Odd chain phenolic lipids in liposomes as a delivery system in food using high power ultrasound

by

Kelly Dornan

A thesis submitted to the Faculty of Graduate and Postdoctoral Affairs in partial fulfillment of the requirements for the degree of

Master of Science

in

Chemistry
(Food Science and Nutrition)

Carleton University

Ottawa, Ontario

ABSTRACT

Odd chain phenolic lipids have gained interest due to their functionality in food and pharmaceuticals owing to their bioactivity, amphiphilic properties, and use for encapsulation and drug delivery. Alkylresorcinols (ARs) are the most studied and found in high concentrations in wheat bran. In parallel, high power ultrasound (US) is an emerging green non-thermal technology with many applications in food. This research aimed to investigate the use of US to extract crude ARs from wheat bran and potential applications for preparation of liposomal solutions for the production of emulsion-filled gels (EFGs) for delivery of functional ingredients and fat reduction in a margarine model system. US proved to be an efficient method of extraction of crude ARs from wheat bran, reducing traditional extraction time from 24 hr to 30 min. Crude ARs and US were then used to develop functional EFGs from US prepared liposomal solutions which were characterized using polarized-light microscopy (PLM), water activity, textural analysis, rancimat, and differential scanning calorimetry (DSC). US and crude ARs improved microstructure, hardness, and oxidative stability of the margarine model system.

ACKNOWLEDGMENTS

First and foremost, I owe the dedication of this work to my supervisor, Dr. Farah Hosseinian. The amount of knowledge and skills that were transferred to me from Dr. Hosseinian will be of value to me for the rest of my life. My greatest resource along the way was paying attention every time she spoke for her wealth of knowledge is an immeasurable asset. Her ability to see potential and encourage her students is inspiring and for that, I am deeply grateful to have had her as a mentor along my academic work.

My gratitude is also owed to Dr. Aynur Gunenc whose experience in research provided me thoughtful guidance in the lab and who patiently taught me a great deal on data interpretation and writing manuscripts. Thank you to Dr. Jeremy Laliberte for allowing me to use his DSC, Hayat El for her training, and Trinda Crippin for kindly allowing us to use her lab for some of the research. Also in need of thanks are my peers in the lab. Nasim Meshginfar, who provided me with much-needed coffee breaks and enriching discussions on science, life, and culture. Minfang Luo and Colleen Celton for their valuable teamwork, and Sandra Gerhards for helping me with obtaining results.

And of course, I must thank my family who has always provided me with the support and encouragement I needed to push myself towards my goals. A special thanks to my mother, my sister, and my grandmother, who fill my life with plain old happiness.

TABLE OF CONTENTS

LIST OF TABLES

LIST OF FIGURES

ABBREVIATIONS

AAPH	2'2'-axobis(2-methylpropionamidine) dihydrochloride
AO	Avocado oil
AR	Alkylresorcinol
AUC	Area under the curve
B	Base (EFG control)
ddH_2O	Double distilled water
DHBA	3,5-dihydroxybenzoic acid
DHPPA	3-(3,5-dihydroxyphenyl) propanoic acid
DM	Dry matter
DSC	Differential scanning calorimetry
EFG	Emulsion-filled gels
GMS	Glycerol monostearate
GSH	Reduce glutathione
GSSG	Oxidized glutathione
HPLC	High-performance liquid chromatography
HDL	High-density lipoprotein
I	Inulin
IC_{50}	Half maximal inhibitory concentration
M	Margarine
Me	Mechanical homogenization
O	Oil
ORAC	Oxygen radical absorbance capacity
PDA	Photodiode array detector
PLM	Polarized-light microscopy
RP	Reverse phase
TA	Traditional acetone wheat bran extract
TAG	Triglyceride
TE	Traditional ethanol wheat bran extract
US	Ultrasound
US30A	Ultrasound-assisted (30 min) acetone extract
US30E	Ultrasound-assisted (30 min) ethanol extract
US-Me	Ultrasound homogenization
UV	Ultra-violet
VLDL	Very low-density lipoprotein
W	Water
WB	Wheat bran
WBE	Wheat bran extract

CHAPTER 1: Literature Review

1.1 Wheat bran

1.1.1 A brief overview

Humans have a long history of consuming wheat. It is believed that people began to consume wheat in prehistoric times, at least 15 000 years B.C. (Symko, 2015). The consumption, farming, and processing of wheat are believed to be deeply entrenched in the rise of civilization. Wild wheat seems to have been discovered in the Fertile Crescent (roughly modern Iraq) where wild emmer wheat and barley were likely the first cereal to be domesticated and grown in large enough quantities for people to settle down and start cultivating cereal for consumption. The large food stocks meant that more people could be fed leading to an increase in population and demand for trade in settlements (Giroux, 2017). Settling down meant that farmers had time to develop new farming, processing, and cooking techniques eventually leading to bread wheat evolution. Today, this old-world agriculture founder crop is now a staple crop in more than 40 countries. It is still deeply entrenched in world economies and people's diets providing 60% of calories, together with rice and maize (Ozkan et al., 2011). In Canada, the grain sector is a key driver of economic growth. In 2017, the country exported 20.5 million tonnes of wheat representing $21 billion in export sales (Agriculture and Agri-Food Canada, 2019). With a total of $549.6 billion in export sales in 2017, wheat export sales represent about 3.8% of this (Statistics Canada, 2018).

Wheat grain is composed of different layers: the germ, endosperm, aleurone layer, and pericarp (Figure 1.1).

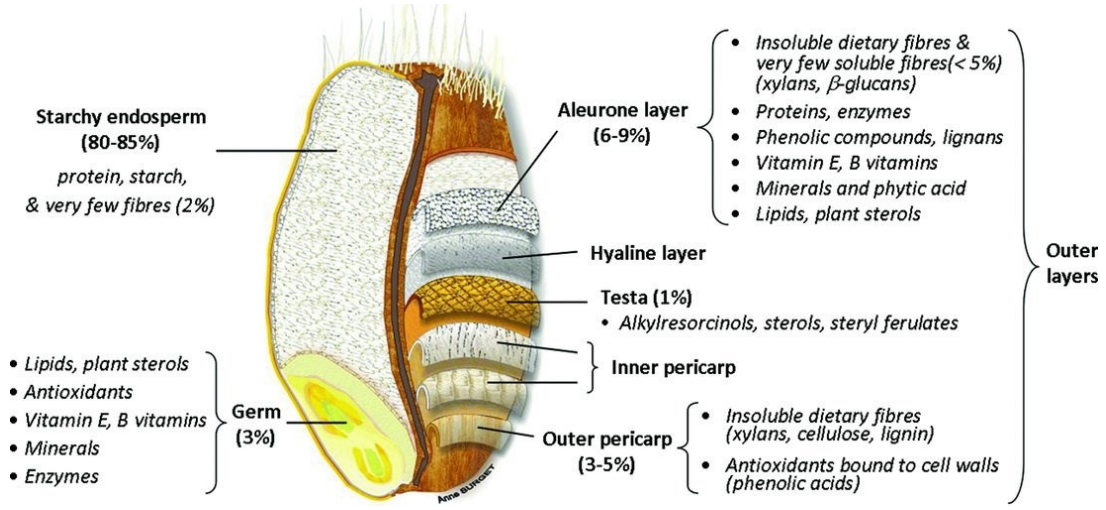

Figure 1.1 Wheat grain structure (Onipe et al., 2015).

Wheat bran, the outer layers (pericarp, seed coat, nucellar epidermis, aleurone), is a major by-product of the wheat industry obtained by de-branning wheat stocks. Wheat bran is removed in the milling process by abrasion and friction before grinding (Galindez Najera, 2014). De-branning of wheat before grinding produces a more refined flour that provides better organoleptic properties in bread making while also removing unstable lipids (from germ) and mycotoxins, pesticide residues, and heavy metals (from peripheral tissues) minimizing storage and contamination issues (Galindez Najera, 2014). But wheat bran is also nutritionally rich in fibre, minerals, vitamin B6, thiamin, folate, vitamin E, and phytochemicals (Stevenson et al., 2012). Wheat bran accounts for 25% of the grain weight and about 150 billion tons of biomass by-product produced per year globally (Puckler et al., 2014). About 90% of the wheat bran by-product produced from wheat grain milling is used as livestock feed while only 10% is used in the food industry as a fibre source in bakery, fried foods, and breakfast cereals (Onipe et al., 2015). Considering the large amount of wheat bran biomass produced from the milling industry and the low value of bran feed products,

there is currently interest in finding novel value-added applications for wheat bran (Puckler et al., 2014).

1.1.2 Nutritional composition of wheat bran

Wheat bran, aside from being an abundant source of dietary fibre, also contains minerals, B vitamins, and bioactive compounds such as phenolic acids, arabinoxylans, alkylresorcinols, and phytosterols. These compounds have been studied and evidence links them to health benefits that may prevent disease (Onipe et al., 2015). Table 1.1 shows the various components that have been identified and measured in wheat bran.

Table 1.1 Nutritional composition of wheat bran (Onipe et al., 2015)

Bran Component	**Range % DM**
Dietary fibre	33.40-63.0
Moisture	8.1-12.7
Ash	3.9-8.10
Protein	9.60-18.6
Total carbohydrates	60.0-75.0
Starch	9.10-38.9
Phytochemicals	**µg g^{-1}**
Alkylresorcinols	489-1429
Phytosterols	344-2050
Ferulic acid	1376-1918
Bound phenolic compound	4.73-2020
Flavonoids	3000-4300
Micronutrients	**mg per 100 g**
Phosphorous	900-1500
Magnesium	530-1030
Zinc	8.3-14.0
Iron	1.9-34.0
Manganese	0.9-10.1
Vitamin E (Tocopherols/tocotrienol)	0.13-9.5
B Vitamins	
Thiamin (B1)	0.51-1.6
Riboflavin (B2)	0.20-0.80
Pyridoxine (B6)	0.30-1.30
Folate (B9)	0.088-0.80

DM: dry matter

About 53% of bran is composed of dietary fibre (xylans, lignin, cellulose, galactan, and fructans). The other components include alkylresorcinols, ferulic acid, flavonoids, carotenoids, lignans, and sterols. Several epidemiologic studies have shown that consuming whole grain (with bran layers) is linked to a decrease in the risk of chronic disease. One example is the Iowa Women's Health Study (Jacobs et al., 2007) which followed a cohort of postmenopausal women(*n*= 41 836) aged 55-69 over 17 years and found an inverse association in inflammation-related death associated with whole-grain intake when comparing hazard ratios to women who rarely or never ate whole-grain foods. The authors suggested the presence of antioxidant constituents in whole grain as the likely mechanism offering a reduction in oxidative stress.

1.1.3 Wheat bran extract (WBE)

One application of wheat bran biomass is the extraction of compounds of interest found within the outer layers of wheat. The extractable plant-based components include fibre, hemicellulose, proteins, polysaccharides, lipids, and phytochemicals. In Canada, one company has received a no-objection notice from Health Canada for the safe use of wheat bran extract (WBE) as a novel food ingredient at levels of 0.6 to 15% w/w, providing a maximum of 3.0 g of WBE per serving of food in baked goods and baking mixes; grain products and pasta; breakfast cereals; beverages; milk products; frozen dairy products; gelatins, puddings, and fillings; jams, jellies, and preserves; processed fruit and fruit juices; and process vegetables and vegetable juices (Health Canada, 2015).

1.2 5-*n*-Alkylresorcinols (ARs)

1.2.1 Structure of ARs

5-*n*-Alkylrercinols (ARs) are a mixture of AR homologues, amphiphilic 1,3-dihydroxybenzene derivatives with an odd-number alk(en)yl chain containing 13-27 carbon atoms (C13:0-C27:0) attached to the 5th position of the benzene ring (Liu et al., 2018). The side chain is predominantly in the saturated form. The C17:0-C25:0 homologues, found in wheat, rye, and triticale bran are shown in Figure 1.2.

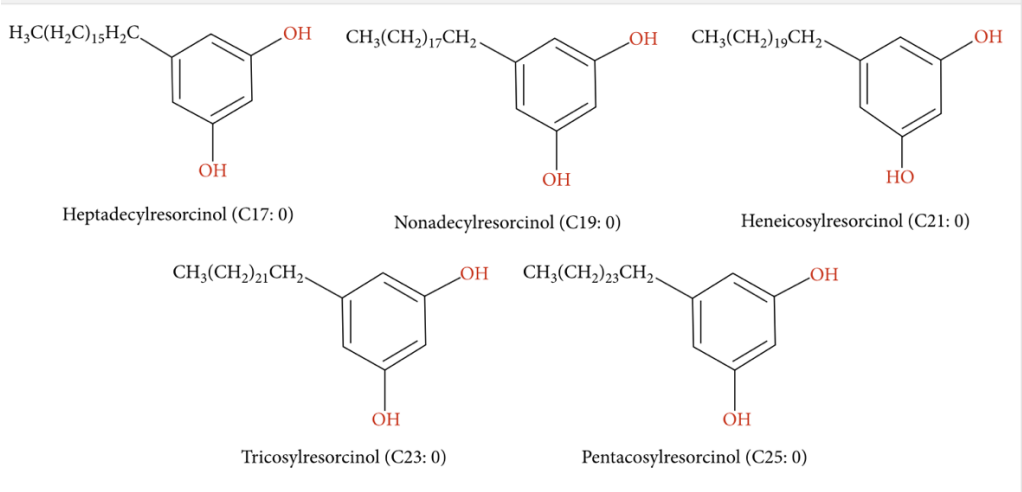

Figure 1.2 Alkylresorcinol homologues found in wheat, rye, and triticale bran (Tian et al., 2020)

1.2.2 Pharmacokinetics of ARs

Figure 1.3 shows the absorption, distribution, and elimination of ARs (Marklund et al., 2014). Research shows that when ingested, approximately 60% of ARs are absorbed by the small intestine through the lymphatic pathway (Linko et al., 2007; Ross et al., 2003). There is also evidence that one-third of ARs undergo first-pass metabolism by being absorbed through the portal vein and subsequently metabolized to DHBA and DHPPA by the liver before entering circulation

(Marklund et al., 2014). ARs absorbed via the lymphatic system are transported in chylomicrons, bypassing the liver, and enter circulation intact where they are incorporated into erythrocytes or lipoproteins (Linko & Adlercreutz, 2007). From circulation they are transferred to the liver, to undergo phase I or phase II metabolism or repackaging into lipoproteins with higher proportions of ARs found in HDL and VLDL (Linko-Parvinen et al., 2007; Marklund et al., 2014). Or they can also be transferred from circulation to adipose tissue where longer chain derivatives are found in higher proportions compared to their shorter chain homologues (Jansson et al., 2010). In the liver, they are believed to undergo metabolism similar to fatty acids, in which cytochrome P450 dependent ω-oxidation is initiated by attaching a hydroxyl group at the terminal carbon and then two-step oxidation converts this hydroxyl group to a carboxylic acid allowing for subsequent shortening of the alkyl chain through several rounds of β-oxidation, ultimately leading to the formation of hydrophilic DHPPA and DHBA as phase I metabolites. DHPPA and DHBA can further be conjugated through phase II metabolism (Marklund et al., 2013). From the liver, these metabolites are either secreted through bile into the intestine, where they are reabsorbed or excreted through feces, or they can be secreted into plasma and eliminated by the kidneys through urine (Marklund et al., 2014).

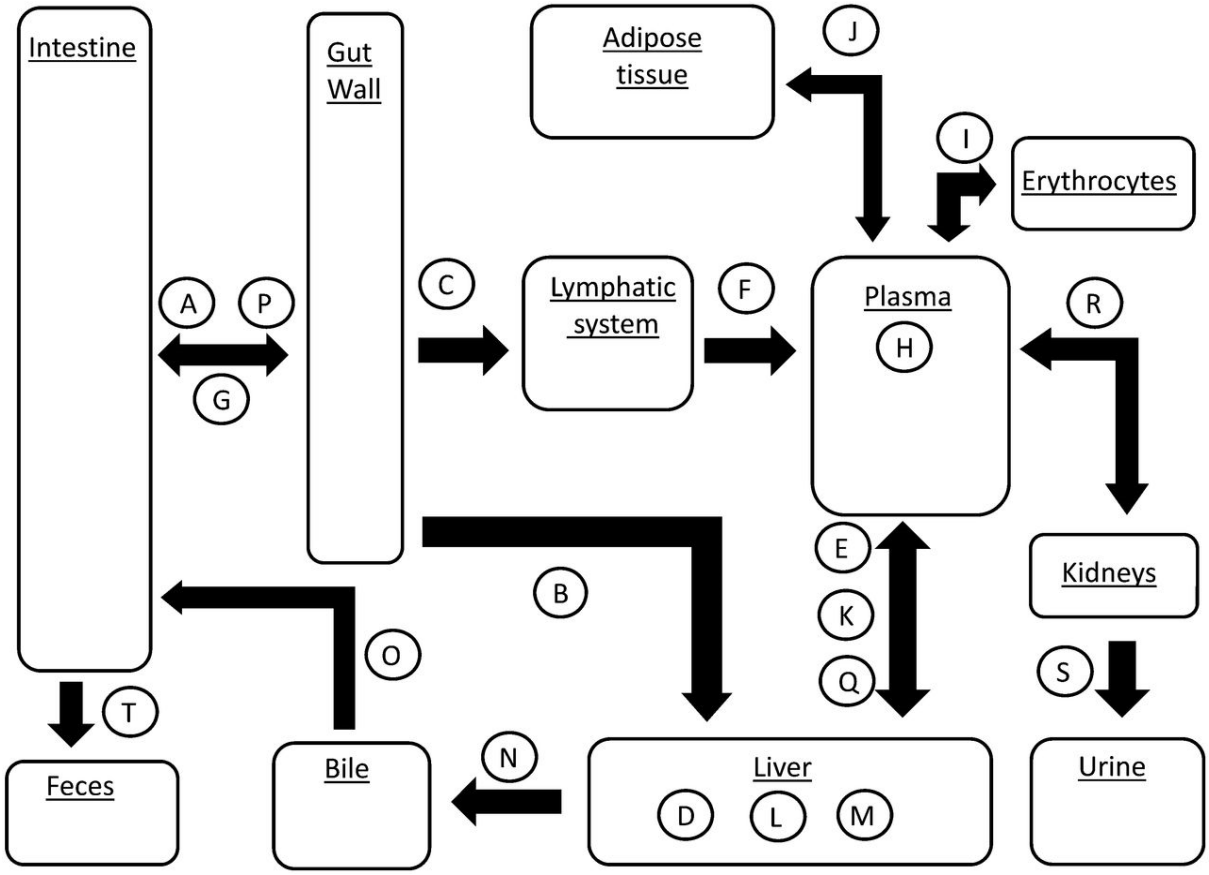

Figure 1.3 Diagram representing the hypothetical absorption, distribution, and elimination of ARs. After absorption from the intestine to the gut wall (A) ARs enter systemic circulation through the portal vein (B) or the lymphatic system (C). The portal vein delivers ARs to the liver where they are metabolized to DHBA and DHPPA (D) before entering systemic circulation (E). Lymphatic absorption is a slower process but ARs absorbed through this pathway avoid hepatic metabolism (F) and enter the plasma intact. Some ARs might undergo metabolism directly in the gut wall before being excreted back to the intestinal lumen (G). In plasma, ARs are mainly incorporated in lipoprotein particles (H) and erythrocytes (I) but can be transferred to other tissues (i.e., adipose tissue (J) or liver (K)). In the liver, ARs are either reassemble to different lipoproteins (L) or undergo phase I and II metabolism (M). Metabolites like DHPPA or conjugated ARs are transferred to the bile (N) and back to the intestine (O) where they are either reabsorbed (P) or excreted into the feces (T). DHBA and DHPPA formed in the liver can also be secreted into plasma (Q) and eliminated by kidneys (R) through urine (S). (Marklund et al., 2014).

1.2.3 Bioactivity of ARs

Many in vitro and in vivo studies have shown the biological activity of ARs. Horikawa et al. (2017) showed that chronic supplementation with ARs from wheat bran prevented glucose intolerance, insulin resistance with hepatic lipid accumulation induced in mice by a high-fat high sucrose diet. They also showed that ARs dose-dependently decreased micellar solubility of cholesterol in an in-vitro biliary micelle model while in-vivo transient AR supplementation with a high-fat high-sucrose diet increased cholesterol and triglyceride excretion in feces while decreasing plasma cholesterol concentrations. The authors suggest that ARs interfere with micellar cholesterol solubilisation in the digestive tract, thereby decreasing cholesterol absorption, which may provide the underlying mechanism for reduced risk of metabolic disorders previously seen in correlation to whole wheat consumption in epidemiological studies. Agil et al. (20 16) showed that supplementation of high-fat diets in mice with 0.5 % ARs and 0.5 % triticale bran led to a significant improvement in antioxidant status of the liver and heart tissues compared to mice fed a non-supplemented high fat diet by increasing levels of reduced glutathione (GSH) and lowering the oxidized glutathione to reduced glutathione ratio (GSSG/GSH). Another study by (Ross et al., 2004) reported elevated levels of γ-tocopherol in the liver and lungs of rats fed purified ARs at concentrations reflecting whole-grain rye (1 g/kg) and rye bran (4 g/kg). Rats fed that highest concentration had 47% less liver cholesterol and 35% less cholesterol in liver lipids compared to the control diet. The study attempted to illustrate this effect in-vivo finding evidence that ARs might mediate γ-tocopherol through competitive inhibition of the γ-tocopherol pathway.

1.2.4 ARs in cell membranes

ARs are amphiphilic odd chain phenolic lipids capable of incorporating into biological membranes (Stasiuk & Kozubek, 2010). The chain length of ARs is related to their bioactivity with longer alkyl chains having better fat solubility and stronger antioxidant activity by binding to adjacent phospholipids in the membrane through hydrogen bonding and exerting resistance to oxidation due to their ability to scavenge free radicals (Tian et al., 2020). Their incorporation into cellular membranes can affect the structure and dynamics of lipid bilayers and has been studied in artificial membranes (Andersson et al., 2011). ARs show good miscibility with phospholipid bilayers with different effects on thermal behaviour (phase transition temperature and enthalpy) observed between saturated (increase) and unsaturated homologues (broadening and lowering, respectively) (Stasiuk & Kozubek, 2010). It is believed that these disturbances are caused by a change in molecular packing of the bilayer components and by acting on the membrane surface charge and mobility of lipids and possibly influenced by chain length and degree of saturation of the AR homologues.

1.2.5 Industrial applications of ARs

ARs have been shown to have applications in several industries. Cardanol, an odd chain phenolic lipid similar to ARs but with one hydroxyl group attached to the benzene ring instead of two, is produced from cashew nutshell liquid and has the potential to be used as a renewable biosource to replace petroleum derived alkylphenols. Cashew nutshell liquid itself can be used as a phenolic source for formaldehyde polymerization. In compounded forms, it can be applied as friction dust for auto parts (Sampietro et al., 2013). The self-assembly of odd chain phenolic lipids can also be exploited in manufacturing biomaterials such as lipid nanotubes, twisted/helical nanofibers, low

molecular weight hydro- and organo-gels, and liquid crystals. These soft materials have shown applications in template synthesis and biosensors (John & Vemula, 2006).

ARs also have applications in drug delivery for encapsulation by self-assembly into liposomes in a solution that can act as carriers for various molecules and delivery systems in the food, pharmaceutical, and cosmetic industries. Atrooz (Atrooz, 2011) investigated the effect of ARs from acetonic extracts from wheat grains on liposome properties and found that ARs from the extract can self-assemble into vesicles (AR liposomes) that have higher size stability, increased permeability than phosphocholine liposomes. AR liposomes and AR-incorporated phosphocholine liposomes also showed increased oxidative stability compared to liposomes made of only phosphocholine.

In food, the amphiphilic and antioxidant properties of ARs have potential for encapsulation of hydrophobic compounds, as an emulsifier, and as a natural antioxidant and antimicrobial agent. (Elder et al., 2021) investigated the antioxidant activity of AR homologues in bulk oils and oil-in-water emulsions and found that ARs were able to inhibit lipid oxidation in both systems with different degrees of activity influenced by chain length. They found that antioxidant activity decreased with alkyl chain length in bulk oils with intermediate alkyl chain lengths (C21:0) offering optimal antioxidant activity in emulsions.

In agriculture, research has shown antifungal properties of AR extracts against the growth of Fusarium Head Blight causal agents with suggestions that commercial formulations be developed for the prevention of fungal disease for crop protection systems (Ciccoritti et al., 2015).

1.2.6 Toxicology of alkylresorcinols (ARs)

Studies show low toxicity of ARs. (Biskup et al., 2016) investigated cytotoxicity of natural AR fraction, individual homologues, and related compounds (resorcinol, orcinol and olivetol) on normal cells using mouse fibroblast (cell Line L929) and reported a dose-dependent structure-activity with decrease in cytotoxicity with increasing chain length that can be described by the quadratic function. Homologue C17:0 showed the strongest inhibition of fibroblast growth (IC_{50} = 171 μM), followed by C19:0 (IC_{50} = 330 μM), and C21:0 (IC_{50}= 551 μM) in comparison to the positive control (Hydroquinone) which showed a toxicity of less than 19.5 μM. Hydroquinone is the positional isomer of resorcinol with the two hydroxyl groups in the para position instead of in the meta position. Resorcinol showed the highest IC_{50} value (11043 μM) and lowest cytotoxicity showing that the position of the hydroxl groups in the benzene ring has an important effect on activity. Resorcinol and its 5-methyl derivative, orcinol, both had higher IC_{50} and lower cytotoxicity compared to ARs with longer carbon chains attached to the benzene ring. The increase in carbon chain is also what allows ARs to incorporate within membrane bilayers which could be the reason why they show a higher activity. The AR concentrations used in this study exceeded the concentrations found in human plasma by 10^4 times and by 50 times in adipose tissue. The study highlighted the safety of ARs while also offering caution to high local AR concentrations that might be possible in fortified foods or cosmetics.

Bilobol, an AR with unsaturation at the 8^{th} carbon of the 15 carbon alkyl chain, found in cashew nut shell liquid is a promising eco-friendly larvicide for vector control of *Aedes aegypti* known to transmit arbovirus that cause arthropod-borne diseases such as dengue, Zika, and chikungunya.

Schulte et al. (2021) recently investigated its degradation profile and acute toxicity on zebrafish, a non-target organism, to ensure the safe use of bilobol with minimal environmental effects and reported no significant toxicity on zebrafish embryos.

1.3 Lipids

1.3.1 Structure and function

Lipids are hydrocarbons with a wide diversity in structure and biochemical function with their primary role to form membranes that act as barriers for cells and organelles (Dowhan et al., 2015). They also serve as an excellent form of energy storage releasing large amounts of energy when oxidized. In adipocytes, they are found as triglycerides, three fatty acids attached to a glycerol head group through an ester linkage. Lipids can also function as intracellular signaling molecules (Scherer, 2006). Fatty acids are the basic form of lipids and consist of a straight chain of mostly even-numbered carbon atoms that can either be saturated or unsaturated.

1.3.2 Saturated fatty acids

Saturated fatty acids have no double bond in their alkyl chain and therefore pack more easily than unsaturated fatty acids and are more ordered with higher melting points. Fats, which are solid at room temperature, consist mainly of saturated fatty acids. Saturated fatty acids are more resistant to oxidation due to the lack of oxidizable double bonds.

1.3.3 Unsaturated fatty acids

Unsaturated fatty acids are fatty acids in which one or more double bonds exist and are categorized as monounsaturated (one double bond) or polyunsaturated (more than one double bond). The

presence of a double bond introduces a kink in the alkyl chain which affects packing. Unsaturated fatty acids pack less closely than saturated fatty acids and are therefore less ordered with lower melting points. Oil, which is liquid at room temperature, consists mainly of unsaturated fatty acids. Because of the presence of the double bond, which can be oxidized, unsaturated fatty acids are more prone to oxidation compared to saturated fatty acids. On the other hand, the position and number of double bonds have a direct relationship to their function. Omega-3 fatty acid, or α linolenic (C18:3 Ω3), is a polyunsaturated fatty acid with three cis double at the 9^{th}, $12^{th,}$ and 15^{th} carbon and a key building block of cell membranes and famously linked to health disease reduction when consumed and is considered an essential fatty acid (Cholewski et al., 2018).

1.3.4 Chain length

Fatty acids can differ in chain length from short-chain (C1-6), medium-chain (C7-12), long-chain (C14-18), and very-long-chain (C>20). For the most part, fatty acids consist of an even number of carbons. Odd chain fatty acids, however, exist in dairy products with saturated carbon chains. Odd chain saturated fatty acids have lower melting points than their even-numbered homologues which can affect cell membrane fluidity (Kurotani et al., 20 17). Epidemiological studies have shown a negative correlation between the presence of odd chain fatty acids in plasma, associated with dairy consumption, and coronary heart disease and type 2 diabetes (Forouhi et al., 20 14; Khaw et al., 20 12; Kurotani et al., 20 17).

1.3.5 Lipid oxidation

Lipid oxidation is a complex set of free radical reactions between fatty acids and oxygen or free radicals which results in rancidity (Mozuraityte et al., 2016). The chain mechanism can be divided

into three stages: initiation, propagation, and termination. A simplified scheme is given in Figure 1.4. Oxidation is initiated in unsaturated lipid molecules in the presence of heat, light/ionizing radiation, and metal ions/metalloprotein. The loss of a hydrogen atom at the double bond produces a free radical that then reacts with oxygen to form a peroxyl radical that attacks a new lipid molecule in a chain reaction. During initiation and propagating, lipid free radicals can be stabilized through resonance leading to a shift of double bonds and cis-trans isomerization. The chain reaction is self-propagating until no hydrogen source is left or the chain is interrupted by an antioxidant. (Shahidi & Zhong, 2010).

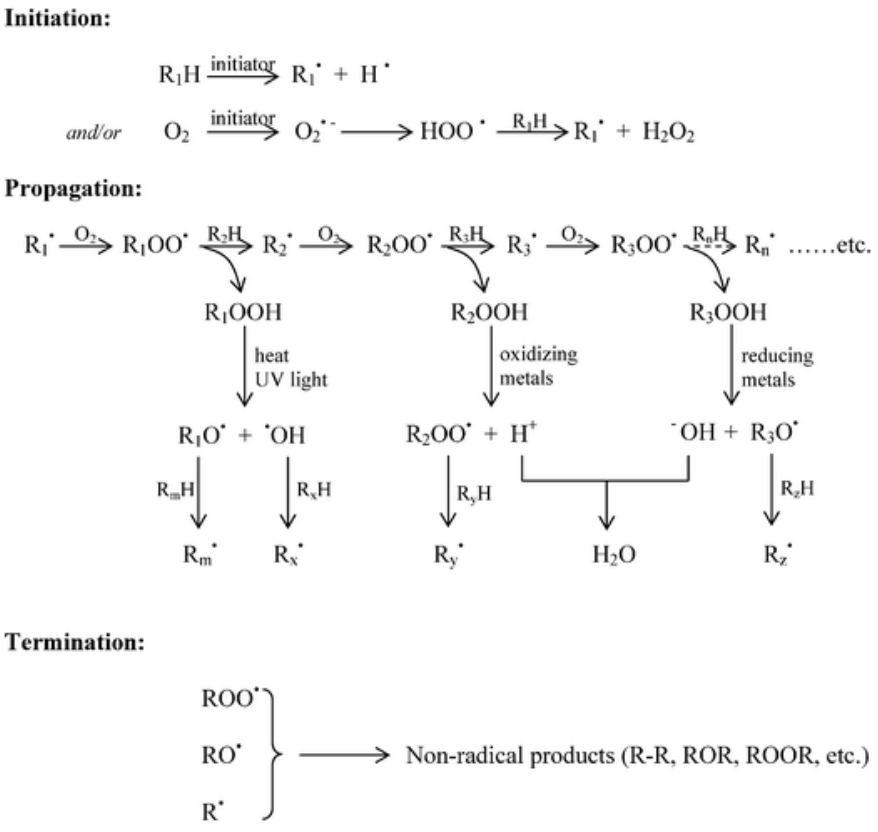

Figure 1.4 Lipid autoxidation pathways (Shahidi & Zhong, 2010)

1.3.6 Crystallization of fats

Crystallization of fats is important for organoleptic and physicochemical properties in foods. Crystallization occurs when a saturated system in equilibrium becomes supersaturated and shifts to a non-equilibrium system. When this happens the characteristics of the system determine the degree of supersaturation that drives formation and growth. The most common methods used to create a supersaturated solution are cooling, solvent evaporation, chemical, reaction, pH modification, and alteration in solvent composition. Controlling crystallization is a key factor in the food industry and is typically achieved through temperature change and solvent evaporation (Deora et al., 2013). The three basic forms of fats crystals, also called polymorphs, are α, β', β in order of increasing melting point, size, density, molecular organization, and thermodynamic stability or decreasing free energy (Gibon, 2006). The length and degree of unsaturation of the fatty acids in triglycerides affect how the molecules will pack and crystallize. Table 1.2 shows the melting points (T_m) of β'and β of common triglycerides (TAG).

Table 1.2 Melting points (°C) of β'and β polymorphs of common TAGs (Ghotra et al., 2002)

TAG	T_m (°C)	
	Polymorph	
	β'	β
PPP	56.7	**66.2**
SSS	64.2	**73.5**
PSP	**68.8**	-
POP	30.5	45.3
SOS	36.7	41.2
SOO	8.8	23.7
OOO	-11.8	5.1
LOO	28.3	-23.3
LLO	3.02	25.2

P: Palmitic, S: Stearic, O: Oleic, L: linoleic acid. Letters in bold indicate the polymorphic tendency of solid TAGS in margarine and shortening.

The polymorph present in fats is responsible for its thermal behaviour. The shape and size of the crystal also affect the hardness of the fat network. β' crystals are small (~1 μm), thin and needle-like, and are the most functional in food. Palm oil is often added to vegetable-based shortenings and margarine to promote the formation of β' crystals due to its high content of palmitic acid, which favours β' formation and also delays and prevents conversion to the less favoured larger crystal structure known as the β polymorph. Stabilizing the somewhat unstable β' crystals is important to the food industry as it results in a better product.

1.4 Emulsions

1.4.1 Brief overview

Emulsions typically consist of two immiscible liquids with one dispersed within the other. The liquid droplets (the dispersed phase) are dispersed within a liquid medium (the continuous phase) with the two most simple classes being oil-in-water (O/W) or water-in-oil (W/O) emulsions (Tadros, 2016). A more complex class of emulsions are double emulsions consisting of either water-in-oil-in-water (W/O/W) or oil-in-water-in-oil (O/W/O) whereby the dispersed phase itself consists of an emulsion, see Figure 1.5 for a simple representation.

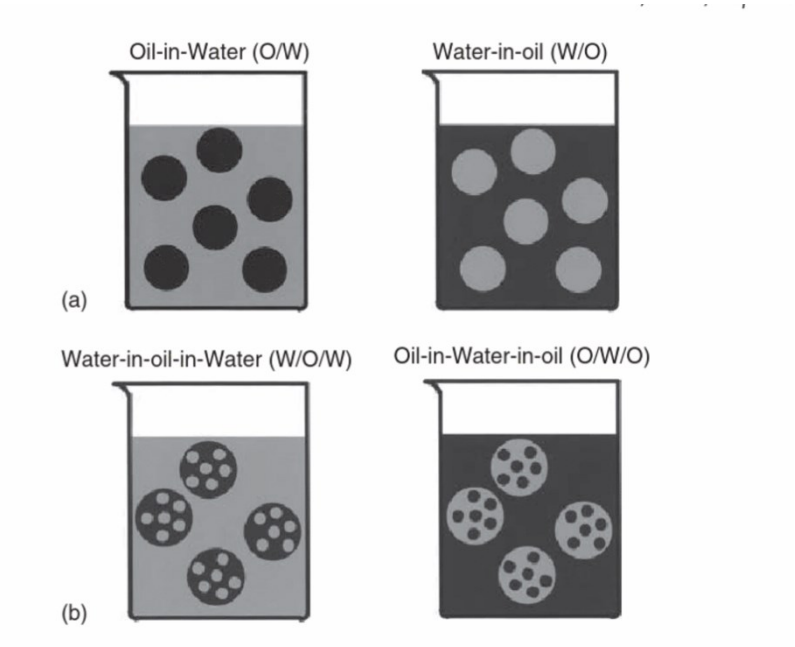

Figure 1.5 (a) oil-in-water (O/W) emulsion and water-in-oil (W/O) emulsion. (b) Water-in-oil-in-water (W/O/W) emulsion and oil-in-water-in-oil (O/W/O) (Schramm, 2014).

Emulsions have well-known applications in food (butter, milk, spreads, etc), pharmaceutics (parenteral nutrition, drug systems), and cosmetics (lotions) (Petersen et al., 2013). Common emulsions in food are butter, margarine, yogurt, milk, ice cream, mayonnaise, and sausages. Table 1.3 shows what type of emulsions these are along with the common stabilizers used for each.

Table 1.3 Dispersed and continuous phases of emulsions and the most common stabilizers used for each adapted from (Schramm, 2014).

	Dispersed phase	**Continuous Phase**	**Stabilizer**
Butter	Water	Fat	Milk proteins
Margarine	Water	Fat	Lecithin, mono-and diglycerides
Yogurt	Fat	Water	Milk proteins
Milk	Fat	Water	Milk proteins
Ice cream	Fat	Water	Egg yolk
Mayonnaise	Water	Oil	Egg yolk
Sausage	Fat	Water containing salts, dissolve, gelled, or suspended proteins	Egg, blood plasma, milk proteins, soy proteins, wheat proteins

1.4.2 Emulsifiers

Emulsions are thermodynamically unstable and require stabilizers such as emulsifiers, thickening agents, gelling agents, weighting agents, and ripening inhibitors to stabilize the dispersed phase within the aqueous phase (McClements & Gummus, 2016). The functionality of emulsifiers lies in their ability to reduce surface tension at the oil-water interface making it easier to disrupt bulk phases into small droplets. The stability and mechanical property of emulsions is influenced by the adsorption and interaction of emulsifiers at the fluid interfaces. Lecithin and GMS are both low-molecular-weight emulsifiers commonly used to stabilize different food products.

Soy lecithin is a mixture of phospholipids found in soybean with phosphatidylcholine (PC) being the major component. Also present in smaller quantities are phosphatidylethanolamine (PE), phosphatidylinositol (PI), and phosphatidic (PA). Phospholipids are polar lipids, amphiphilic in nature, containing a hydrophilic phosphate head-group attached to two non-polar hydrocarbon chains that are either saturated or unsaturated (Pichot et al., 2013). Figure 1.6 shows two examples of the chemical structure of phosphatidylcholine containing different acyl chains.

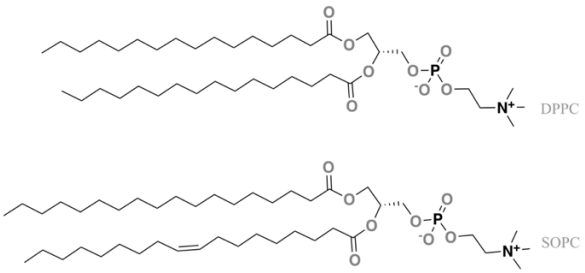

Figure 1.6 Two examples of saturated and unsaturated phosphatidylcholines found in lecithin, namely 1,2-dipalmitoyl-*sn*-glycero-3-phosphocholine (DPPC) and 1-stearoyl-2-oleoyl-*sn*-3-phosphocholine (SOPC) (Kafle et al., 2020)

Phosphatidylcholine from soybean swells by incorporating water and forms a lamellar liquid crystalline phase. The behaviour of this phase is directly influenced by the chain length and degree of saturation of the hydrocarbon chain (van Hoogevest & Wendel, 2014). Table 1.4 shows the phospholipid composition and the fatty acid composition (area%) of de-oiled soy lecithin.

Table 1.4 Phospholipid composition (%) and fatty acid composition (%area) of de-oiled soy lecithin adapted from (van Hoogevest & Wendel, 2014)

De-oiled soy lecithin			
Phospholipid	**(%)**	**Fatty Acid**	**(% area)**
PC	20-22	C14:0	0.1
PE	16-22	C16:0	21
PI	13-16	C18:0	4.7
PA	5-10	C18:1	9.9
LPC	<3	C18:2	57
		C18:3	5.0
		C20:0	0.1
		C22:0	0.4

Phospholipids are ionizable emulsifiers capable of providing stability to emulsions as a mechanical and electrostatic barrier to coalescence (Moran-Valero et al., 2017)

Soy lecithin can be used to manufacture nanostructured drug delivery systems by assembling itself into bilayers, also known as liposomes. Liposomes have utility in pharmaceuticals for drug delivery and, in research can be used as model artificial cell membranes as they mimic the core basic structure of cells to study the effect of drugs on membrane permeability and fluidity. For drug delivery, surface modification can be used to enhance drug delivery and has applications in cancer treatment, brain targeting vaccinology. Demands for food-approved liposome nanoparticles are increasing. Liposomes can be used to affect the rheological properties of food, fat, and sugar reduction.

Glycerol monostearate (GMS) is a monoglyceride, a glycerol ester of stearic acid (C18:0), see Figure 1.7. It is a non-ionic surfactant with a hydrophilic glycerol group and a hydrophobic saturated acyl chain.

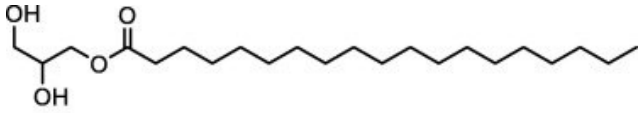

Figure 1.7 GMS chemical structure (Zhao et al., 2018)

GMS is commonly used in low-fat products (spreads, cakes, bread, creams, whipping, and cream substitutes) as an emulsifier due to its ability to enhance organoleptic and textural properties by affecting the liquid crystalline phases present.

GMS and lecithin can be used in combination to impart a favourable synergistic effect on emulsions. Moran-Valero et al. (2017) studied this synergistic performance in oil/water emulsions and attributed it to their interactions in both the bulk phase and at the interface. GMS, which is more hydrophobic than lecithin due to its lack of an ionizable phosphate group, is believed to mainly interact with the oil phase while the more amphiphilic nature of phospholipids interacts at the interface, with the ionic phosphate group interacting with water and the acyl chains anchoring into the oil phase. GMS seems to enhance this anchoring by interacting with the phospholipid acyl chains, see Figure 1.8.

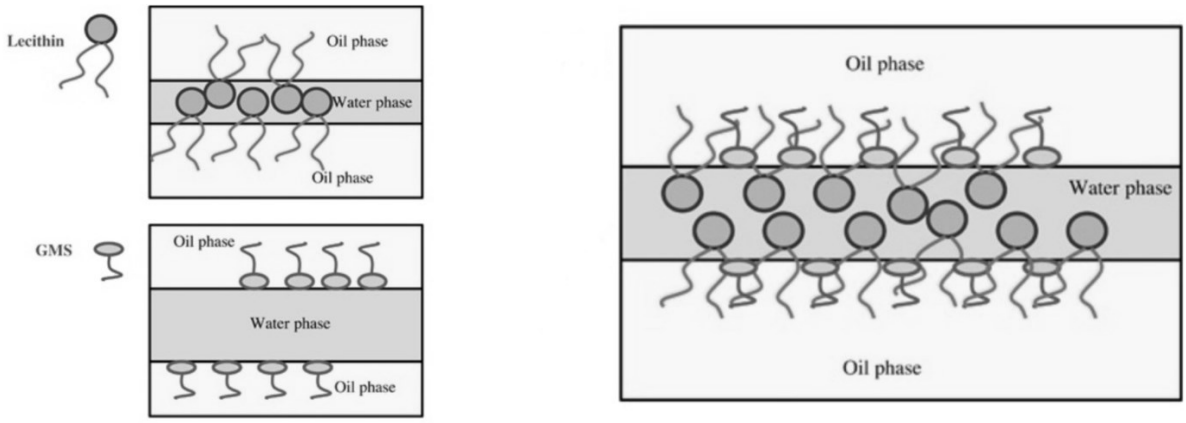

Figure 1.8 Interaction of Lecithin and GMS with the oil/water interface individually and together (adapted from (Moran-Valero et al., 2017).

Inulin is a carbohydrate polymer that is widely used in food and commonly labeled as a dietary fibre. It can be used to form gels by creating a network of small particles that trap water and mimic fat crystals making it a good fat substitute in food (Paglarini et al., 2021). Inulin can be described as a fructan carbohydrate, a polymer of D-fructose units linked by β (2 → 1) linkages with a terminal glucose residue, Figure 1.9. Depending on the amount of repeating fructose units, or degree of polymerization, it exists either as an oligosaccharide or a polysaccharide.

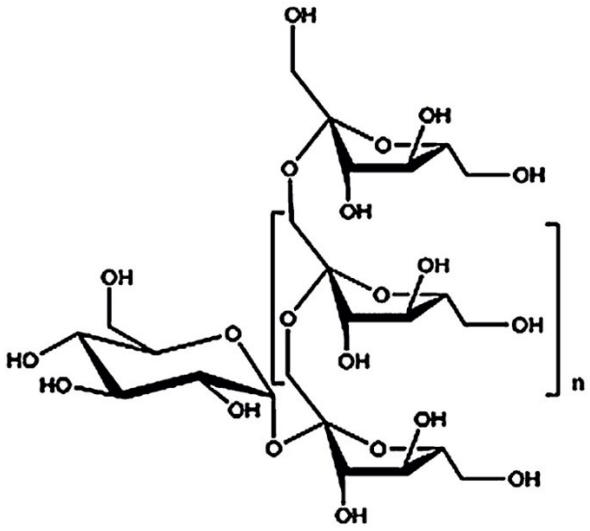

Figure 1.9 Chemical structure of inulin (Shoaib et al., 2016)

1.4.3 Emulsion-filled gels

Emulsion-filled gels (EFGs) can be described as oil droplets dispersed within a gel matrix to act as fillers. The oil droplets can be characterized as active fillers or inactive fillers depending on the way they interact with the gel matrix, a representation of which can be seen in Figure 1.10

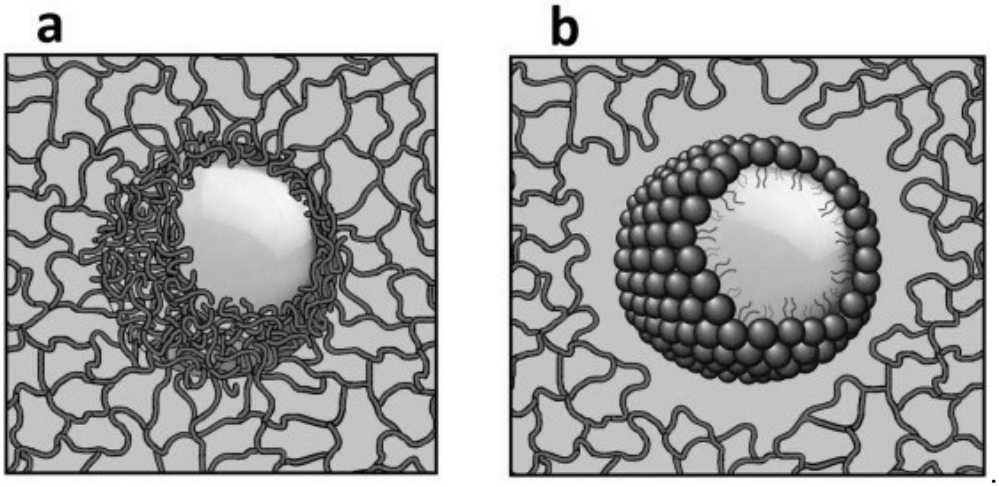

Figure 1.10 Representation of emulsion-filled gels with a) oil droplets acting as active filler particles, and b) oil droplets acting as inactive filler particles (Farjami & Madadlou, 2019)

The oil droplets in emulsion-filled gels are stabilized within a hydrogel, a three-dimensional solid-like aqueous network, preventing them from coalescing through steric hindrance. Hydrogels by themselves have application in food due to their ability to stabilize food texture but due to their aqueous nature are not suited for the delivery of hydrophobic compounds. Emulsion-filled gels however can be utilized for delivery of both hydrophobic and hydrophilic compounds by dissolving them within the stabilized oil droplets and within the aqueous phase, respectively.

1.4.4 Liposomes

Liposomes are synthetic lipid vesicles made of a phospholipid bilayer with an aqueous core as seen in Figure 1.11

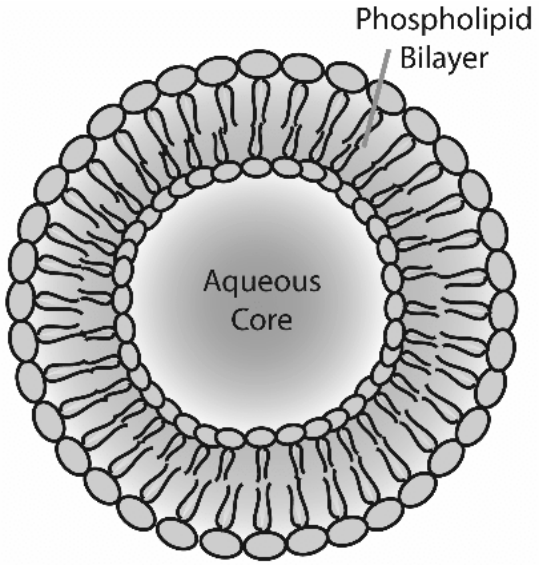

Figure 1.11 Schematic cross-section of liposome (Leung et al., 2019).

Phospholipids self-assemble into bilayers within a solution to minimize contact of hydrophobic acyl chains with the hydrophilic environment while the hydrophilic phosphate groups interact with the aqueous environment. An input of mechanical and thermal energy is required to manufacture liposomes from a dispersion of lipid/phospholipid molecules in an aqueous solution as seen in Figure 1.12 (Mozafari et al., 2008). The resulting liposomes can be used to encapsulate hydrophilic or hydrophobic compounds within the aqueous core or the lipid membrane, respectively. Increasingly, they are being used as delivery methods for drugs in pharmaceutics which can be targeted by modifying the surface of the liposome. They can also be used in research as an artificial model of cell membranes to investigate the effect of various compounds on membrane properties.

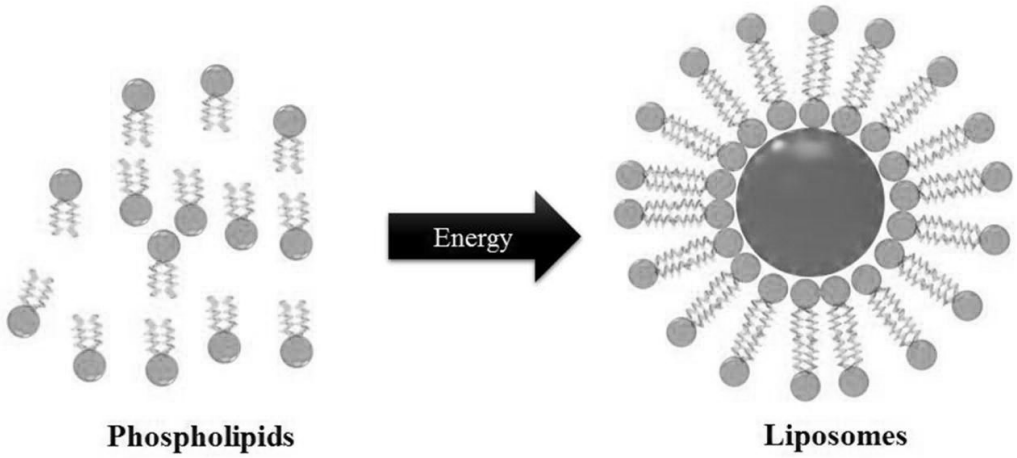

Figure 1.12 Mechanism of liposome particle formation (Shukla et al., 2017)

In food, the demand for encapsulation of ingredients using food-safe liposomes is increasing as they can be used to protect sensitive ingredients or increase the efficacy of food additives through encapsulation (Mozafari et al., 2008; Shukla et al., 2017). Large-scale production of liposomes is limited by poor encapsulation, lack of a continuous process, and the use of toxic organic solvents in their preparation that can remain entrapped within the liposomes (Mozafari et al., 2008). One solution is the use of high-power ultrasound to provide enough energy to lipid/phospholipid dispersions in water to manufacture liposomes which can also be adapted to form a continuous process (Guner & Oztop, 2017; Hielscher).

1.5 High power ultrasound (US)

High power ultrasound (also called low frequency or high-intensity ultrasound) is an emerging non-thermal green technique in the food industry. While low-intensity ultrasound is non "destructive" and used for detection purposes in food, high-frequency ultrasound can be applied to manipulate processes by damaging cellular walls of microorganisms, denaturing proteins, stimulating seed germination, and enhancing crystallization in foods (Bermudez-Aguirre et al.,

2010). Another common application is cell destruction and extraction of intracellular material. The underlying phenomenon of high-intensity ultrasound is acoustic cavitation. Sound waves at high frequencies (20 kHz-10 MHz) are propagated through a liquid medium the mechanical effect of which generates small bubbles that grow and shrink with each wave eventually leading to unstable bubbles that collapse and release energy absorbed creating localized areas of extreme high heat (4500 ºC) and high pressure (100 MPa) capable of damaging cells walls and particles surfaces through microjets that are generated when bubbles implode (Servili et al., 2019). Figure 1.13 shows the application of the acoustic phenomena and the effect of microjets for the release of intracellular materials.

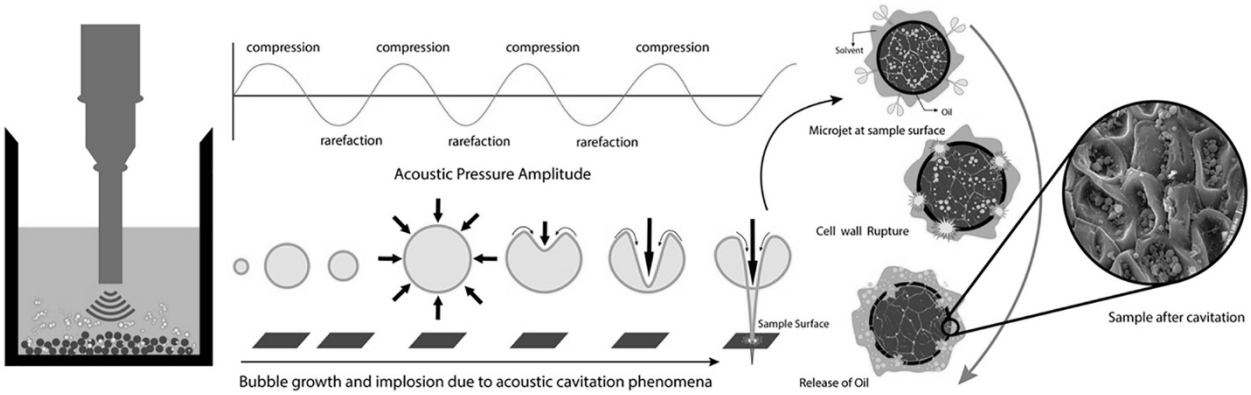

Figure 1.13 Mechanism of ultrasonic acoustic cavitation phenomena for the destruction of cell wall and release of intracellular material (Senrayan & Venkatachalam, 2020)

US energy can also be applied to improve the crystallization process by controlling nucleation and is known as sonocrystallisation. When ultrasound is applied, nucleation is initiated at higher temperatures or in shorter times leading to smaller and more uniform crystals (Petersen et al., 2013). Research has shown that ultrasound induces nucleation at much lower supersaturation levels compared to conventional mechanical agitation and may eliminate the need for crystal seeding (Ruecroft et al., 2005). The application of sonocrystallization in food has been shown

capable of inducing the formation of more stable polymorphs in cocoa butter capable of delaying blooming in chocolate (Martini, 2013). Sonocrystallization is an emerging technique that requires additional attention in the food industry due to its potential to improve process efficiency and product quality.

US can also be applied to produce liposomes from lipid/phospholipid dispersions in an aqueous medium (Guner & Oztop, 2017; Hielscher, 2021). Acoustic cavitation within the aqueous solution allows for mass transport of constituents in a non-homogenous fashion allowing for the fast formation of vesicles (Silva et al., 2010). Hielscher, an ultrasonic technology manufacturer, advertises the use of its ultrasonic processors for the preparation of liposomes for pharmaceutical and cosmetics that can be adapted into a continuous process (Hielscher, 2021).

In the research presented in this paper, low frequency (20 kHz) high power (90 W) was applied using a UIP500hd processor (Hielscher, Germany), shown in Figure 1.14 to extract crude ARs from wheat bran and to produce food-grade liposomal solutions for the preparation of EFGs.

Figure 1.14 The UIP500hd ultrasonic processor (Hielscher, Germany) used in this study.

1.6 Hypothesis and objectives

1.6.1 Hypothesis

It is hypothesized that:

(1) Low-frequency high power Ultrasound can be used to make stable emulsion filled gels as a delivery system of crude ARs in food using margarine model

(2) If low-frequency high power Ultrasound can help ARs, acting as a delivery antioxidant system to reduce lipid oxidation in liposomal membranes

1.6.2 Objectives

The objectives of this study were to:

(1) Extract and characterize crude ARs from wheat bran using low-frequency high power ultrasound

(2) Use low-frequency high power ultrasound to make stable emulsion-filled gels from liposomal solution.

(3) Investigate the effect of low-frequency high power ultrasound on physicochemical properties of emulsion-filled gels

(4) Incorporate crude ARs into emulsion-filled gels as a delivery system for a margarine model system

(5) Investigate incorporation of emulsion-filled gels on physicochemical properties of margarine

CHAPTER 2: Extraction and quantification of alkylresorcinols in wheat (*Triticum aestivum)* bran

2.1 Abstract

The traditional extraction of ARs from wheat bran is time-consuming (24h) and uses acetone, a somewhat non-polar toxic solvent. Ethanol is more polar and less toxic (food-grade) and has been shown able to extract ARs from wheat bran. The application of ultrasound is also increasingly being used as a green non-thermal technique for extraction due to its ability to break down the cell wall through the cavitation phenomenon and releasing solutes into the solvent. In this study, two traditional solvent-based extraction methods using acetone (TA) and ethanol (TE) were used and then low frequency (20 kHz) high power (90W) ultrasound was applied for 30 min (US30A, US30E) in an attempt to decrease extraction time. Using RP-HPLC-PDA, AR homologues C17:0, C19:0, C21:0, and C23:0 were identified and quantified in all extracts. Traditional extraction yields with acetone (TA) and ethanol (TE) were 29.52 $\pm$ 1.91 mg/g of dry bran and 53.33 $\pm$ 1.72 mg/g of dry bran, respectively. Total ARs represented 2.29 $\pm$ 0.10 mg and 2.04 $\pm$ 0.27 mg of these total yields for TA and TE, respectively. Ultrasound-assisted extractions resulted in significantly ($p<0.05$) higher extraction yield when using acetone (US30A) at 35.61 $\pm$ 1.05 mg/g of dry bran compared to TA, while ultrasound-assisted extractions using ethanol (US30E) showed no significant difference in yield compared to TE at 55.38 $\pm$ 1.72 mg/g of dry bran. Total ARs represented 2.87 $\pm$ 0.34 mg and 2.94 $\pm$ 0.18 mg of the total yield for US30A and US30E, respectively, with no significant difference in total ARs observed between all samples. Antioxidant activity of extracts were measured at 292.83 $\pm$ 6.00, 1386.45 $\pm$ 76.15, 321.68 $\pm$ 47.06, and 402.49 $\pm$ 15.30 μmol TE/g for TA, TE, US30A, and US30E, respectively. While US significantly ($p<0.05$) decreased antioxidant activity of ethanol extracts (TE compared to US30E) due to the higher lipid

content of ethanol extracts, the was no significant difference observed between TA, US30A, and US30E. This study shows that the application of US for extraction of crude ARs from wheat bran can significantly decrease extraction time from 24 h to 30 min and using ethanol as a solvent yields the same amount of total AR extraction. Conclusively, combining US and ethanol can be used as a green non-toxic extraction method to extract crude ARs.

2.2 Introduction

Alkylresorcinols (ARs) are phenolic lipids found in numerous plant, fungal and bacterial species. Due to their strong antimicrobial activities, it is believed that these compounds serve primarily as a defense mechanism (Baerson et al., 2010). ARs are well studied odd chain phenolic lipids capable of incorporating into the cell wall and providing bioactivity. They have also been shown to have applications in the pharmaceutical and food industry due to their amphiphilic nature and self-assembling properties. Wheat bran, a by-product of wheat milling, is a rich source of ARs. The traditional extraction of crude ARs is time-consuming (24 hr) and used harsh solvents (acetone, ethyl acetate, methanol, chloroform). Meanwhile, ultrasound technology is increasingly being used to assist in the extraction of natural plant chemicals due to its generation of shear force through acoustic cavitation which is capable of destroying the cell wall and releasing solutes into the solvents. This study aimed to investigate the use of high power (90W) low frequency (20 kHz) ultrasound for 30 min to assist in the extraction of crude ARs from wheat bran using acetone and food-grade ethanol as the solvent. The effect of US on extraction yields of crude ARs was investigated by characterizing and quantifying AR homologues using RP-HPLC-PDA and antioxidant activity using the oxygen radical absorbance capacity (ORAC) assay.

2.3 Materials and Methods

2.3.1 Materials

Wheat bran was kindly provided by Agriculture Canada. Acetone and HPLC grade methanol are from Chemicals VWR International (Ontario, Canada). Ethanol (100%) is from Caledon Laboratories LTD (Ontario, Canada). Acetic acid is from Aldrich Chemical Company INC. AR standards (C15:0, C17:0, C19:0, C21:0, C23:0, and C25:0) with 95% purity is from Sigma-Aldrich.

2.3.2 Traditional solvent-based extraction of ARs from wheat bran

Crude ARs were extracted from wheat bran using two traditional solvents, acetone, and ethanol, to compare yields. Wheat bran was added to the respective solvents at a 1:40 w/v ratio and stirred at room temperature for 24 hours. The samples were then filtered using Whatman double filter paper (number 9). The residue was discarded while the filtrate was evaporated under a vacuum using a Rotavapor (Buchi-Brinkman, R100 Switzerland). The remaining extract was redissolved with a minimal amount of solvent to transfer from the rotovapor flask to a smaller storage container. The solvent was then evaporated using nitrogen gas. The dried extract was then weighed and stored at -20 for further analysis. All extractions were conducted in triplicates.

2.3.3 Ultrasound-assisted extraction of ARs from wheat bran

Crude ARs were extracted from wheat bran using US with acetone and ethanol to compare yields. Wheat bran was added to the respective solvents at a 1:40 w/v ratio. The samples were placed in an ice bath with the ultrasound transducer submerged into the solvent. Direct low frequency (20

kHz) high power (90 W) ultrasound, using a UIP500hd ultrasonic processer (Hielscher, Germany) was applied for 30 minutes with constant stirring. During the 30 min US treatment, 1ml of solvent was collected at every 5 min interval (0,5,10,15,20, 25, 30 min) to determine the time course of AR extraction into the solvent. After 30 minutes, the samples were filtered using Whatman double filter paper (number 9). The residue was discarded while the filtrate was evaporated under a vacuum using a Rotavapor (Buchi-Brinkman, R100 Switzerland). The remaining extract was redissolved with a minimal amount of solvent to transfer from the rotovapor flask to a smaller storage container. The solvent was then evaporated using nitrogen gas. The dried extract was then weighed and stored at -20 for further analysis. All extractions were conducted in triplicates.

2.3.4 Reversed-phase high-performance liquid chromatography

The concentration of ARs in extracts was determined by RP-HPLC-PDA using an Alliance® HPLC system e2695 Separation Module coupled with a 2998 Photodiode Array Detector from Waters (Milford, Massachusetts) and a C18 column (4.6 x 150mm, inner diameter 5μm). Solvent A consisted of 4% acetic acid in ddH_2O, and solvent B consisted of 1% acetic acid in methanol. A gradient program was used as follows:

Table 2.1 Gradient program for RP-HPLC-PDA analysis of ARs

	Time (min)	Flow (ml/min)	Solvent (%)	
			A	B
1	0 -10	1.00	10.0	90.0
2	10-35	1.00	00.0	100.0
3	35-45	1.00	10.0	90.0

Compounds were detected using a UV detector that measured absorbance at 280 nm wavelength. The area under the curve for detected peaks was used to measure concentration using a standard curve. Retention times were determined, and a standard curve was generated using a AR standard

mixture that contained homologues C15:0, C17:0, C19:0, C21:0, C23:0 and C25:0 dissolved in methanol at concentrations of 0.05, 0.0625, 0.20, 0.25, 0.30 and 0.35 g/mL. Extracts were also dissolved in methanol at 50mg/ml concentration and filtered through a polytetrafluorethylene (PTFE) syringe tip filter (0.45µm, 13mm; Acrodisc^{TM}, Ann Arbor, MI).

2.3.5 Oxygen radical absorbance capacity assay (ORAC)

The method for investigating antioxidant capacity using ORAC is adapted from (Huang et al., 2002). The antioxidant standard was Trolox, peroxyl radical generator was AAPH, positive control was rutein, and the probe was fluorescein. Briefly, standards, samples and rutin were loaded into a 96-well fluorometric microplate and then fluorescein was added to each well. After incubation at 37 ^{o}C for 20 min, APPH was added. Absorbance was read using FLx800TM Multi-Detection Microplate Reader with Gen5TM software over 60 min (excitation wavelength = 485 nm; emission wavelength= 525 nm). Final ORAC values were calculated using a Trolox standard curve and net AUC of each sample. Values are expressed as µmol Trolox equivalent per g of sample.

2.3.6 Statistical Analysis

All experiments were performed in triplicates (n=3). One-way ANOVA was performed using SAS software with a significant difference of $p<0.05$ to determine the statistical significance of the results.

2.4 Results and Discussion

2.4.1 Traditional solvent-based extraction of ARs from wheat bran

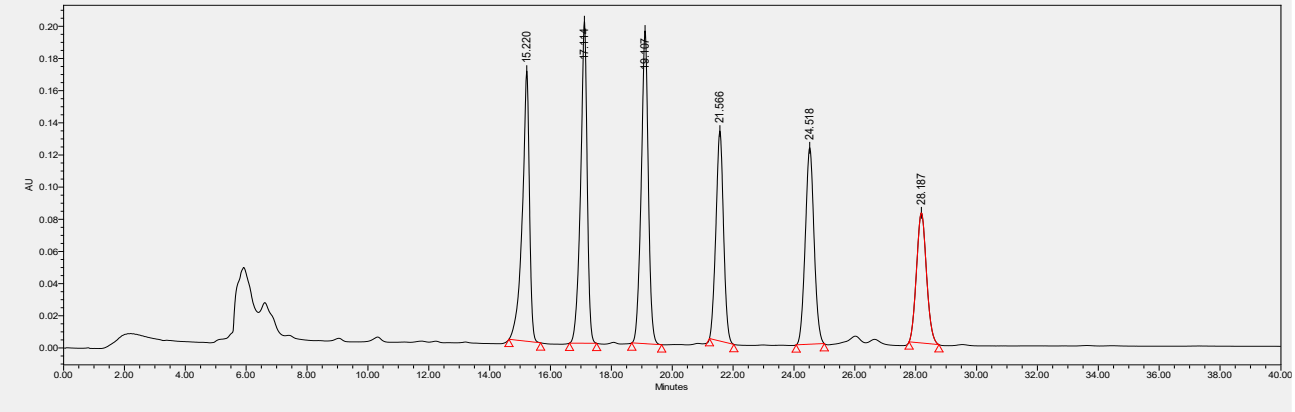

Figure 2.1 RP-HPLC-PDA Chromatogram of AR standard mixture. Homologue peaks in increasing order of chain length (C15:0, C17:0, C19:0, C21:0, C23:0, C25:0) are in increasing order of retention times.

Table 2.2 Retentions times of each homologue in the AR standard mixture used in RP-HPLC-PDA.

AR Monologue	Retention Time (min)
C15	15.22
C17	17.11
C19	19.11
C21	21.57
C23	24.52
C25	28.19

Crude ARs were extracted from wheat bran using two different solvents (acetone and ethanol) to compare yields of different homologues. A standard mixture of AR homologues was used to identify retention times for each and generate a standard curve, see Figure 2.1. As shown in Table 2.2, retention times for C15:0, C17:0, C19:0, C21:0, C23:0, and C25:0 are 15.22, 17.11, 19,11, 21.57, 24.52, and 28.19 min, respectively.

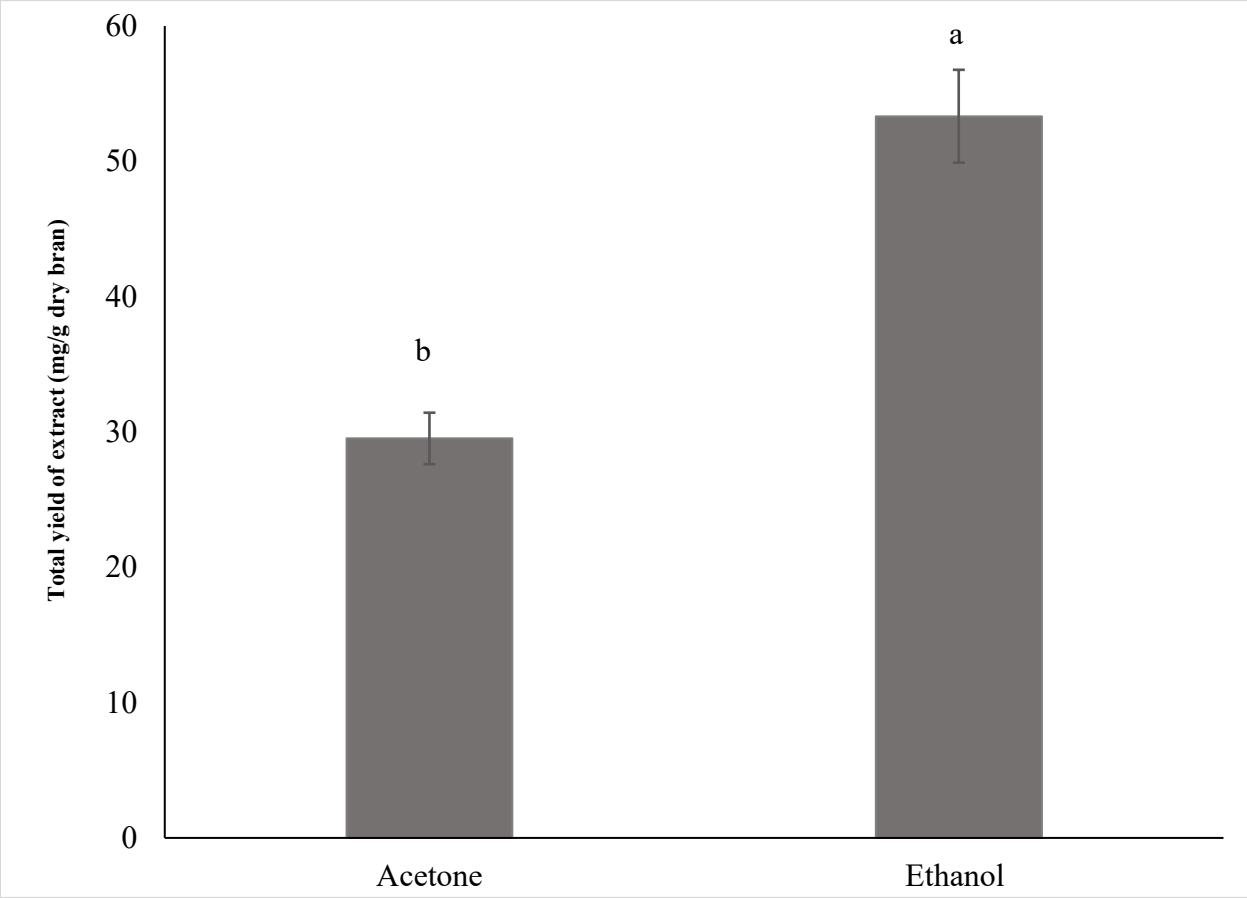

Figure 2.2 Extract yield (mg/g dry bran) of wheat bran extract using traditional extraction with acetone or ethanol as the solvent. Different letters represent significant difference and results are expressed as mean of triplicates ± SEM.

The total yield (mg/g dry bran) of crude AR extract obtained from wheat bran using acetone and ethanol are shown in Figure 2.2. Using acetone as the solvent yields an average of 29.52 ± 1.91 mg/g of dry bran which was significantly ($p < 0.05$) lower than the yield obtained using ethanol as the solvent with an average of 53.33 ± 1.72 mg/g of dry bran. This is because the more polar ethanol is less selective compared to acetone and extracts with more impurities (e.g. the presence of flavonoids, phytic acid, and phenolic acids).

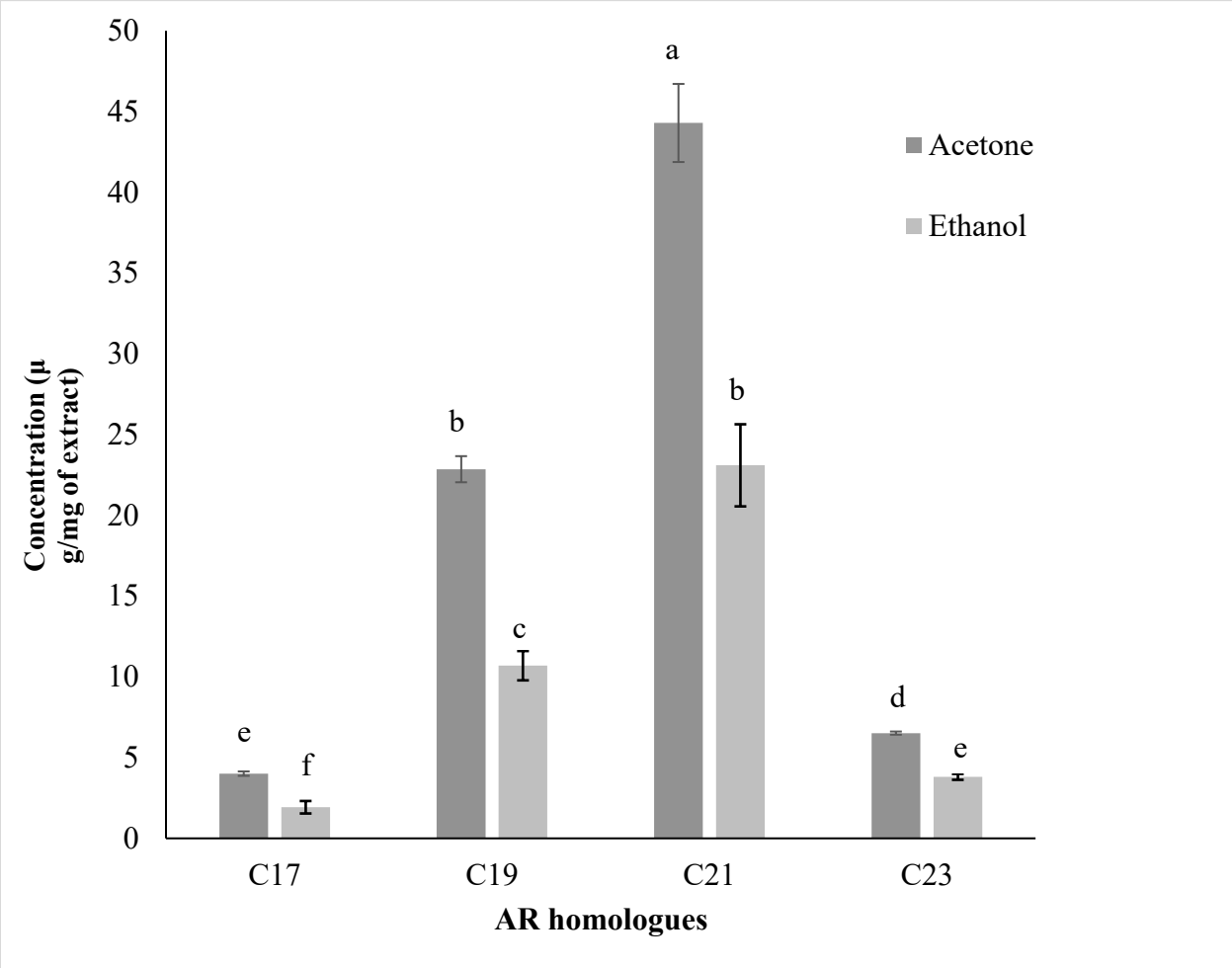

Figure 2.3 Concentration of AR homologues in wheat bran extract using acetone or ethanol traditional extraction Different letters represent significant difference and results are expressed as mean of triplicates ± SEM.

After analyzing the crude extracts with RP-HPLC-PDA, the homologues identified in both extracts were C17:0, C19:0, C21:0, C23:0, see Figure 2.3. The concentration of each homologue in acetone extracts was 4.01 ± 0.14, 22.86 ± 0.81, 44.29 ± 2.42, and 6.52 ± 0.10 µg/mg of extract for C17:0, C19:0, C21:0, and C23:0, respectively. Ethanol extracts had significantly ($p<0.05$) lower concentrations of each homologue compared to acetone extracts with an average of 1.92 ± 0.39,

10.69 ± 0.91, 23.10 ± 2.54, and 3.81 ± 0.18 μg/mg of extract for C17:0, C19:0, C21:0, and C23:0, respectively.

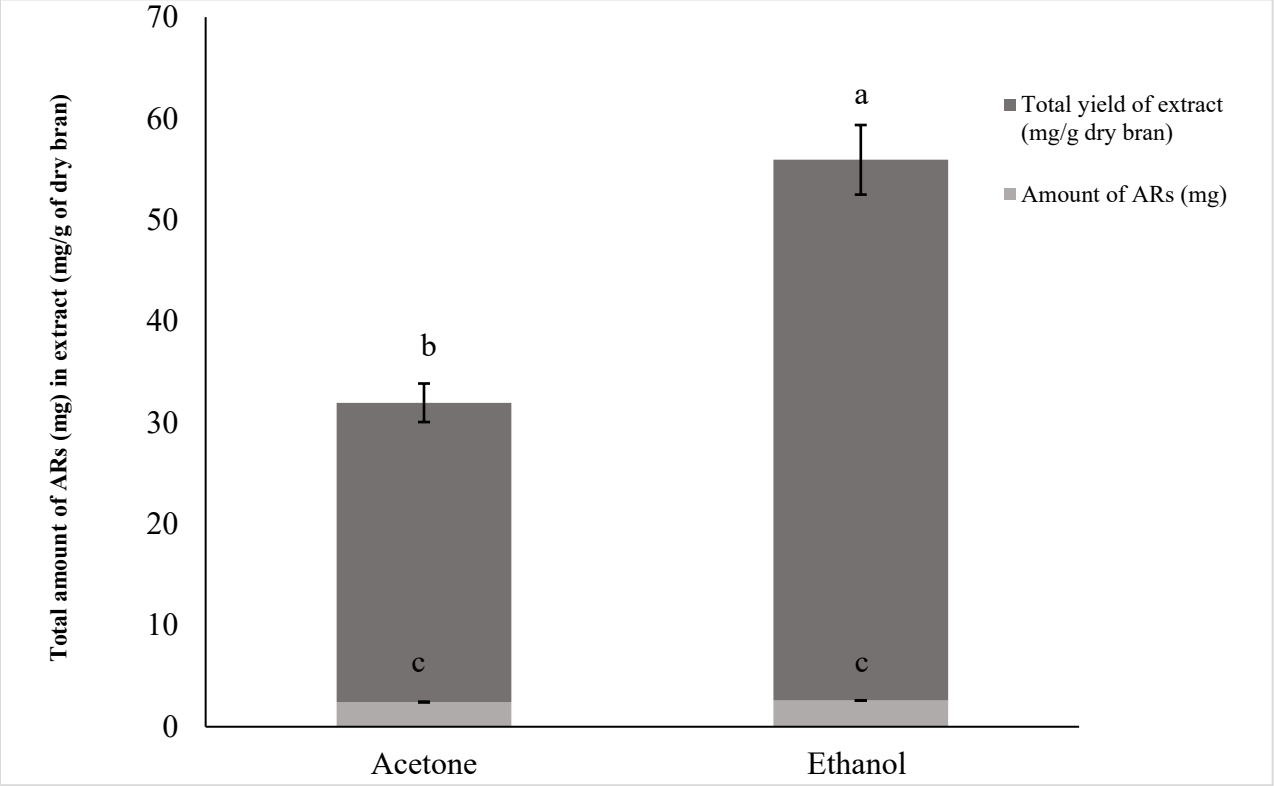

Figure 2.4. Amount of ARs (mg) present in wheat bran extracts (mg/g of dry bran) using acetone or ethanol as solvent. Different letters represent significant difference and results are expressed as mean of triplicates ± SEM.

While the concentration of ARs in the crude extract is significantly lower when using ethanol, the total amount of ARs extracted compared to acetone is not. Figure 2.4 shows the total amount of ARs (mg) measured in the total yield of the extract (mg/g of dry bran). For acetone, of the 29.52 mg of extract/g of dry bran, the total amount of ARs represents 2.29 ± 0.10 mg (~7.75%). For ethanol, the total amount of ARs represents 2.04 ± 0.27 mg (~3.83%) of the 53.33 mg of extract/g of dry bran. There is no significant difference between the total amounts of ARs found in each

crude extract. The concentration of total ARs, however, is significantly lower in ethanol crude extracts because ethanol results in a higher total yield of extract. This is because ethanol extracts more oil compared to acetone.

2.4.2 Ultrasound-assisted extraction of ARs

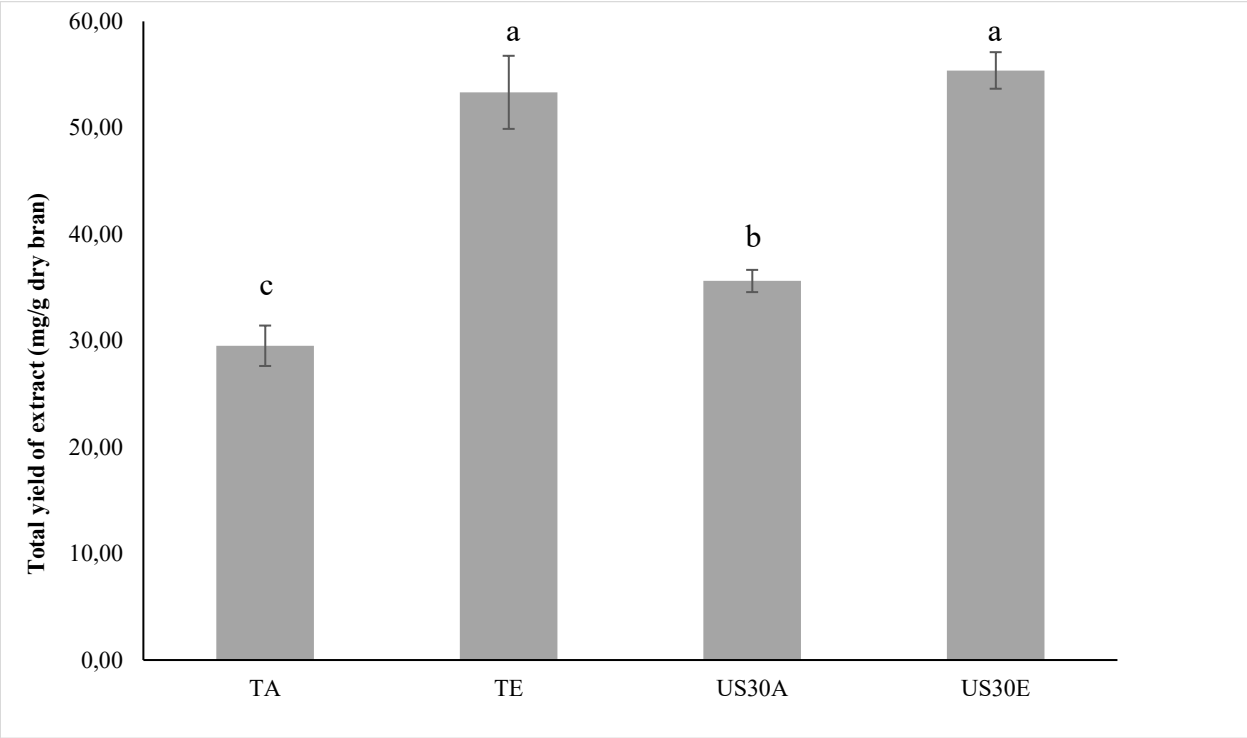

Figure 2.5. Extract yield (mg/g dry bran) of wheat bran extract using traditional and US-assisted extraction with acetone or ethanol as the solvent. Different letters represent significant difference and results are expressed as mean of triplicates ± SEM.

The total extract yield (mg/g of dry bran) for traditionally (24hr) extracted ARs compared to ultrasound-assisted (30 min) extract ARs are shown in Figure 2.5. Using acetone as the solvent, the total yield of extract was slightly significantly ($p<0.05$) higher in ultrasound-assisted (US30A) extracts at 35.61 ± 1.05 mg/g of dry bran compared to traditional extractions (TA) at 29.52 ± 1.91 mg/g of dry bran. This is significant because it means that the application of ultrasound cut down the extraction time from 24 h to 30 min. Using ethanol as the solvent, no significant difference

was seen in the total yield of extract between traditional (TE) and ultrasound-assisted extracts (US30E) at 53.33 ± 3.43 mg/g of dry bran and 55.38 ± 1.72 mg/g of dry bran, respectively. Again, ultrasound cut down the extraction time here from 24h to 30 min with the same yield. As expected, using ethanol in both extractions resulted in significantly ($p<0.05$) higher extraction yields compared to using acetone due to extracting more oil from the wheat bran.

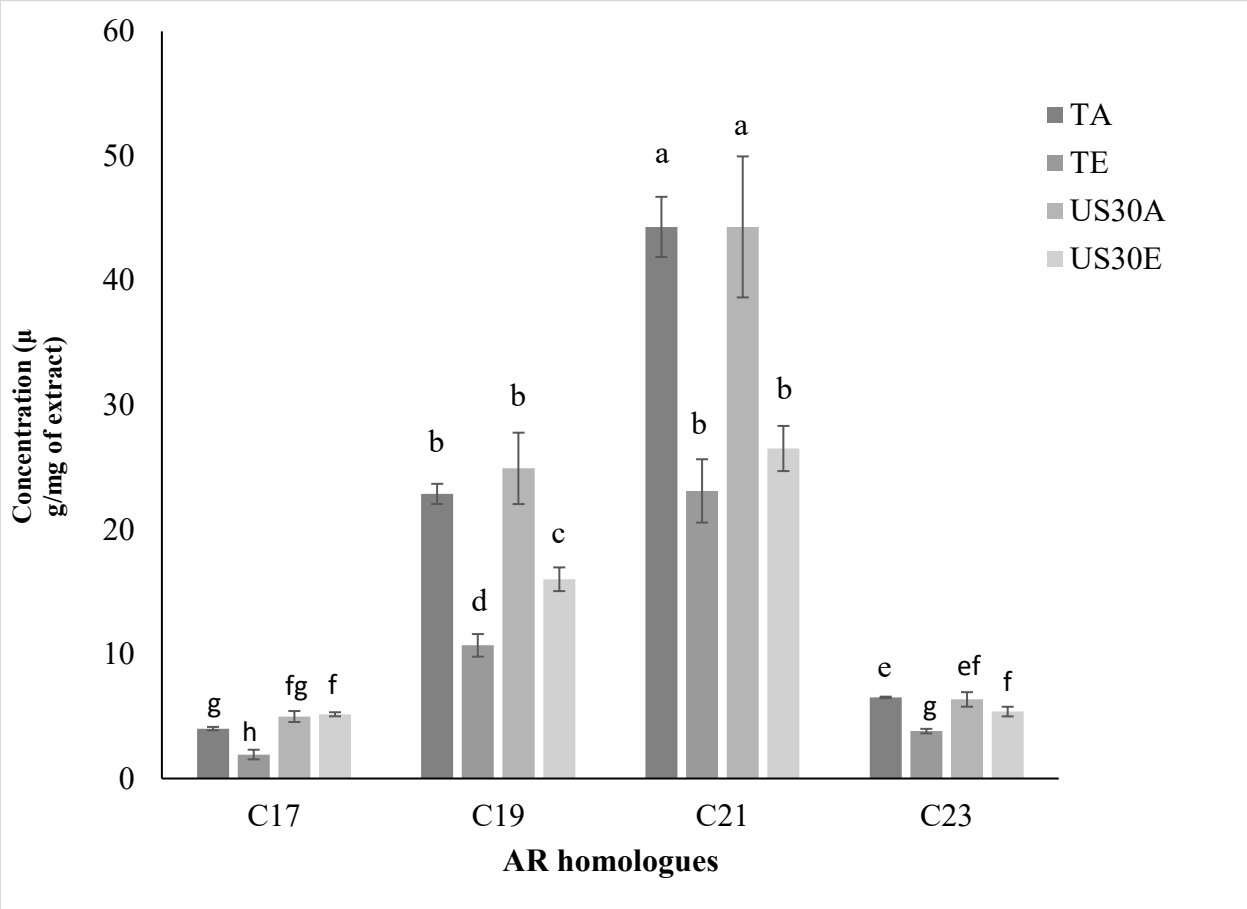

Figure 2.6. Concentration (µg/mg of extract) of AR homologues in wheat bran extract using acetone (TA), ethanol (TE), and ultrasound-assisted using acetone (US30A) and ethanol (US30E). Different letters represent significant difference and results are expressed as mean of triplicates ± SEM.

The concentration of AR homologues in traditional (TA, TE) and ultrasound-assisted (US30A, US30E) extracts are shown in Figure 2.6. For AR homologue C17:0, the concentration is

significantly ($p<0.05$) higher in traditional extracts using acetone (TA) compare to using ethanol (TE), as was seen in Figure 2.3. For ultrasound-assisted extracts, US30A did not have a significantly different concentration of C17:0 (4.98 $\pm$ 0.44 μg/mg of extract) compared to TA (4.01 $\pm$ 0.14 μg/mg of extract). Surprisingly, US30E had a C17:0 concentration of 5.16 $\pm$ 0.16 μg/mg of extract which was significantly ($p<0.05$) higher than both TA (4.01 $\pm$ 0.14 μg/mg of extract) and TE (1.92 $\pm$ 0.39 g/mg of extract) while not statistically different than US30A. This means that ultrasound-assisted extraction with ethanol (US30E) seems to have extracted the same amount of C17:0 as ultrasound-assisted extraction with acetone (US30A) and twice the amount of traditional extractions with ethanol (TE). A similar trend is seen for all homologues where slightly higher concentrations are seen for US30E compared to TE while US30A and TA have no significant difference in homologue concentration pointing to the implication of a synergistic effect between ultrasound and solvent used. For C19:0, the concentration in the extracts is significantly ($p<0.05$) higher in TA (22.85 μg/mg of extract) compared to TE (10.69 $\pm$ 0.91 μg/mg of extract). No significant difference is seen in C19:0 concentration for US30A (24.91 $\pm$ 2.87 μg/mg of extract) compared to TA (22.85 μg/mg of extract) but it is significantly ($p<0.05$) higher than TE (10.69 $\pm$ 0.91 μg/mg of extract) and US30E (16.00 $\pm$ 0.95 μg/mg of extract). Meanwhile, US30E is significantly ($p<0.05$) higher than TE with about a 50% increase in C19:0 concentration seen in US30E compared to TE. For C21:0, which represents the highest concentration of AR homologues for all samples, is found in higher amounts in acetone extracts at 44.29 $\pm$ 2.42 μg/mg of extract in TA and at 44.30 $\pm$ 5.66 μg/mg of extract in US30A with no significant difference between the two. Both are significantly ($p<0.05$) higher than extracts using ethanol (TE, US30E). Meanwhile, extracts using ethanol showed no significant difference in C21:0 concentration between TE (23.10 $\pm$ 2.54 μg/mg of extract) and US30E (26.50 $\pm$ 1.81 μg/mg of extract). This is the only homologue

where no difference in concentration is seen between these two extracts. For C23:0, no significant difference is seen between TA (6.52 $\pm$ 0.06 μg/mg of extract) and US30A (6.35 $\pm$ 0.58 μg/mg of extract). C23:0 concentration is significantly ($p<0.05$) higher in TA compared to TE (3.81 $\pm$ 0.18 μg/mg of extract) and US30E (5.38 $\pm$ 0.39 μg/mg of extract). However, no significant difference is observed in C23:0 concentration between US30A and US30E while the latter is significantly ($p<0.05$) higher than TE with about a 40% increase in concentration observed in US30E compared to TE. Again, when comparing ultrasound-assisted extractions compared to traditional, no significant difference in homologue concentration is seen when using acetone while a slight significant increase in homologues C17:0, C19:0, and C23:0 can be seen when using ethanol in ultrasound-assisted extractions. This confirms that not only does the application of ultrasound result in the same amount of extract yield compared to traditional extractions, as was seen in Figure 2.5, but also in the same concentration of AR homologues when using acetone but also a slight increase in the concentration of certain homologues when using ethanol.

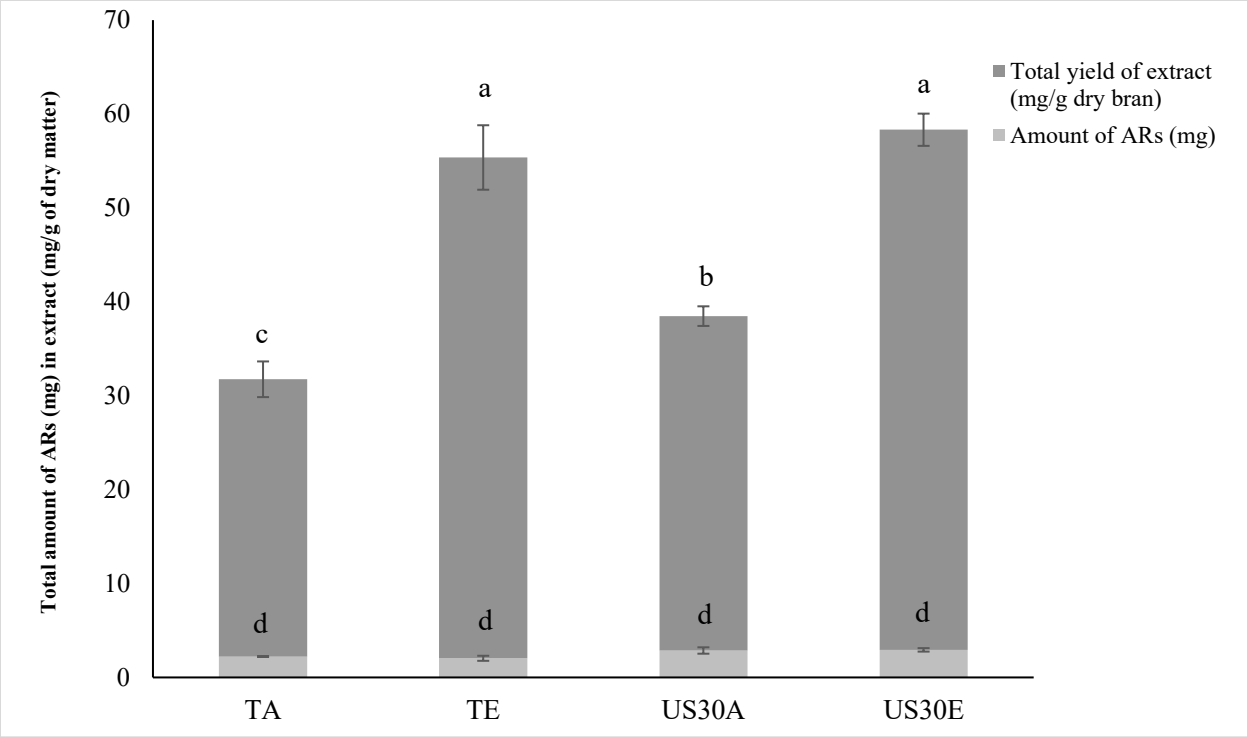

Figure 2.7 Amount of ARs (mg) present in wheat bran extracts (mg/g of dry bran) using acetone (TA), with ethanol (TE), and ultrasound-assisted with acetone (US30A) and with ethanol (US30E). Different letters represent significant difference and results are expressed as mean of triplicates ± SEM.

Figure 2.7 shows the total amount of ARs (mg) measured in the total yield of the extract (mg/g of dry bran) of ultrasound-assisted extracts (US30A, US30E) compared to traditional extracts (TA, TE). As was confirmed in Figure 2.4, no significant difference in total ARs is seen between different solvents used in traditional extracts (TA compared to TE). Also, when comparing traditional to ultrasound-assisted extracts no significant difference in total ARs is seen between the samples. For US30A, of the 35.61 ± 1.05 mg of extract/g of dry matter, the total amount of ARs represents 2.87 ± 0.34 mg with no significant difference compared to TA (2.29 ± 0.10 mg), US30E (2.94 ± 0.18 mg) and TE (2.04 ± 0.27 mg). Figure 2.7 shows that applying ultrasound to extractions results in a slightly higher amount of total yield of extract when comparing TA and US30A and

the same amount of extract yield when comparing TE and US30E while extracting the same amount of total ARs in all extracts with ethanol samples (TE and US30E) having lower concentrations of ARs due to the higher amount of yield (due to ethanol extracting more oil). This is significant in the case of extracting ARs from WB which traditionally takes 24 h but these results show that when low frequency (20 kHz) high power (90W) ultrasound is applied, extraction time can cut down that time to 30 min.

2.4.3 Oxygen radical absorbance capacity (ORAC)

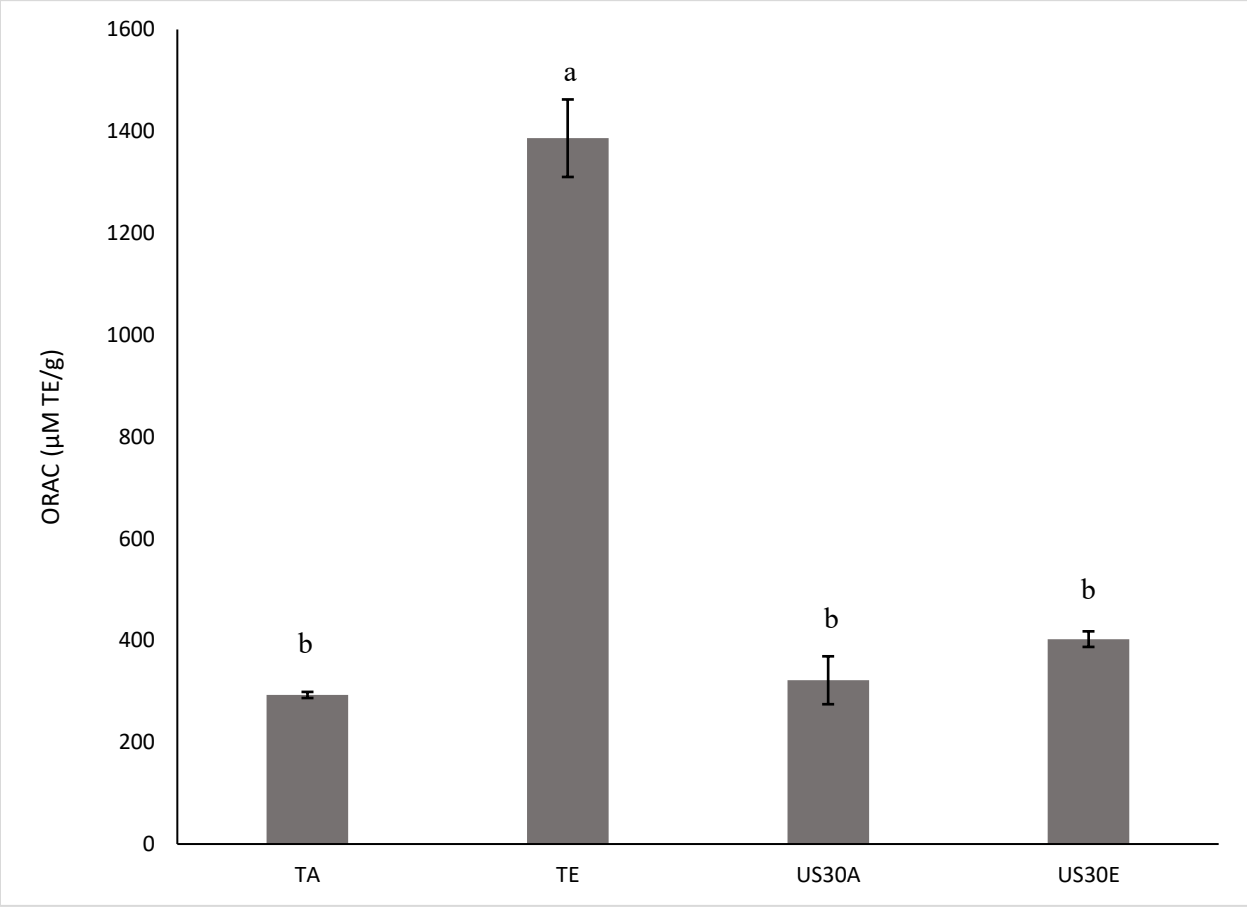

Figure 2.8. ORAC antioxidant activity of traditional wheat bran extract with acetone (TA), with ethanol (TE), and ultrasound-assisted with acetone (US30A) and with ethanol (US30E) expressed

in μmol TE/g. Different letters represent significant difference and results are expressed as mean of triplicates ± SEM.

Because ultrasound is capable of generating free radicals and causing oxidation, antioxidant activity was measured to see if a difference would be observed between traditional extracts compared to ultrasound-assisted extracts. Figure 2.8 shows the ORAC antioxidant activity of the different extracts expressed in μmol TE/g. The highest antioxidant activity was observed in traditional extracts using ethanol (TE) which was significantly ($p<0.05$) higher than all the other samples at 1386.45 ± 76.15 μmol TE/g. Compared to traditional extracts with acetone (TA) at 292.83 ± 6.00 μmol TE/g, this represents a ~ 373% increase in antioxidant activity when using ethanol compared to acetone in the traditional method. Ethanol, being more polar and less selective, extracts more water-soluble antioxidants that are present in the wheat bran which would explain this significant increase in antioxidant activity. But when ultrasound is applied with ethanol for extraction a significant ($p<0.05$) decrease is observed in US30E at 402.49 ± 15.30 μmol TE/g, representing a ~70% decrease in antioxidant activity. This is where ultrasound results in a decrease in antioxidant activity likely caused by oxidation of impurities within the ethanol extract and of polyunsaturated lipids from wheat bran. When comparing US30A to TA, extracts using acetone, no significant difference is seen when ultrasound is applied (321.68 ± 47.06 μmol TE/g) compared to the traditional extract (292.83 ± 6.00 μmol TE/g). When comparing US30E to these two samples (US30A and TA) no significant difference in antioxidant activity is observed despite being significantly lower than TE. So, while ethanol may extract more antioxidants when used in traditional extractions (TE) leading to a higher antioxidant activity than when using acetone (TA), when ultrasound is applied (TE), this antioxidant activity is decreased but still results in the same

antioxidant activity compared to using acetone in traditional extractions (TA) or with ultrasound (US30A).

2.5 Conclusion

Results from this study are the first to report the efficiency and applicability of high power (90 W) and low frequency (20 kHz) ultrasound in decreasing extraction times of crude ARs from wheat bran from 24 h to 30 min with no difference in extraction yield or total AR concentration of extracts. The results provide a more efficient, economical, and environmentally method for extracting crude ARs from wheat bran using food-grade ethanol and green non-thermal ultrasound technology. Crude ARs can then be used as a functional ingredient in food or for other industrial applications (biomaterials, pharmaceuticals).

CHAPTER 3: Production and characterization of emulsion filled gels from liposomal solution using US, inulin, crude ARs as a delivery system for fat reduction in margarine

3.1 Abstract

Emulsion-filled gels (EFG) have applications for ingredient delivery and fat reduction in foods. This study evaluated physicochemical properties of EFGs made with canola and avocado oil, inulin, a gel-forming prebiotic carbohydrate polymer, and wheat bran extract (WBE), containing crude ARs known for their antioxidant and lipid-modifying properties. EFGs were produced from liposomal solutions homogenized with mechanical shearing (Me) and ultrasound homogenization (US-Me). The resulting EFGs were then incorporated into margarine as a delivery system for fat reduction and functional ingredients. EFGs and EFG-incorporated margarine showed differences in microstructure, pH, water activity, hardness, oxidative stability, and thermal behavior. Compared to Me, EFG produced from liposomal solutions using US-Me showed improved physicochemical properties characterized by a more homogenous microstructure observed through polarized light microscopy, increase in hardness, and change in thermal behavior when incorporated into margarine, with no negative impacts on oxidative stability. The study showed that US-Me can be used to make functional EFGs for delivery of functional ingredients, inulin and crude ARs, and fat reduction in food.

3.2 Introduction

As consumers become more health-conscious, demand is increasing for lower-fat foods without minimal effect on organoleptic properties. Several authorities have recommended decreasing intake of saturated fats causing a challenge for food producers who wish to provide healthy alternatives without giving up the desirable texture that saturated fats provide. Emulsion-filled gels combine gelling agents and oils in an effective approach to reach this goal. Polar lipids (lecithin, GMS) and polysaccharides (inulin) can be used as gelling agents in EFGs. Inulin is recognized as a functional ingredient due to its prebiotic status. It is neither hydrolyzed nor absorbed by the small intestine and can be used for targeted delivery to the colon where it is fermented by bacteria. Inulin gels work by trapping a large amount of water in its small crystallite network that resembles that of a network of fat crystals in oil providing similar organoleptic properties. Studies have looked at the application of inulin in EFG for producing low-or zero-fat products in spreads, mayonnaise (Alimi et al., 2013; Glibowksi, 2010; Paglarini et al., 2021). Although the introduction of polyunsaturated fats in emulsions or EFGs can make them more susceptible to oxidation, the delivery of antioxidants can counteract this susceptibility by providing resistance to oxidation. Crude ARs from WBE are natural antioxidants that can provide this resistance while also having antifungal properties and health benefits, making them a functional ingredient.

Ultrasound technology is increasingly employed as a homogenization technology in the production of EFGs with many studies demonstrating it to be an advantageous tool in developing stable functional EFGs (Geng et al., 2021; Hu et al., 2021; Huerta et al., 2020; Paradiso et al., 2015). Most EFGs made using US in the literature apply sonication to the oil phase and water phase in combination which can have deleterious effects on the oil phase through oxidation introduced by

acoustic cavitation. In this study, low frequency (20 kHz) high power (90W) direct ultrasound was applied to first produce liposomal solutions to encapsulate inulin and crude ARs from WBE, which were then emulsified using two different oils (canola and avocado) using mechanical homogenization to make functional EFGs. Effects on microstructure and oxidative stability of EFGs and EFG-incorporated margarine were investigated using polarized light microscopy (PLM), pH, water activity, hardness, oxidative stability, and thermal behaviour.

3.3 Materials and Methods

3.3.1 Materials

Wheat bran extract was obtained by traditional extraction from wheat bran using ethanol as described in the previous section. Soy lecithin (90%) is from Alfa Aesar. Canola oil is Perla brand (Quebec, Canada). Avocado oil is cold-pressed extra-virgin from President's Choice (Canada). Margarine (Crystal brand, Canada) is canola based with 91% canola oil and 9% vegetable oils (modified palm oil, palm kernel oil, dextrose, vegetable monoglycerides, soy lecithin, potassium sorbate, natural flavor, annatto, turmeric, vitamin A palmitate, vitamin D2). Glycerol monostearate (GMS) is from Axenic. Inulin from Jerusalem Artichoke is from Nutra Food Ingredients (Canada).

3.3.2 EFG production

Five formulations of EFG were selected after preliminary trials based on the evaluation of consistency and visual homogeneity (data not shown). Two different kinds of oil, canola oil (CO) and avocado oil (AO) were used to compare the use of two oils with different compositions of unsaturated and saturated fatty acids, see Table 3.2. Glycerol monostearate (GMS) and lecithin (L) were used as emulsifiers in all formulations. Inulin (I) was added to some EFG replacing some

of the oil. And then finally wheat bran extract (WBE), extracted using ethanol, was added to EFGs containing AO to replace oil. Formulations are shown in Table 3.1.

Table 3.1 Composition (%) of EFG with canola oil and avocado oil.

Sample	Homogenization technology	Water	Canola oil	Avocado oil	GMS	Lec	I	WBE
B	Me	47	47	N/A	5	1	N/A	N/A
B-US	US-Me	47	47	N/A	5	1	N/A	N/A
I10	Me	47	37	N/A	5	1	10	N/A
I10-US	US-Me	47	37	N/A	5	1	10	N/A
I20	Me	47	27	N/A	5	1	20	N/A
I20-US	US-Me	47	27	N/A	5	1	20	N/A
B-AO	Me	47	N/A	47	5	1	N/A	N/A
B-AO-US	US-Me	47	N/A	47	5	1	N/A	N/A
AO-WBE-I20	Me	47	N/A	17	5	1	20	10
AO-WBE-I20-US	US	47	N/A	17	5	1	20	10

N/A: Not applicable. Values are mean $\pm$ standard deviations.

The EFGs were prepared in 100g batches. First, a food-grade liposomal solution was prepared according to a method adapted from (Guner & Oztop, 2017). Briefly, GMS (5% w/w) and lecithin (1% w/w) were added to water and homogenized using the two different techniques described below. Inulin and WBE extract were also added to the water phase for samples containing these ingredients. After homogenization, the oil phase was added and emulsified by mechanical homogenization for 2 minutes, as described below:

-Me: mechanical homogenization with Tissuemiser (Fischer Scientific, United States) at 33, 000 RPM was used to mix water phase containing emulsifiers for 2 min. After, oil is mixed in with a mechanical homogenizer for another 2 min. Finally, EFG is cooled and stored at 4^{o}C. Mechanical

homogenization of EFGs was done in a water bath at 65ºC to control for the temperature reached (65ºC) in the US-EFGs due to the heat that is produced by sonication.

-US-Me: direct low frequency (20 000kHz) high power (90 W) ultrasound (UI500D, Hielscher, Germany) applied for 2 min by submerging transducer into water phase containing emulsifiers. After US, oil is mixed in with a mechanical homogenizer for 2 minutes. Finally, EFG is cooled and stored at 4ºC.

Table 3.2 Composition (%) of the common fatty acids in Canola oil, avocado oil, and margarine.

	Canola Oil	**Avocado Oil**	**Margarine**
Variety and/or Country of Origin	Canada	New Zealand	Crystal
Capric C10:0	N/A	N/A	1.00
Lauric C12:0	N/A	N/A	4.00
Myristic C14:0	N/A	N/A	2.00
Palmitic 16:0	4.75 ± 0.11	20.61 ± 0.16	15.00
Stearic C18:0	1.43 ± 0.01	0.30 ± 0.01	6.00
Palmitoleic C16:1 Ω7	0.26 ± 0.06	10.31 ± 0.03	0.50
Oleic C18:1 Ω9	57.56 ± 0.13	50.97 ± 0.30	35.00
Linoleic C18:2 Ω6	22.67 ± 0.09	16.10 ± 0.11	20.00
α linolenic C18:3 Ω3 (cis 9,12,15)	11.47 ± 0.02	1.72 ± 0.02	14.50
Arachidic C20:0	0.53 ± 0.09	N/A	N/A
Eicosenoic C20:1 Ω9	1.12 ± 0.16	N/A	N/A
Mono-unsaturated fatty acids	58.94 ± 0.35	61.28 ± 0.33	35.50
Poly-unsaturated fatty acids	34.14 ± 0.11	17.82 ± 0.13	34.50
Saturated fatty acids	7.83 ± 0.21	20.91 ± 0.17	24.00
Reference	(Mungure & Birch, 2014)	(Flores et al., 2019)	(Galindo-Cuspinera et al., 2017)

N/A: Not applicable. Values are mean ± standard deviations.

3.3.3 Incorporation of EFG in margarine

Based on results obtained in this study, the best EFGs were selected for incorporation into margarine. All samples mixed using US-Me were selected due to their improved texture compared to Me alone. Namely, B-US, I20-US, B-AO-US, and AO-WBE-I20-US were selected. The final samples, MB-US, MB-AO-US, MI20-US, and MAO-WBE-I20-US are composed of 20% EFG and 80% margarine (Crystal brand).

3.3.4 Microscopy

Microscope images were taken using an Axioplan 2 imaging microscope (ZEISS, Germany) with a Retiga 1200 camera (Quantitative Imaging Corporation, Canada) using Northern Eclipse software. The samples were observed under polarized light and images were captured after mixing of ingredients (with Me or US-Me) before the addition of oil, after addition of oil, and after 24 h stored at 4^{o}C.

3.3.5 pH

The pH of each sample was measured using an Orion Star benchtop pH meter (Thermo Scientific, United States) after formation.

3.3.6 Water activity (a_w)

Water activity was measured using a water activity meter from Aqualab (Washington, USA). Samples (2g) were loaded on plastic capsules and then place into the meter to measure the partial pressure of water (p). The results are given as values between 0 (no water activity) and 1 (high

water activity) and calculated using the following equation where p= partial pressure of water, and p_o = saturated pure pressure of water at the same temperature.

$$aW = \frac{p}{p0}$$

3.3.7 Texture analysis

Texture analysis of the different EFG formulations was performed using the CT3 Texture Analyzer (Brookfield, United States). Analysis was done on samples 24h at 4ºC, after initial preparation. The single compression cycle was carried out with a trigger of 5 g, a deformation of 2 mm at a 2mm/s speed. The deformation is measured and expressed as hardness (g).

3.3.8 Oxidative Stability

Oxidative stability was determined according to the AOAC official method Cd12b-92 (AOCS, 2017) of all EFG formulation after 24h at 4ºC using Rancimat (Metrohm, Switzerland). For this, 6g of sample was used and Rancimat was set at 120ºC with airflow at 20L/h.

3.3.9 Differential scanning calorimetry (DSC)

Thermal behaviour curves were obtained for EFG-incorporated margarine using a differential scanning calorimeter (DSC Q20 series, TA Instruments, United States) and based on a method by Teles dos Santos et al (2016). Samples were loaded onto tzero alodined pans at a weight of 10mg. The sample pan and an empty reference pan were placed into the DSC. Heating and cooling cycles were done at a rate of 5ºC/min. Samples were initially cooled down from 20ºC to -20ºC and held at this temperature for 5 min before heating up to 90ºC. Samples were held at 90ºC for 5min and cooled back down to -20ºC. The thermal behavior curves obtained show the heat flow (W/g) as a

function of temperature with each peak representing a certain thermal event, as shown in the following figure:

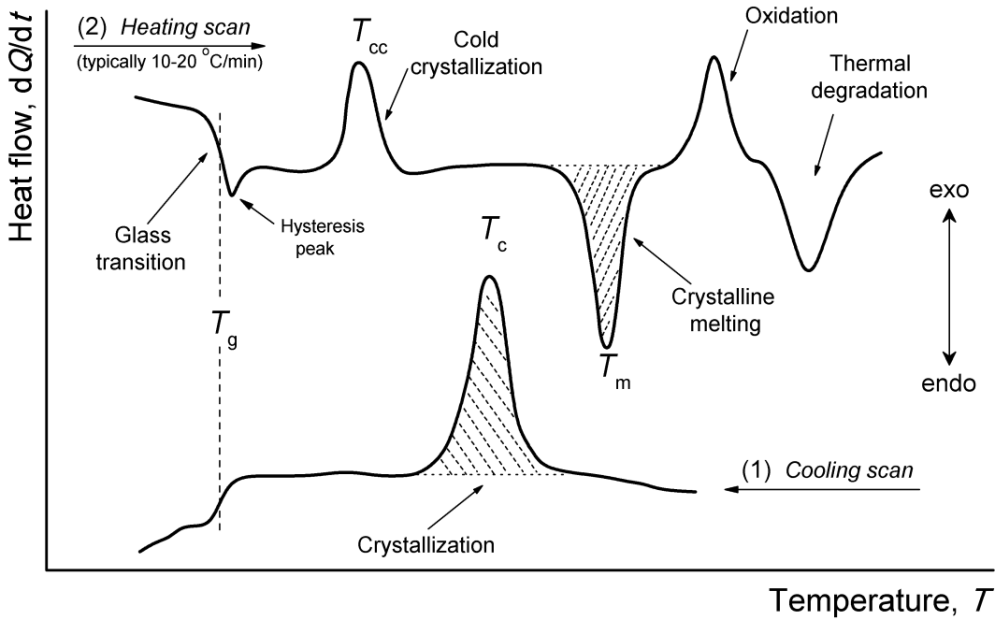

Figure 3.1. Different peaks obtained in a thermal behaviour curve from differential scanning calorimetry (Kalogeras, 2016).

3.4.10 Statistical Analysis

All experiments were performed in triplicates (n=3) except for DSC (due to time constraints and machine access). One-way ANOVA was performed using SAS software with a significant difference of $p<0.05$ to determine the statistical significance of the results.

3.4 Results and Discussion

3.4.1 EFGs with and without Ultrasound

Table 3.3 Picture of EFG with and without US

Sample	Me	US-Me
B		
I10	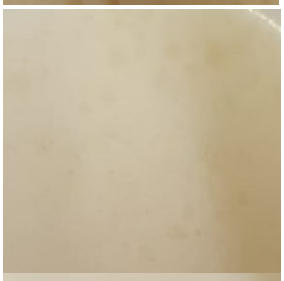	
I20	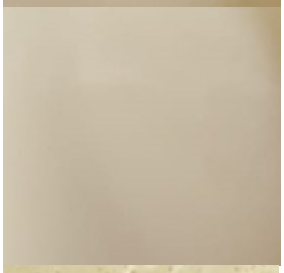	
B-AO		
AO-WBE-I20	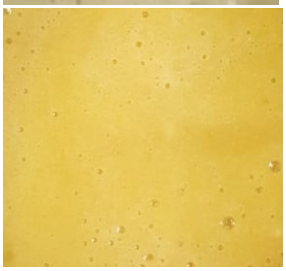	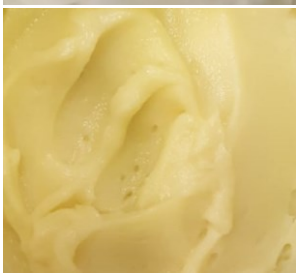

All pictures in Table 3.3 were taken after being store at 4ºC for 24 h after production. There is a marked difference between samples with and without ultrasound. Samples without ultrasound (first column) were non-homogenous and liquid in texture compared to sonicated samples (second column) which were much thicker and homogenous. Inulin seemed to improve the texture of samples without ultrasound when comparing the control (B) to I10 and I20. B showed phase separation with large oil bubbles forming at the surface, while samples with 10% inulin (I10) showed less phase separation with smaller oil bubbles forming at the surface, and finally, samples with 20% inulin (I20) showed no phase separation. Inulin has been shown to have applications in emulsions as a gelling agent capable of stabilizing oil droplets within its gel network (Paglarini et al., 2021). Also observed, was a difference in colour in samples prepared with canola oil (B, I10, I20) and avocado oil (B-AO, AO-WBE-I20). Canola oil-based samples were whiter while avocado oil samples were more yellow. For B-AO, this can be attributed to the presence of carotenoid pigments in cold-pressed avocado oil (Ashton et al., 2006). Samples with wheat bran (AO-WBE-I20) extract were even more yellow compared to the avocado oil control (B-AO). WBE extracted traditionally with ethanol is naturally yellow owing to the simultaneous extraction of carotenoids (Fu et al., 2017). WBE samples without inulin (not shown) showed obvious phase separation in the optimization process and were therefore not chosen for analysis. Therefore, the homogeneity shown in the pictures for AO-WBE-I20 is attributed to the presence of 20% inulin. It was believed that WBE would stabilize the solution due to its high content of ARs but likely the presence of polyunsaturated fatty acids in the ethanol extracted WBE, as well as other compounds present in the crude extract, may be responsible for phase separation and oil migration that was observed. It

is believed that the WBE failed to delay, maybe even induced, the transformation of small beta prime crystals to larger beta crystals which is responsible for oil migration (da Silva et al., 2020).

3.4.2 Polarized-light microscopy of EFGs

Table 3.4 PLM images (500x) of samples taken at three different stages of production: 1) After mixing of water phase with emulsifiers, 2) After mixing oil with water phase, 3) After 24 h at 4ºC.

Sample	After mixing water phase	After adding oil	After 24 h at 4ºC
B	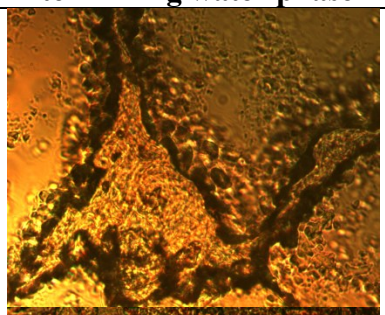	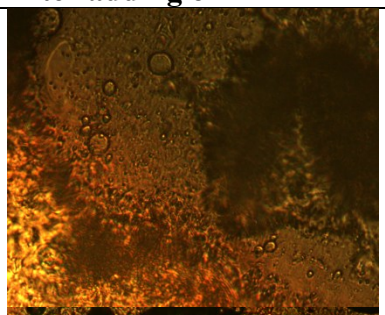	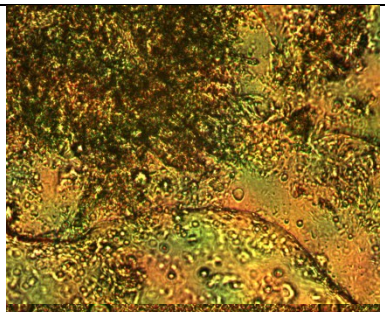
B-US	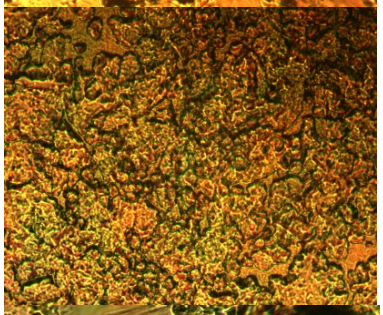	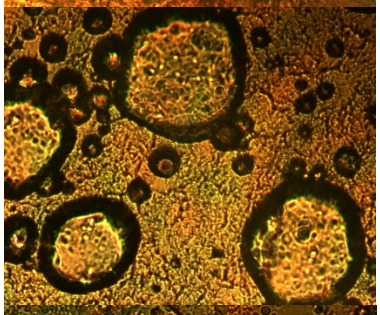	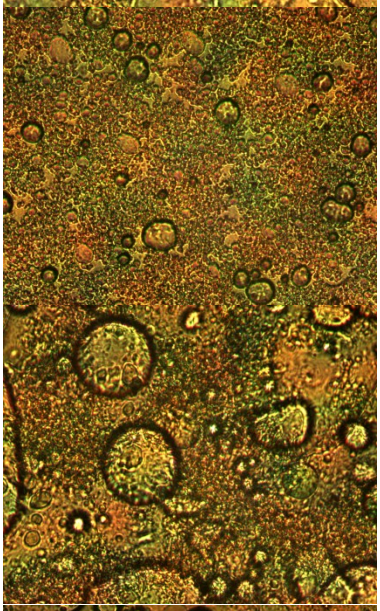
I20	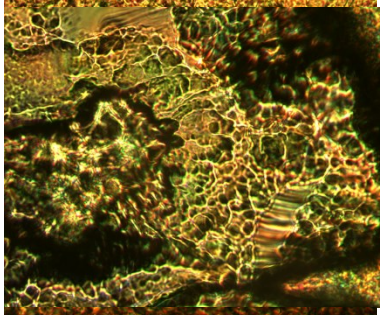	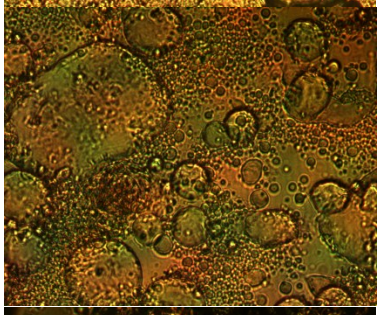	
I20-US	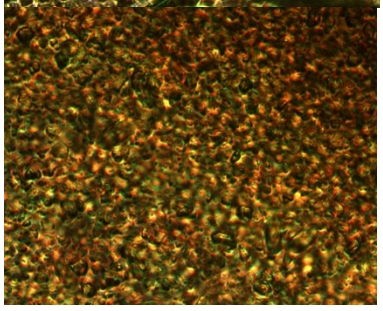	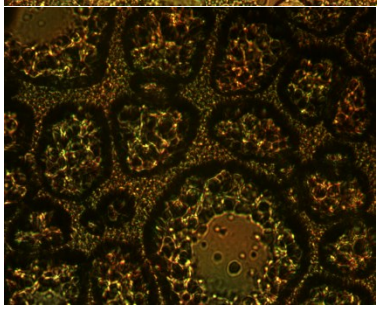	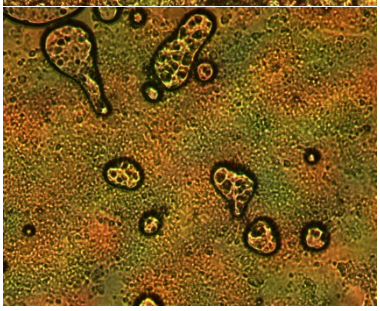

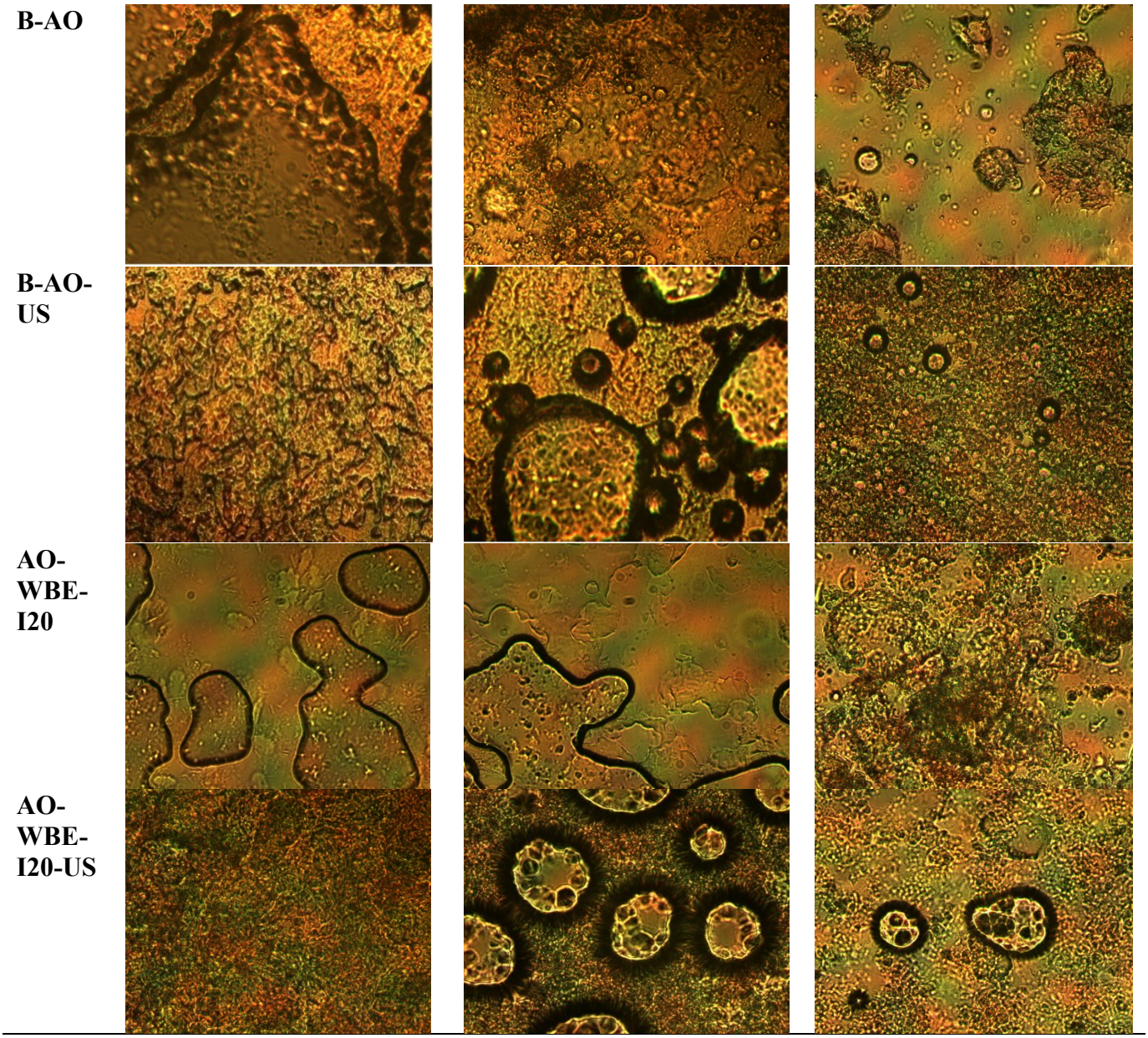

The microstructure of emulsions is an important indicator of rheological properties. Microscopic images presented in Table 3.4 were taken at three different stages of the production process. The first column of images was taken after Me or US-Me mixing of water phase with emulsifiers (lecithin, GMS) with some samples also containing inulin and WBE. Images in the second column

were taken after mixing in the oil phase. And images in the third column were taken after 24 h of storage at 4^{o}C.

In the first step, Me mixing of emulsifiers in the control (B) seems to have created aggregates of the dissolved lecithin and GMS which can be seen in a triangle shape in the center of the image positioned against a more diluted water phase. When 20% inulin (I20) was added in this step, you can see the solution has more dissolve particles but is still heterogeneous compared to the sonicated sample with 20% inulin (I20-US). B-US and I20-US both show a more homogenous network of particles dissolved in the water phase. Again, when comparing both these samples the one with 20% inulin added (I20-US) has a denser network compared to the control (B-US) with only lecithin and GMS. As expected, before adding oil, B is the same as B-AO and B-US is the same as B-AO-US because at this step of the process they are the same sample (water phase with lecithin and GMS. When WBE is added to this step with 20% inulin in AO-WBE-I20, a clear difference is seen compared to I20. As previously stated, the WBE used was extracted with ethanol and contains polyunsaturated oils, as such dissolving it in the water phase created large amorphic bubbles. It seems to also have affected the network seen in I20 resulting in a more dissolved aqueous phase. When US is applied at this step in AO-WBE-I20-US, a more homogenous network of particles is seen with no large visible bubbles compared to AO-WBE-I20. The particles also appear smaller than those observed in I20-US suggesting that WBE and inulin may act in synergy to produce smaller particles when ultrasound is applied.

When looking at the second step, after the addition of oil, B shows oil bubbles dissolved in the aqueous phase and large aggregation of lecithin and GMS that was also seen in the previous step, before adding oil. B-US shows a more homogenous network with big and small oil bubbles

dispersed through the system. The dark rim observed around the bubbles is likely lecithin and gms interacting at the phase interface. The same is seen in B-AO and B-AO-US, with avocado oil, with not much difference seen compared to B and B-US. When 20% inulin is present (I20) a more homogenous network of particles is seen with more bubbles that are smaller in size compared to B showing that inulin alone can be used to stabilize emulsions through its gelling behavior as previously reported (Paglarini et al., 2021). When ultrasound is applied with inulin present (I20-US) an even more homogenous and denser network is seen compared to I20. The image is darker as less light is getting through due to the presence of a dense crystal network. Inulin seems to also be interacting at the interface where a dark rimming effect can be seen around the bubbles that is thicker and more network-like than the one seen in B-US. When looking at the sample with avocado oil, inulin, and WBE (AO-WBE-I20) a more dissolved system is observed with large amorphic phase separation similar to that observed in the previous step, before oil addition, suggesting that the addition of WBE with inulin affects how inulin dissolves within the two phases. When ultrasound is applied however in AO-WBE-I20-US, a more homogenous network within the aqueous phase is seen with equal-sized bubbles dissolved throughout. When comparing it to I20-US, the image is brighter suggesting that the network created is less dense allowing more light to pass through. The rimming effect around the bubbles is wider and fuzzier compared to B-AO-US suggesting that inulin is also interacting at the interface with GMS and lecithin. Also interesting for this sample is the apparent presence of bubbles within the oil bubbles suggesting that a double emulsion stabilized within a gel network was created when combining inulin, WBE, and ultrasound.

In the third step, after cooling at 4 ºC for 24 h, a difference can be observed in the microscopic images between samples that were liquid after cooling and samples that were solid after cooling,

namely the non-sonicated and sonicated samples, respectively. B shows concentrated large aggregations, seen as dark structure in the upper left corner of the picture, and non-homogenous crystals dissolved throughout. B-AO is similar with aggregation and obvious phase separation occurring. AO-WBE-I20 appears even more similar to B, perhaps influenced by the larger amount of polyunsaturated fatty acids present in WBE compared to avocado oil. The only non-sonicated sample that is different in microscopic structure at this step is I20 with 20% inulin. I20 appears more homogenous compared to the other non-sonicated samples with obvious bubbles dispersed through a more homogenous network of particles. This again confirms the ability of inulin by itself to stabilized oil bubbles within an emulsion through its gelling capabilities and water-holding capacity. When looking at the sonicated samples (B-US, I20-US, B-AO-US, AO-WBE-I20-US) an explanation as to why these samples are solid compared to the liquid non-sonicated samples begins to emerge. All show a more homogenous network of particles with bubbles dissolved within the network, an indication that the bubbles are stabilized within a gel network. B-US shows this with small bubbles while I20-US shows a network of smaller particles with larger somewhat amorphic bubbles. The bubbles themselves appear to have crystals dissolved within them when comparing I20-US to B-US as dark sports can be seen within the bubbles in I20-US which are absent in B-US. B-AO-US is similar to B-US with somewhat smaller bubbles and a denser network of particles. This could be due to the presence of more saturated fats in avocado oil that is more easily crystallized. AO-WBE-I20-US shows larger bubbles compared to the other sonicated samples but like I20-US the bubbles appear to have crystals within them, again suggesting that a double emulsion was produced. The particle network appears less dense than B-AO and more similar than that observed in B-US. This is likely because the 10% WBE was added to replace the avocado oil and contains more polyunsaturated fatty acids.

3.4.3 Images and polarized-light microscopy of EFG-incorporated margarine

Table 3.5 Images and polarized light microscopy images of EFG-incorporated margarine

Sample	Images	PLM
M		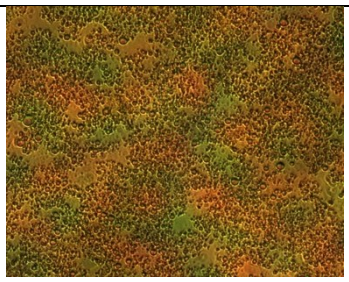
MB-US		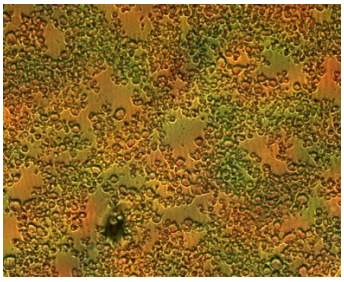
MI20-US		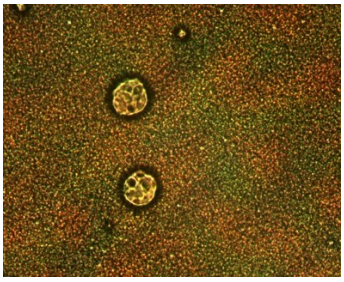
MB-AO-US		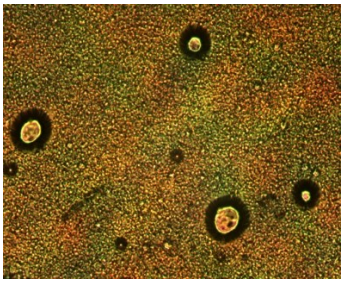
MAO-WBE-I20-US		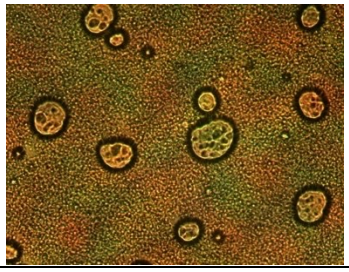

Table 3.5 shows real-life images and polarized light microscopy images of margarine (M) and margarine incorporated with 20% EFG samples. When looking at the colour, MB-US and MI20-US are whiter compared to M while MB-AO-US and M-AO-WBE-I20 are more yellow. This was expected as B-US and I20-US are whiter in colour whereas AO-US and AO-WBE-I20-US are more yellow due to the presence of yellow pigments in cold-pressed avocado oil and WBE. When looking at the microscopic structure of M, a homogenous network of fat crystals can be seen. MB-US shows a more diluted network of fat crystals. MI20-US shows a denser network likely composed of both fat and inulin crystals with a few bubbles. Since by incorporating the O/W EFGS into the margarine, the system is now an O/W emulsion meaning that the bubbles seen are either water droplets or oil droplets encapsulated by GMS, lecithin, and inulin. MB-AO-US also shows bubbles dispersed through the lipid crystals. Since no bubbles were shown in MB-US, likely because B-US was canola based liked that margarine making it dissolve more easily, suggesting that the bubbles observed in MB-AO-US are likely encapsulated oil bubbles that contain more saturated fats and are less dissolved within the margarine. MI20-US and MAO-WBE-I20-UUS show a denser crystal network with MAO-WBE-I20-US having more bubbles than MI20-US. Both these samples show dark spots within the bubbles suggesting a double emulsion was formed.

3.4.4 pH measurement of EFGs

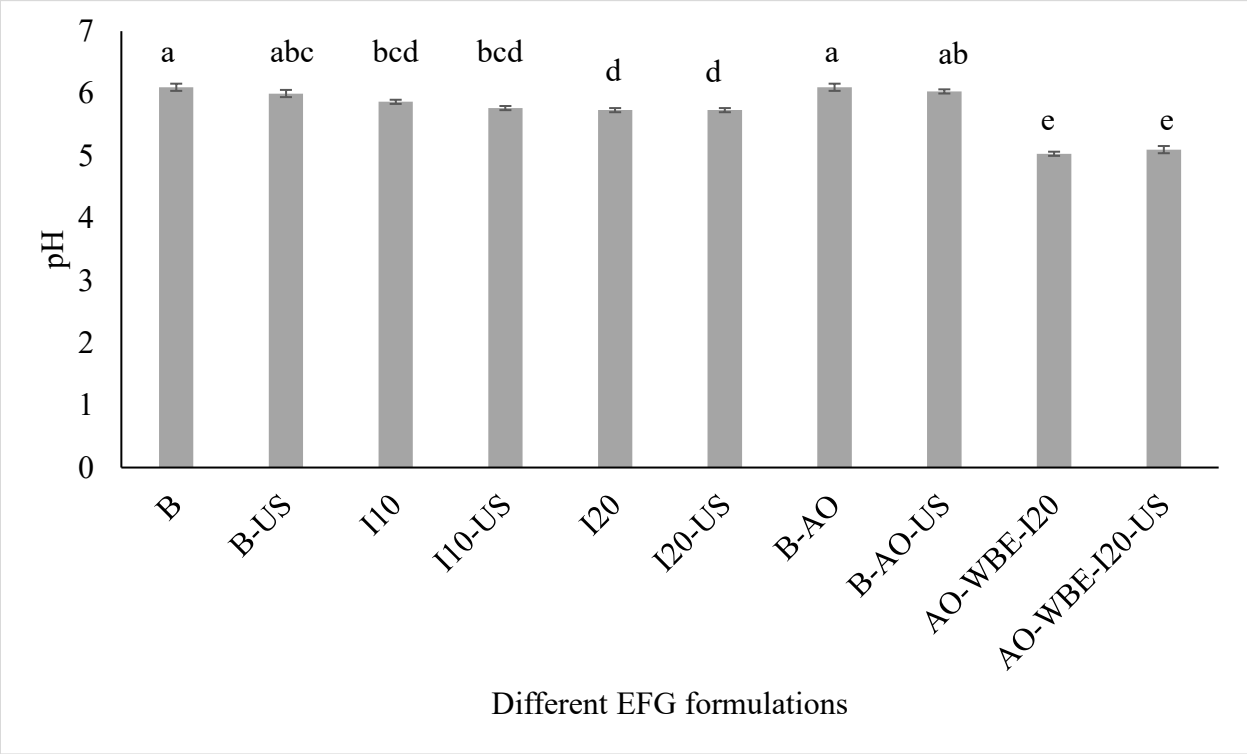

Figure 3.2 pH of different EFG formulations. Different letters represent significant difference and results are expressed as mean of triplicates ± SEM.

The pH of each EFG formulation was measured and is shown in Figure 3.2. Since pH can affect gelling properties, especially when inulin is used, the pH of the samples was measured to see if a difference could be observed. When comparing sonicated samples (B-US, I10-US, I20-US, B-AO-US, and AO-WBE-I20-US) with non-sonicated samples (B, I10, I20, B-AO, AO-WBE-I20) using US-Me to mix the samples had no significant effect on pH. When adding 10% inulin (I10, I10-US), no significant difference is seen compared to the control (B, B-US). Adding 20% inulin however significantly decreased the pH from 6.10 ± 0.06 and 6.00 ± 0.06 for B and B-US, respectively, to 5.73 ± 0.03 and 5.70 ± 0.03 for I20 and I20-US, respectively. Inulin is known to decrease the pH of fermented products and the gut but usually through its fermentation by probiotics that produce organic acids (Loh et al., 2006). While searching the literature there is no

evidence that inulin alone can decrease pH without fermentation. It is possible that the inulin powder used in this study contained organic acid present in the Jerusalem Artichoke source material. Adding both 20% inulin and WBE further decreased the pH to 5.03 ± 0.03 and 5.10 ± 0.06 for AO-WBE-I20 and AO-WBE-I20-US, significantly lower than all other samples. The WBE was responsible for this significant decrease in pH and may be due to the extraction of organic acids from wheat bran which is known to contain a high amount of phenolic acids (Katileviciute et al., 2019).

3.4.5 Water activity (a_w) of EFGs

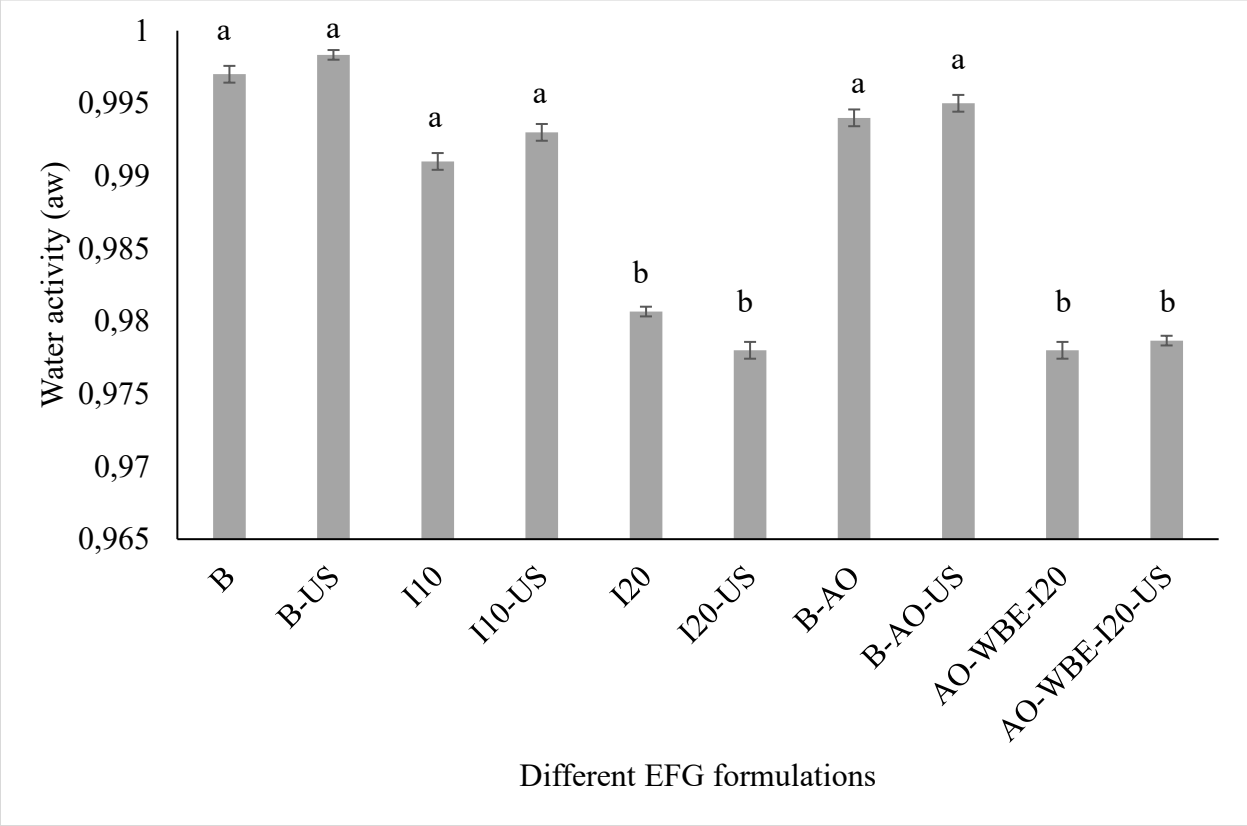

Figure 3.3 Water activity (a_w) of different EFG formulations. Different letters represent significant difference and results are expressed as mean of triplicates ± SEM.

Water activity (a_w) was measured for all EFG formulations and is shown in Figure 3.3. When comparing sonicated samples (B-US, I10-US, I20-US, B-AO-US, and AO-WBE-I20-US) with non-sonicated samples (B, I10, I20, B-AO, AO-WBE-I20) using US-Me to mix the samples had no significant effect a_w values. The only significant ($p<0.05$) difference was seen when adding 20% inulin to the samples which decreased a_w from 0.997 $\pm$ 0.001 and 0.998 $\pm$ 0.001 for B and B-US, respectively, to 0.981 $\pm$ 0.001 and 0.978 $\pm$ 0.001 for I20 and I20-US, respectively, and from 0.994 $\pm$ 0.001 and 0.995 $\pm$ 0.001 for B-AO and B-AO-US, respectively, to 0.978 $\pm$ 0.001 and 0.979 $\pm$ 0.001 for AO-WBE-I20 and AO-WBE-I20-US, respectively. Inulin, like most polysaccharides, is known to reduce water activity by binding to water (Paglarini et al., 2021). It was expected that I20 would decrease water activity by binding to water and decreasing the amount of free water available in the sample, but at least 20% inulin is required to reach this effect as 10% inulin (I10) did not show a significant decrease in a_w value compared to the control (B). Other researchers have shown that a 20% inulin concentration is required to form a three-dimensional network providing a gelling effect (Glibowksi, 2010).

3.4.6 Textural analysis of EFGs and EFG-incorporated margarine

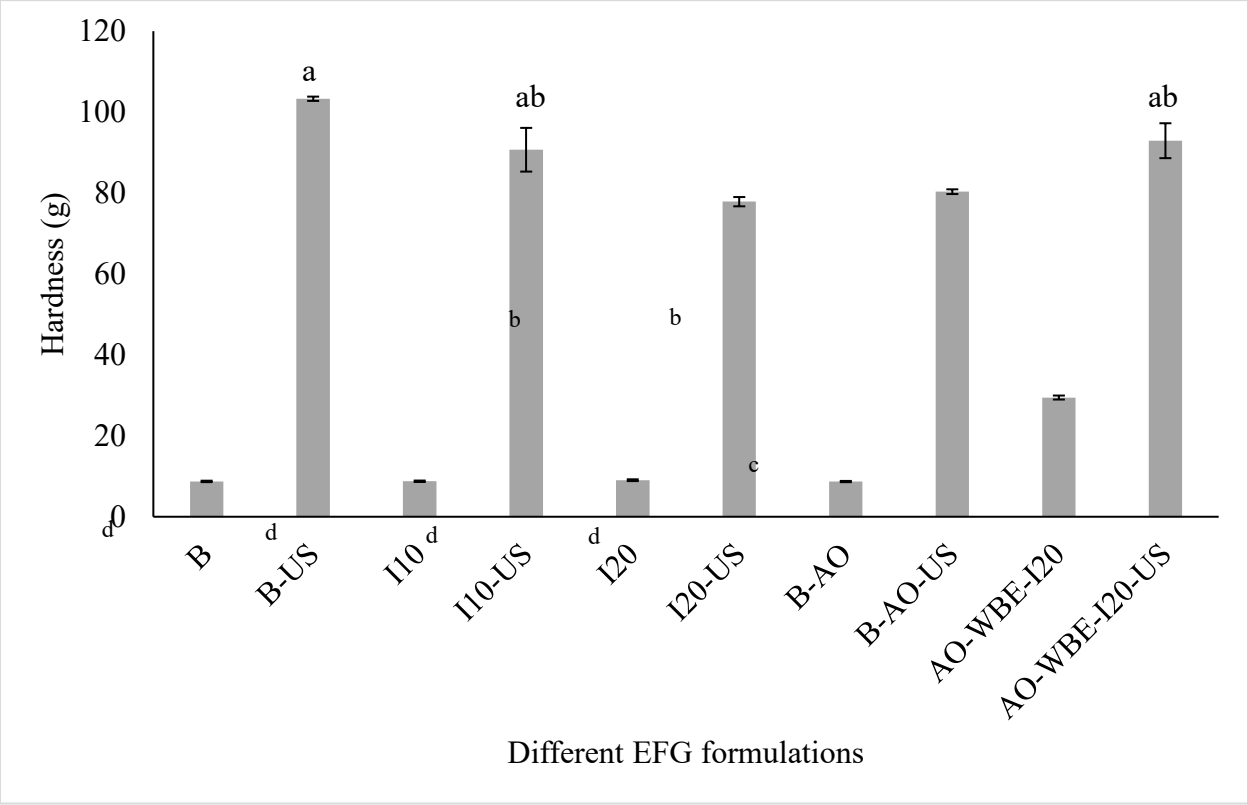

Figure 3.4 Hardness (g) of different EFG formulations at room temperature (21°C). Different letters represent significant difference and results are expressed as mean of triplicates ± SEM.

The hardness (g) of the different EFG formulations was measured with a texture analyzer and the values are presented in Figure 3.4. Measuring hardness provides insight into the microstructure fat crystal networks, or the degree to which a solid fat crystal network has been formed (Boodhoo et al., 2008). Hardness is also an important measure for spreads in the food industry. For example, margarine or butter that is too hard at room temperature is hard to spread and leads to consumer dissatisfaction. When comparing sonicated samples (B-US, I10-US, I20-US, B-AO-US, and AO-WBE-I20-US) with non-sonicated samples (B, I10, I20, B-AO, AO-WBE-I20) using US-Me to mix the samples significantly ($p<0.05$) increased hardness (g) in all samples. The highest value was observed in B-US at 103.3 ± 0.5 g suggesting that this sample had the most stable fat crystal

network. It is interesting to note that while adding inulin alone in I10 and I20, no difference is seen compared to the control B, but when ultrasound is applied a slight nonsignificant decrease is observed in I10-US with 10% inulin addition at 90.7 $\pm$ 5.4 g and a significant ($p<0.05$) is seen in I20-US with 20% inulin addition at 77.9 $\pm$ 1.1 g compared to B-US. Another interesting observation is the significant ($p<0.05$) difference in hardness observed in B-US (103.3 $\pm$ 0.5 g) and B-AO-US (80.33 $\pm$ 0.6 g). The difference between these two samples is the type of oil (canola for B-US and avocado for B-AO-US) added to the sonicated water phase containing GMS and lecithin. B-AO-US is significantly lower in hardness compared to B-US showing that the type of oil used likely interacts differently with the dispersed GMS and lecithin in the water phase. Avocado oil has more saturated fatty acids compared to canola oil, as shown in Figure 3.1. The addition of 20% inulin and WBE increased that hardness enough in AO-WBE-I20-US, at 92.9 $\pm$ 4.3 g, that it was not significantly different to B-US. When looking at the non-sonicated samples, only the sample with wheat bran extract (AO-WBE-I20) has a significantly ($p>0.05$) higher hardness value compared to all other samples while the addition of 20% inulin shows no significant difference in hardness. This is important as it shows that WBE alone, or in synergy with inulin, may be responsible for changing the microstructure of the fat network. It is theorized that the saturated alkyl chains of ARs may be responsible for increasing packing at the phase interface by interacting with GMS and lecithin at the water/oil interface. With sonicated samples addition of 20% inulin leads to a significant decrease. So, for AO-WBE-I20-US the increase in hardness is likely due to the addition of WBE, or a synergistic effect with inulin is responsible.

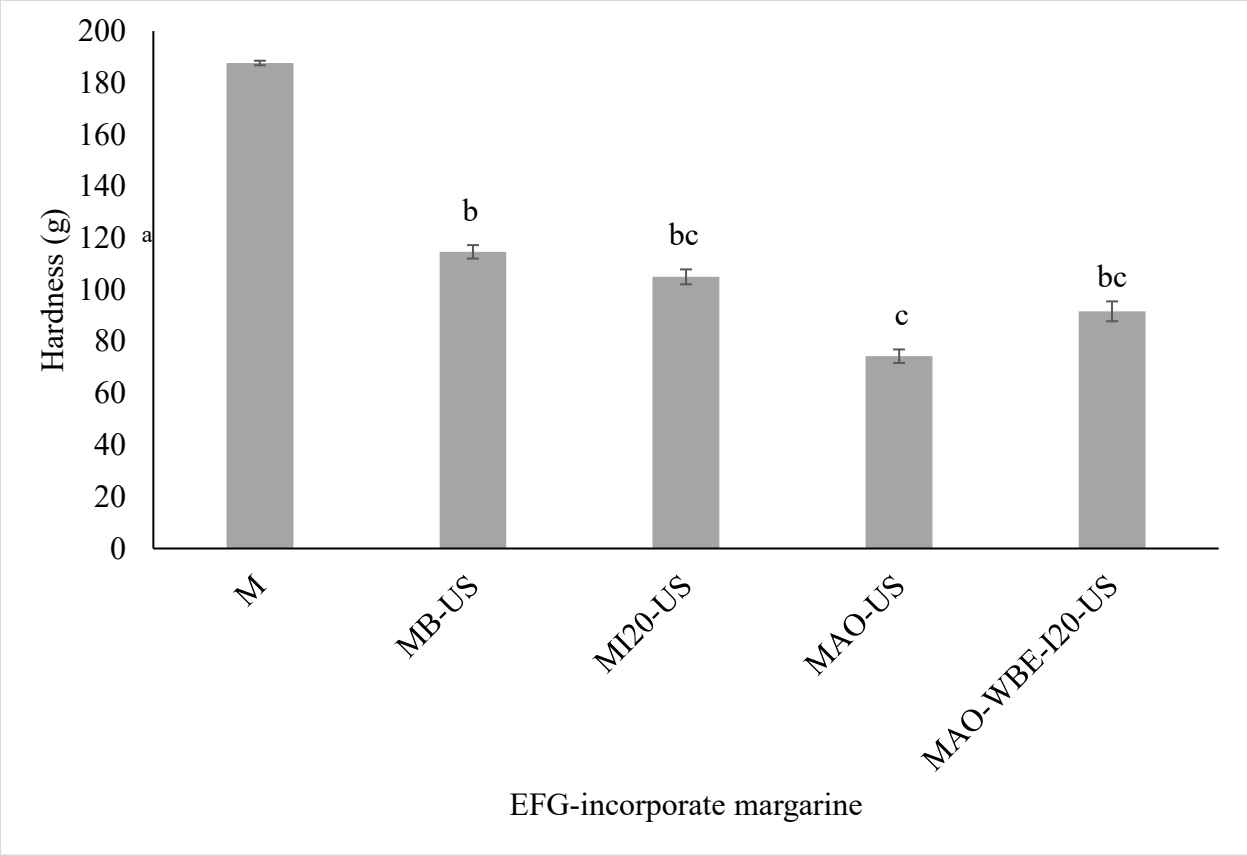

Figure 3.5 Hardness (g) of EFG-incorporated margarine. Different letters represent significant difference and results are expressed as mean of triplicates ± SEM.

The hardness (g) of EFG-incorporated margarine was measured with a texture analyzer and the values are presented in Figure 3.5. Only sonicated EFG were used since they were shown to have improved texture and stability. Margarine (M) by itself has a hardness of 187.7 ± 0.9 g. The hardness is significantly ($p<0.05$) decreased when EFG is incorporated in all samples showing that their incorporation leads to microstructural changes in the fat crystal network. When comparing to M, incorporating B-US led to a ~40% decrease in MB-US (114.7 ± 2.6 g). Incorporating I20-US led to a ~44% decrease in MI20-US (105 ± 2.9 g) compared to M. The lowest value of hardness was observed in MAO-US with 74.3 ± 2.6 g, a ~60% decrease in hardness compared to M, while the incorporation of AO-WBE-I20-US showed a ~51% decrease in MAO-WBE-I20-US at 91.7 ±

3.8 g. The significant decrease in hardness with MAO-US may be due to the more saturated fats in the avocado oil not mixing well with the canola-based margarine affecting rheological properties.

3.4.7 Oxidative stability of EFGs and EFG-incorporated margarine

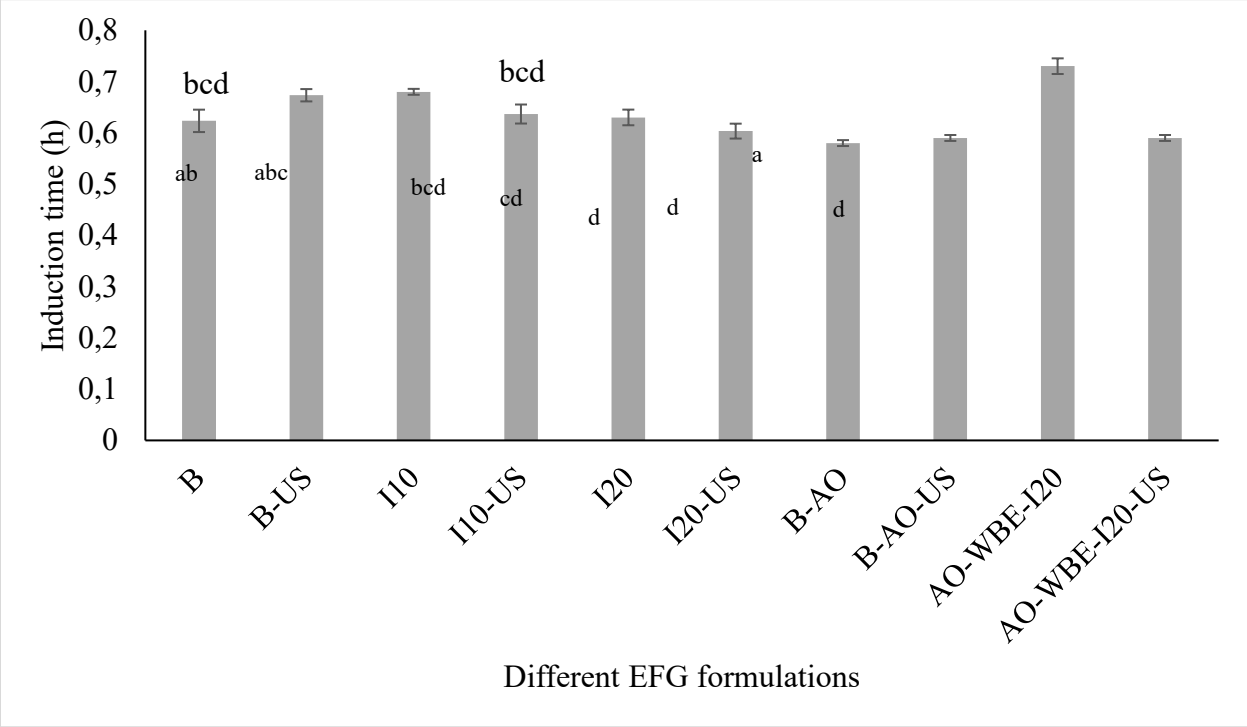

Figure 3.6 Induction time (h) of different EFG formulations. Different letters represent significant difference and results are expressed as mean of triplicates ± SEM.

Another important measure is oxidative stability which shows the ability of samples to withstand oxidation at a high temperature (121 ^{o}C) when exposed to air (20 L/h) and is measured as induction time (h), the time it takes before oxidation begins. The longer the induction time the more resistant the sample is to oxidation. Induction time (h) was measured in all EFG formulations and is presented in Figure 3.6. The longest induction time was observed in AO-WBE-I20 at 0.73 ± 0.02 h while the lowest was observed in B-AO at 0.58 ± 0.01 h. When comparing non-sonicated samples to sonicated samples, no significant difference is seen between B, I10, I20, B-AO, and B-US, I10-

US, I20-US, BAO-US. The only sample where sonication seems to have significantly ($p<0.05$) decreased oxidative stability is AO-WBE-I20-US at 0.59 ± 0.01 h, a ~19% decrease compared to AO-WBE-I20. Since the WBE used in this formulation was extracted using food-friendly ethanol as the solvent, it contained polyunsaturated oils and impurities that are prone to oxidation, as was seen in Figure 2.8 where WBE extracted with ultrasound and ethanol had a significantly lower antioxidant activity compared to the traditionally extract WBE with ethanol. This is likely what led to the decrease of induction time seen here when ultrasound was applied to the water phase containing GMS, lecithin, 20% inulin, and WBE.

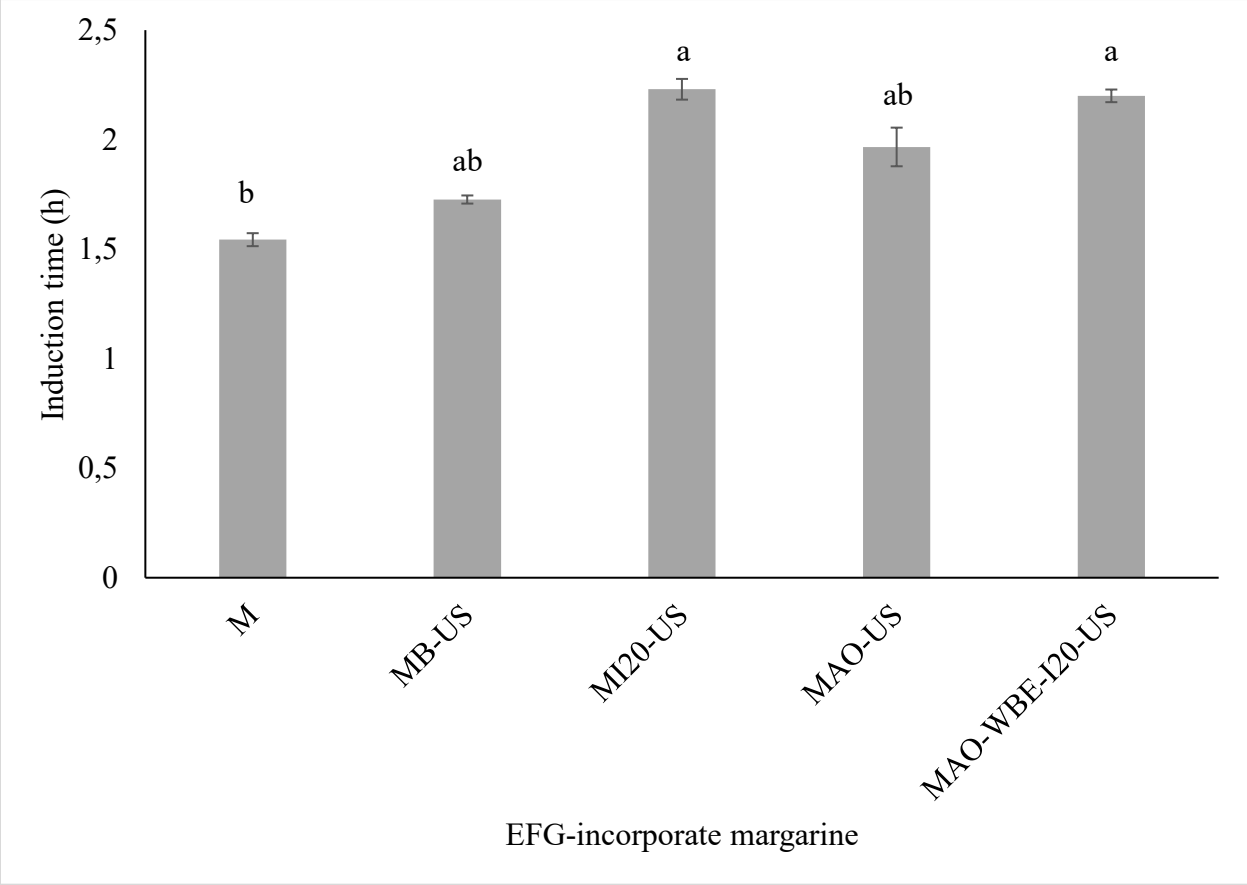

Figure 3.7 Induction time (h) of EFG-incorporated margarine. Different letters represent significant difference and results are expressed as mean of triplicates ± SEM.

Induction time (h) was measured in all EFG-incorporate margarine samples and is presented in Figure 3.7. Margarine (M) by itself had the lowest induction time of 1.54 $\pm$ 0.03 h but was not significantly different from MB-US and MAO-US at 1.72 $\pm$ 0.02 h and 1.97 $\pm$ 0.09 h, respectively. Compared to M, a significant ($p<0.05$) increase was observed in M120-US and MAO-WBE-I20-US 2.23 $\pm$ 0.05 h and 2.20 $\pm$ 0.03 h, respectively, representing a ~ 45% and ~43% increase, respectively. This is significant as it shows that the incorporation of EFGs produce in this study with 20% inulin and WBE can significantly increase the oxidative stability of margarine, something that is desired for stable shelf life in the food industry. Inulin has previously been shown capable of scavenging hydroxyl and superoxide radicals (Stoyanova et al., 2011). ARs in WBE are also well-known antioxidants capable of scavenging free radicals. The WBE also likely contained more hydrophilic antioxidants such as some flavonoids and phenolic acids that can also be present in ethanol extracts. Combining both WBE and inulin provides both hydrophilic and hydrophobic antioxidants to the margarine.

3.4.8 Thermal behaviour of EFG-incorporated margarine

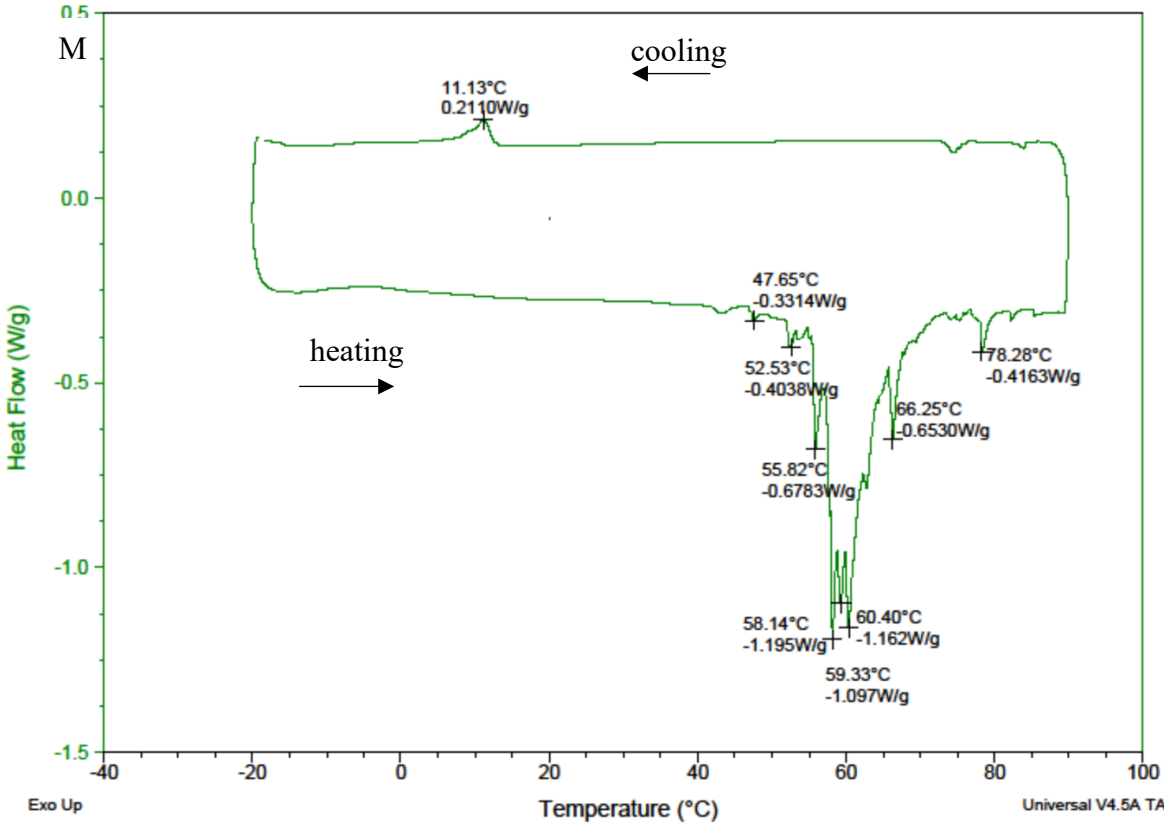

Figure 3.8 Melting and cooling DSC curves of Margarine (M)

The thermal behaviour of margarine (M) was investigated using DSC. Figure 3.8 shows the DSC graph obtained for M while Figure 3.9 shows graphs for margarine with the incorporation of non-sonicated EFG (MB, MI20, MAO, MAO-WBE-I20) and sonicated EFG (MB-US, MI20-US, MAO-US, MAO-WBE-I20-US). The complexity of the melting curves with several peaks shows the heterogeneous profile of crystallized fats. The melting profile of margarine shows the onset point (T_{onset}) of melting at 47.65 °C and melting peak (T_m) at 58.14 °C. When cooling, after melting, the crystallization peak (T_c) is observed at 11.12 °C. The several melting peaks observed are likely a combination of β' and β crystals with different TAG β' polymorph melting at a lower temperature

(55.82, 58.14, and 60.40 ºC) and the more stable β polymorph melting at higher temperatures (66.25 and 78.28 ºC). Table 3.6 shows melting points (T_m) of different TAG polymorphs.

Table 3.6 Melting point (T_m) of different TAG polymorphs (Ghotra et al., 2002)

TAG	**T_m (ºC)**	
	Polymorph	
	β'	**β**
PPP	56.7	**66.2**
SSS	64.2	**73.5**
PSP	**68.8**	-
POP	30.5	45.3
SOS	36.7	41.2
SOO	8.8	23.7
OOO	-11.8	5.1
LOO	28.3	-23.3
LLO	3.02	25.2

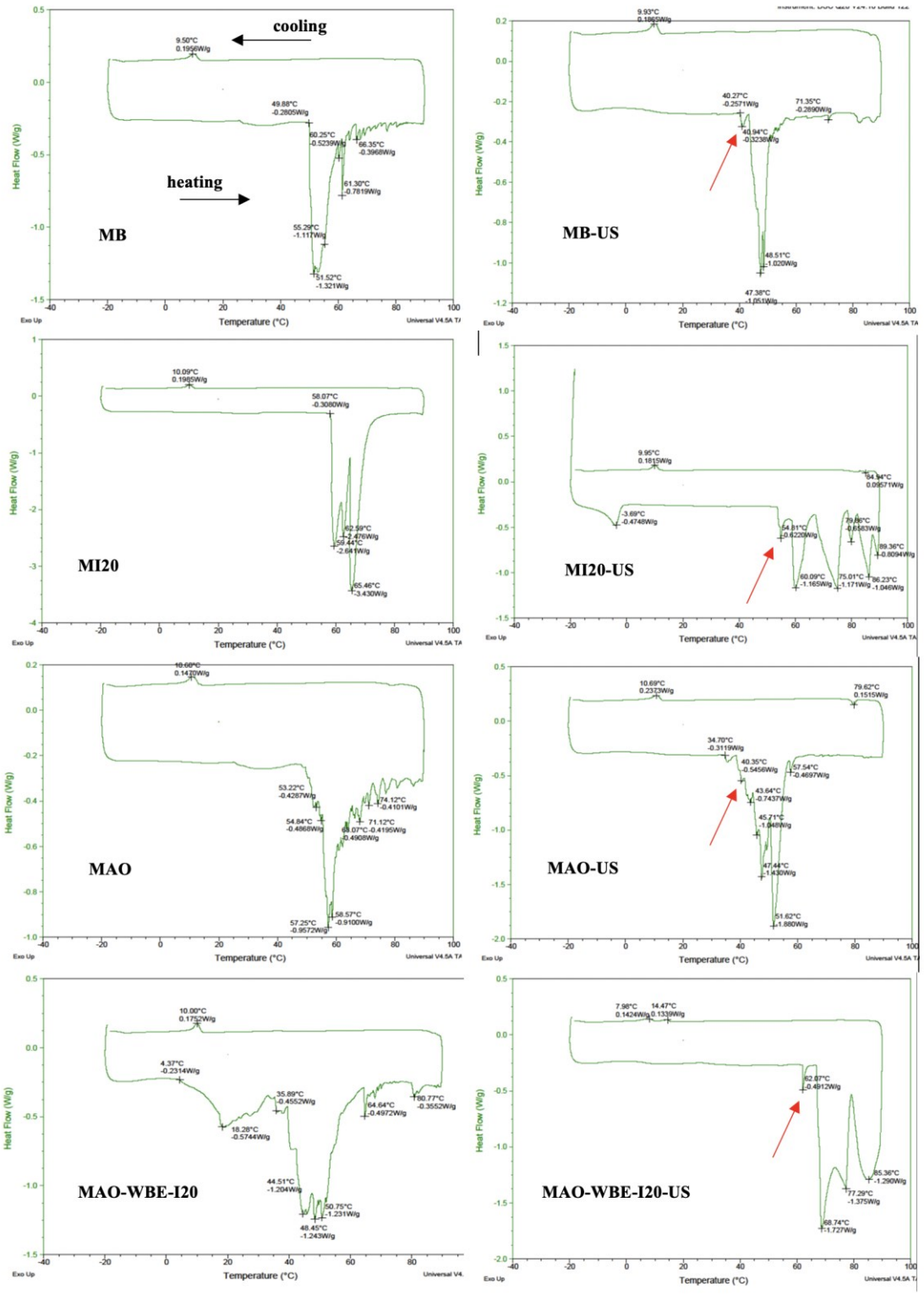

Figure 3.9 Melting and cooling DSC graphs of EFG-incorporated margarine. Red arrows indicate the characteristic liposome melting point (T_m).

Table 3.7 Crystallization peak (T_c) and melting peak (T_m) of EFG-incorporated margarine from DSC graphs

Sample	T_c peak	T_m onset	T_m peak
M	11.13	47.65	58.14
MB	9.50	49.88	51.52
MB-US	9.93	40.27	47.38
MI20	10.09	58.07	65.46
MI20-US	9.95	53.00	75.01
MAO	10.60	53.00	57.25
MAO-US	10.69	34.70	51.62
MAO-WBE-I20	10.00	4.37	48.45
MAO-WBE-I20-US	7.98	61.35	68.74

DSC graphs of EFG-incorporated margarine are shown in Figure 3.9. When comparing T_c peak of EFG incorporated margarine samples to the control (M), shown in Table 3.7, incorporation of EFG decreases the peak of crystallization with the largest decrease observed in MAO-WBE-I20-US at 7.98 ^oC compared to 11.13 ^oC for M. When comparing T_m peaks of EFG incorporated margarine samples to M, the largest increase was seen in MI20-US at 75.01 ^oC compared to 58.15 ^oC in M, while the largest decrease was seen in MB-US at 47.38 ^oC.

The melting behavior of MB is the most similar to control which is not surprising as the EFG incorporated is canola based. When US-Me is used to produce the EFG incorporated in MB-US a decrease in the onset and peak of T_m and is observed with almost no characteristic β melting peaks observed at higher temperatures. This could be due to a shift from β to β' crystals caused by unsaturated TAG β' polymorphs that melt at a lower temperature. The presence of smaller β' crystals in B-US could also explain the increase in hardness observed in Figure 3.4 compared to the other EFGs.

The incorporation of I20 into margarine (MI20), increased the melting temperature onset by 10 ºC and resulted in three distinct melting peaks at 59.44, 62.59, and 65.46 ºC. MI20-US shows 6 distinct melting peaks at 54.81, 60.09, 75.01, 79.66, 86.23, and 89.26ºC. These samples show that incorporation of I20 and I20-US in margarine can affect its melting behavior. The distinction of the peaks compared to the complexity of peaks observed in the control (M) suggests that the addition of inulin may lead to a more proportional formation of different fat crystal polymorphs. Incorporating B-AO into margarine (MAO) also shows similar thermal behaviour to the control M with several more melting peaks introduced at a higher temperature (71.12, 74.14 ºC) likely due to the presence of saturated fatty acids from avocado oil. When B-AO-US is incorporated in MAO-US, the higher temperature peaks disappear and T_m onset is decreased compared to M, suggesting a shift formation of β to β' crystals. When incorporating AO-WBE-I20 into margarine (MAO-WBE-I20-US) several lower melting peaks are introduced at 18.38, 44.51, 48.45, and 50.75 ºC, and T_m onset is decreased to 4.37 ºC. The presence of polyunsaturated lipids in the WBE may be responsible for the lower melting peaks compared to the control (M) and could be either unsaturated TAG β' or β, both of which have lower melting points than their saturated counterparts, or lower melting and unstable α crystals. Also seen are two higher melting with lower enthalpy at 64.64 and 80.77 ºC that are similar to those observed in M at 66.25 and 78.25 ºC and could be the characteristic higher melting point of saturated TAG β crystals. The lower melting peaks observed in MAO-WBE-I20 are absent in MAO-WBE-I20-US where 4 distinct peaks are observed at higher temperatures (62.07, 68.74, 77.29, and 85.36º). These peaks point to the presence of larger β crystals. A significant decrease in hardness was observed with the introduction of inulin in I20-US compared to B-US providing further evidence that sonicated EFGs containing

inulin promoted the formation of larger β crystals while B-US promoted the formation of smaller β' crystals.

All crystallization temperatures (T_c) were similar or lower than the control (M). A decrease is likely due to the introduction of lower melting unsaturated TAGs into the margarine which crystallize at lower temperatures.

Also of note is the introduction of a shoulder peak, shown with red arrows in Figure 3.9. in all margarine samples that were incorporated with EFGs made with US-Me that is not present in EFGs made with Me. The endothermic shoulder peak observed at 40.94 ºC in MB-US is characteristic of the melting point (T_m) of the transition phase of soy lecithin membranes from the gel phase to the liquid crystalline phase typically observed between 40-50 ºC (Yokota et al., 2012). The absence of these characteristic shoulder peaks in non-US EFG-incorporated margarine infers that Me homogenization of the water phase with emulsifiers did not provide the energy necessary for self-assembly of liposomes while US-Me did. The presence of inulin in MI20-US shows a shoulder peak at 54.81 ºC suggesting an increase in order and stability of liposomes with the presence of inulin. Inulin, a fructose polymer, likely stabilized the liposomes by actively interacting with the hydrophilic phosphate head groups and immobilizing them in a sort of coating effect (Mensink et al., 2015). When looking at the presence of WBE and inulin in AO-WBE-I20-US a further increase in temperature can be seen for shoulder peak at 62.07 ºC likely due to the presence of crude ARs from the WBE. The crude ARs characterized in the WBE in chapter 2, are long-chain and saturated. ARs have been shown to incorporate in liposomal membranes and cause a rigidifying effect on bilayer fluidity by increasing packing of the acyl chains within the membrane (Gubernator et al., 1999). The PLM images shown in Table 3.4 and Table 3.5 show a clear presence

of vesicles in US samples. Combined with the information on melting behaviour obtained with DSC and the presence of characteristic peaks of the melting point of lecithin liposomes, it is clear that encapsulation was successful using US.

3.5 Conclusion

The EFGs produced from liposomal solutions in this study show different characteristics (microstructure, hardness, water activity, pH, oxidative stability, thermal behavior) dependent on formulation and homogenization technology used. Microstructure and hardness were significantly improved when high power low frequency direct US was used as the homogenization technology. EFGs produced from liposomal solutions homogenized with US-Me also had a greater effect on the thermal behavior of margarine, an indication that crystal polymorphism is affected. Further studies, such as X-ray diffraction to investigate the effect of US and EFGs containing inulin and WBE on fat crystal polymorphism are warranted. Overall, the results showed that producing EFGs from liposomal solutions homogenized with US-Me is an efficient way to encapsulate and deliver functional ingredients, such as crude ARs and inulin, into food products.

CHAPTER 4: Conclusion and proposal for a future study: Functionality of odd chain phenolic lipids in cellular membrane

4.1 Conclusion

Numerous studies show that crude ARs found in WBE can be applied as a functional ingredient in food. Obstacles stand in the way of its widespread application in the food and pharmaceutical industry namely: cost-effective extraction. In parallel, direct power ultrasound is a green-non thermal with numerous studies showing a wide variety of applications in food. This research demonstrated that high power (90 W) low frequency (20 kHz) ultrasound can be employed as a tool for 1) significantly ($p<0.05$) decreasing extraction time of crude ARs from wheat bran from 24h to 30m while retaining the same antioxidant activity as traditionally extracted crude ARs and 2) improving physicochemical properties of EFGs prepared from liposomal solutions and EFG-incorporated margarine in combination with inulin and crude ARs. Further studies are warranted such as investigation and confirmation of effect on crystal polymorphisms through X-ray diffraction. A study investigating the shelf-life of EFGs such as time-course studies on oxidative stability and antimicrobial activity is also required to show the effect of crude ARs and US on these properties. The mechanism by which ARs may enhance liposomal and cellular membranes is also of interest for research due to their proven ability to incorporate within bilayers. Below, a future study is proposed to investigate the structure-function relationship of odd chain phenolic lipids in cellular membranes and their ability to prevent lipid peroxidation.

4.2 Future study: Functionality of odd chain phenolic lipids in cellular membrane

4.2.1 Introduction

Phenolic lipids are plant secondary metabolites providing defense against environmental stress. They are mono- and dihydroxyl phenol derivatives with odd-numbered alkyl chains that can vary in chain length and degree of saturation. They are amphiphilic with a hydrophilic phenol ring and hydrophobic alkyl chain and have been shown to incorporate into biological membranes. They are believed to affect the packing of phospholipids in membrane bilayers affecting permeability, fluidity, and surface charge through interaction with phospholipids and may provide resistance to oxidative stress. Liposomes can be used as artificial membranes to study the effects of compounds on these properties. This proposal suggests investigating the effect of phenolic lipids with varying chain length on cellular membrane properties using liposomes as an artificial model based on a previous study by (Malekar et al., 2015) that investigated phenolic compounds on liposomal membrane properties. Odd chain lipids should be investigated alongside to determine the effect of phenol rings. The hypothesis is that a relationship exists between odd chain phenolic lipid structure and their functionality in the liposomal membrane. Artificial liposomal membranes can be produced using phospholipids such as phosphocholine. Nuclear magnetic resonance (NMR), differential scanning calorimetry (DSC), dynamic light scattering (DLS), and zeta potential (ZP), conjugated dienes assay can be used as complementary analytical techniques to determine the location of compounds within the bilayer and their effect on bilayer characteristics and stability (Malekar et al., 2015). ^{1}H-NMR can help determine the structure of molecules by giving information on the number of protons and can offer insight into localization within the membrane with changes observed in samples vs the blank indicating presence of phenolic compounds near

the head group of phosphocholine within the membrane bilayer. Changes in aromatic peaks of phenolic compounds indicate incorporation in vesicles. ^{31}P-NMR can be used to analyzed compounds containing phosphorous, such as phospholipids. Changes in peaks observed in the samples vs the blank indicate interaction with the phosphorous head group of phospholipids. Thermal analysis using DSC can provide information on the interaction of phenolic compounds with glycerol region or different regions of the alkyl chain (C_1-C_{10} or C_{10}-higher) of phospholipids (Chiu & Prenner, 2011). A cooperative unit exits in the gel phase of a bilayer due to transmission of motion among the packed and ordered fatty acids. The transition from the gel to the liquid crystalline phase is endothermic, as heat is required to go from a highly ordered phase to a less ordered phase. In cellular membranes, the center of the bilayer tends to be more fluid and less ordered compared to the outer regions of the membrane. When packing of the cooperative unit is altered, an increase or decrease in transition temperature (T_m) occurs. DSC can measure this transition temperature. If the transition temperature peak is broadened, it indicates an interaction with the cooperative unit in the gel phase at C_1-C_{10} of the alkyl chain. If the peak sharpens, the interaction is located at C_{10} or higher as the cooperative unit is not affected. A shoulder peak at a lower temperature indicates interaction with the glycerol region. DLS can be used to determine particle size by measuring the amount of light scattered within the solution with smaller particles scattering more light than larger particles. It can be used to study the stability of colloidal suspension by measuring particle size over time to determine the delay of aggregation. Zeta-potential can be used to determine the surface charge of liposomes to indicate the surface exposure of the charged phosphate group in liposomes and the presence of phenolic compounds and their effect on surface exposure of the phosphate groups. The results can be correlated with ^{31}P-NMR to identify the presence of phenolic compounds near the head group. Finally, the relationship

between odd chain phenolic lipids and resistance to oxidative stress in the liposomal membrane can be investigated by the conjugate dienes assay. Conjugated dienes are a by-product of lipid peroxidation which can be initiated by a free radical generator (i.e. AAPH). Their presence can be measure using UV-spectrophotometry at 234 nm.

4.2.2 Materials and methods

4.2.2.1 Materials

- 1,2-dipalmitoyl-sn-glycero-2-phosphocholine (DPPC) monohydrate
- Odd chain phenolic lipid standards:
    - 5-heptadecylresorcinol (C17:0)
    - 5-nonadecylresorcinol (C19:0)
    - 5-heneicosylresorcinol (C21:0)
- Odd chain fatty acid standards:
    - heptadecanoic acid (C17:0)
    - nonadecanoic acid (C19:0)
    - heneicosanoic acid (C21:0)
- Phosphate buffer (pH 7.4)

4.2.2.2 Preparation of artificial membranes

Prepare liposomes at 17 mM lipid (DPPC)/2mM phenolic lipid concentration. Blank DPPC liposomes should contain only DPPC. For ^{31}P-NMR, vesicles should be made with 90:10 (water/D_2O) and with 100% D_2O for ^{1}H-NMR and 137 mM PBS (pH 7.4), adapted from (Malekar et al., 2015). Samples should be diluted to a lipid concentration of 1 mM for DLS and zeta-potential and 0.1 mM for nano-DSC using 137 mM PBS. Liposome preparation using thin-film hydration adapted from (Hosseinian et al., 2006). Briefly, for blank, dissolve 12.5 mg of DPPC in 1 mL chloroform and evaporate under nitrogen to obtain a thin film. Then rehydrate film with 1mL of appropriate media (PBS for DLS, zeta potential, DSC, and conjugated dienes measurements; 100% D_2O for ^{1}H-NMR; and 10% D_2O for ^{31}P-NMR). Mix the resulting solution with a vortex for 1 min

and then sonicate in an ultrasound bath for 10 min. The liposomes can then be prepared using a liposome extruder (Avanti Polar Lipids) using a 200 nm porous polycarbonate membrane. The suspension is passed through the membrane 21-times to obtain a homogenous unilamellar liposomal solution. For odd chain phenolic and odd chain fatty acids containing liposomes add the following amounts with the 12.5 mg of DPPC at the beginning:

Table 4.1 Amount (mg) required for 2mM liposomal solution

	Amount to add (mg) for 2mM solution
Odd chain phenolic lipid	
C17:0	0.64
C19:0	0.76
C21:0	0.81
Odd chain fatty acid	
C17:0	0.54
C19:0	0.60
C21:0	0.65

4.2.2.3 Nuclear Magnetic Resonance (NMR)

NMR protocols are adapted from (Malekar et al., 2015). Use liposome formulation prepared with 10% *v/v* D_2O in water for ^{31}P-NMR and 100% D_2O for ^{1}H-NMR to provide a deuterium lock signal. Collect ^{31}P-NMR data at 202.3 MHz for 60-K scans with 35.7 kHz sweep width using 131-K data points. Acquisition time should be 1.3 s with a relaxation delay of 0.5 s with a line broadening of 50 Hz applied to all spectra. Reference spectra to H_3PO_4 set to 0ppm and acquire data without spinning. For ^{1}H-NMR, collect data at 499.8 MHz.

4.2.2.4 Differential scanning calorimetry (DSC)

DSC protocol adapted from (Malekar et al., 2015). Using 0.1 mM lipid solution, load 10 mg into Tzero hermetic alodined aluminum pan and seal with hermetic alodined aluminum lid. Place the pan onto the cell sensor with a reference pan (empty). Scan sample at 1 ^{o}C min $^{-1}$ over a range of 10 to 60 ^{o}C.

4.2.2.5 Dynamic Light Scattering (DLS)

DLS protocol adapted from (Malekar et al., 2015). DLS measurements can be performed using a Zetasizer. Samples should be stored at 37 ^{u}C and analyzed at 0, 3, and 5 days to determine particle size.

4.2.2.6 Zeta-potential

Zeta-potential protocol adapted from (Malekar et al., 2015). Dilute an aliquot from each formulation with 137 mM PBS for a final lipid concentration of 1mM. Using a laser doppler procedure with a Zetasizer at 25^{o}C to measure zeta-potential. Airdrop interference should be eliminated before each measurement.

4.2.2.7 Conjugated dienes assay

Conjugated dienes assay adapted from (Hosseinian et al., 2006). Add 50 µL of each liposomal formulation into quartz cuvettes. Initiate oxidation reaction at ambient temperature by adding 150 µL of 40 mmol/L AAPH (free radical generator). Measure samples kinetically for 120 min using UV-visible spectrophotometer at 134 nm. Trolox, a water-soluble antioxidant, can be used as a positive control. The blank should be 50 µL of 137 mM PBS buffer.

REFERENCES

Agil, R., Patterson, Z., Mackay, H., Abizaid, A., & Hosseinian, F. (20 16). Triticale bran alkylresorcinols enhance resistance to oxidative stress in mice fed a high-fat diet. *Foods*, *5*(1), 5.

Agriculture and Agri-Food Canada. (2019). *Government of Canada helps the wheat sector increase export market share* https://www.canada.ca/en/agriculture-agri-food/news/2019/03/government-of-canada-helps-the-wheat-sector-increase-export-market-share.html

Alimi, M., Mizani, M., Naderi, G., & Shokoohi, S. (2013). Effect of Inulin Formulation on the Microstructure and Viscoelastic Properties of Low-Fat Mayonnaise Containing Modified Starch. *Journal of Applied Polymer Science*, *130*(2), 801-809.

Andersson, U., Dey, E. S., Holm, C., & Degerman, E. (2011). Rye bran alkylresorcinols suppress adipocyte lipolysis and hormone-sensitive lipase activity. *Food and Function*, *55*(S290-S293).

AOCS. (2017). *Official Method Cd 12b-92: Oil Stability Index* (M. W. Collision, Ed. 7 ed.). AOCS Press.

Ashton, O. B. O., Wong, M., McGhie, T. K., Vather, R., Wang, Y., Requejo-Jackman, C., Ramankutty, P., & Woolf, A. B. (2006). Pigments in Avocado Tissue and Oil. *Journal of Agricultural and Food Chemistry*, *54*, 10151-10158.

Atrooz, O. M. (2011). Efects of Alkylresorcinolic Lipids Obtained from Acetonic Extract of Jordanian Wheat Grains on Liposome Properties. *International Journal of Biological Chemistry*, *5*, 314-321.

Baerson, S. R., Schroder, J., Cook, D., Rimando, A. M., Pan, Z., Dayan, F. E., Noonan, B. P., &

Duke, S. O. (2010). Alkylresorcinol biosynthesis in plants: New insights from an ancient enzyme family? *Plant Signaling & Behaviour*, *5*(10), 1286-1289.

Bermudez-Aguirre, D., Mobbs, T., & Barbosa-Canova, G. V. (2010). Ultrasound applications in food processing. In *Ultrasound Technologies For Food and Bioprocessing* (Vol. 65-105, pp. 43-50). Springer.

Biskup, I., Kyrø, C., Marklund, M., Olsen, A., van Dam, R. M., Tjønneland, A., Overvad, K., Lindahl, B., Johansson, I., & Landberg, R. (2016). Plasma alkylresorcinols, biomarkers of whole-grain wheat and rye intake, and risk of type 2 diabetes in Scandinavian men and women. *The American Journal of Clinical Nutrition*, *104*(1), 88-96. https://doi.org/10.3945/ajcn.116.133496

Boodhoo, M. V., Humphrey, K. L., & Narine, S. S. (2008). Relative Hardness of Fat Crystal Networks Using Force Displacement Curves. *International Journal of Food Properties*, *12*(1), 129-144.

Chiu, M. H., & Prenner, E. J. (2011). Differential scanning calorimetry: An invaluable tool for a detailed thermodynamic characterization of macromolecules and their interactions. *Journal of Pharmacy and BioAllied Sciences*, *3*(1), 39-59.

Cholewski, M., Tomczykowa, M., & Tomczyk, M. (2018). A Comprehensive Review of Chemistry, Sources and Bioavailability of Omega-3 Fatty Acids. *Nutrients*, *10*(11), 1662.

Ciccoritti, R., Pasquini, M., Sgrulletta, D., & Nocente, F. (2015). Effect of 5-*n*-alkylresrocinol extracts from durum wheat whole grain on the growth of fusarium head blight causal agents. *Journal of Agricultural and Food Chemistry*, *63*(1), 43-50.

da Silva, T. L., Marsh, M., Gibon, V., & Martini, S. (2020). Sonocrystallization as a tool to reduce oil migration by changing physical properties of a palm kernel fat. *Journal of Food Science*,

85(4), 964-971.

Deora, N. S., Misra, N. N., Deswal, A., Mishra, H. N., Cullen, P. J., & Tiwari, B. K. (2013). Ultrasound for Improved Crystallisation in Food Processing. *Food Engineering Reviews*, *5*(1), 36-44.

Dowhan, W., Bogdanov, M., & Milieykovska, E. (2015). Functional Roles of Lipids in Membranes. In (6 ed.). Elsevier Science & Technology.

Elder, A. S., Coupland, J. N., & Elias, R. J. (2021). Effect of alkyl chain length on the antioxidant activity of alkylresorcinol homologues in bulk oils and oil-in-water emulsions. *Food Chemistry*, *346*, 128885.

Farjami, T., & Madadlou, A. (2019). An overview on preparation of emulsion-filled gels and emulsion particulate gels. *Trends in Food Science & Technology*, *86*, 85-94.

Flores, M., Saravia, C., Vergara, C. E., Avila, F., Valdes, H., & Ortiz-Viedma, J. (2019). Avocado Oil: Characteristics, Properties, and Applications. *Molecules*, *24*(11), 2172.

Forouhi, N. G., Koulman, A., Sharp, S. J., Imamura, F., Kroger, J., Schulze, M. B., Crowe, F. L., Huerta, J. M., Guevara, M., Beulens, J. W. J., van Woudenbergh, G. J., Wang, L., Summerhill, K., Griffin, J. L., Feskens, E. J. M., Amiano, P., Boeing, H., Clavel-Chapelon, F., Dartois, L., Fagherazzi, G., Franks, P. W., Gonzalez, C., Jakobsen, M. U., Kaaks, R., Key, T. J., Kaw, K.-T., Kuhn, T., Mattiello, A., Nilsson, P. M., Overvad, K., Pala, V., Palli, D., Quiros, J. R., Rolandsson, O., Roswall, N., Sacerdote, C., Sanchez, M.-J., Slimani, N., Spijkerman, A. M. W., Tjonneland, A., Tormo, M.-J., Tumino, R., van der A, D. L., van der Schouw, Y. T., Langenberg, C., Riboli, E., & Wareham, N. J. (20 14). Differences in the prospective association between individual plasma phospholipid saturated fatty acids and incident type 2 diabetes: The EPIC-Interact case-cohort study. *Lancet Diabetes Endocrinol*,

2(10), 8 10-18.

Fu, B. X., Chiremba, C., Pozniak, C. J., Wang, K., & Nam, C. (2017). Total Phenolic and Yellow Pigment Contents and Antioxidant Activities of Durum Wheat Milling Fractions. *Antioxidants (Basel)*, *6*(4), 78.

Galindez Najera, S. P. (2014). *A compositional breakage equation for first break roller milling of wheat* University of Manchester]. Manchester, England.

Galindo-Cuspinera, V., Valenca de Sousa, J., & Knoop, M. (2017). Sensory and analytical characterization of the "cool-melting" perception of commercial spreads. *Journal of Texture Studies*

48(4), 302-312.

Geng, M., Hu, T., Zhou, Q., Taha, A., Lang, Q., Lv, W., Xu, X., Pan, S., & Hu, H. (2021). Effects of different nut oils on the structures and properties of gel-like emulsion induced by ultrasound soy protein as an emulsifier. *International Journal of Food Science and Technology*, *56*(4), 1649-1660.

Ghotra, B. S., Dyal, S. D., & Narine, S. S. (2002). Lipid shortenings: a review. *Food Research International*, *35*(2002), 1015-1048.

Gibon, V. (2006). Fraction of lipids for use in food. In F. D. Gunstone (Ed.), *Modifying lipids for use in food* (pp. 201-233). Woodhead Publishing Limited.

Giroux, G. A. (2017). Accounting history and the rise of civilization. In (Vol. 1). Business Expert Press.

Glibowksi, P. (2010). Effect of thermal and mechanical factors on rheological properties of high performance inulin gels and spreads. *Journal of Food Engineering*, *99*(1), 106-113.

Gubernator, J., Stasiuk, M., & Kozubeck, A. (1999). Dual effect of alkylresorcinols, natural

amphiphilic compounds, upon liposomal permeability. *Biochimica et Biophysica Acta (BBA) - Biomembranes*, *1418*(2), 253-260.

Guner, S., & Oztop, M. H. (2017). Food grade liposome systems: Effect of solvent, homogenization types and storage conditions on oxidative and physical stability. *Colloids and Surfaces A: Physicochemical and Engineering Aspects*, *513*(2017), 468-478.

Health Canada. (2015). *Novel Food Information - Wheat Bran Extract as a novel food ingredient*. Government of Canada. Retrieved March 20th from https://www.canada.ca/en/health-canada/services/food-nutrition/genetically-modified-foods-other-novel-foods/approved-products/wheat-bran-extract-food-ingredient.html

Hielscher. *Ultrasonic Liposome Preparation*. Retrieved April 17th from https://www.hielscher.com/ultrasonic-liposome-preparation.htm

Hielscher. (2021). *Ultrasonic Liposome Preparation*. Retrieved April 17th 2021 from https://www.hielscher.com/ultrasonic-liposome-preparation.htm

Horikawa, K., Hashimoto, C., Kikuchi, Y., Makita, M., Fukudome, S.-i., Okita, K., Wada, N., & Oishi, K. (2017). Wheat alkylresorcinols reduce micellar solubility of cholesterol in vitro and increase cholesterol excretion in mice. *Natural Product Research*, *31*(5), 578-582.

Hosseinian, F. S., Muir, A. D., Westcott, N. D., & Krol, E. S. (2006). Antioxidant Capacity of Flaxseed Lignans in Two Model Systems. *Journal of the American Oil Chemists' Society*, *83*(10), 835-840.

Hu, S., Wu, J., Zhu, B., Du, M., Wu, C., Yu, C., Song, L., & Xu, X. (2021). Low emulsion gel stabilized by defatted Antarctic krill (Euphausia superba) protein using high-intensity ultrasound. *Ultrasonics Sonochemistry*, *70*, 105294-105294.

Huang, D., Ou, B., Hampsch-Woodill, M., Flanagan, J. A., & Prior, R. L. (2002). High-Throughput Assay of Oxygen Radical Absorbance Capacity (ORAC) Using a Multichannel Liquid Handling System Coupled with a Microplate Fluorescence Reader in 96-Well Format [research-article]. *Journal of Agricultural and Food Chemistry*, *50*(16), 4437-4444. https://doi.org/10.1021/jf0201529

Huerta, R. R., Silva, E. K., El-Bialy, T., & Saldana, M. D. A. (2020). Clove essential oil emulsion-filled cellulose nanofiber hydrogel produced by high-intensity ultrasound technology for tissue engineering applications. *Ultrasonics sonochemistry*, *64*, 104845-104845.

Jacobs, D. R. J., Anderson, L. F., & Blomhoff, R. (2007). Whole-grain consumption is associated with a reduced risk of noncardiovascular, noncancer death attributed to inflammatory diseases in the Iowa Women's Health Stud. *The American Journal of Clinical Nutrition*, *85*(6), 1606-1614.

Jansson, E., Landberg, R., Kamal-Eldin, A., Wolk, A., Vessby, B., & Aman, P. (2010). Presence of alkylresorcinols, potential whole grain biomarkers, in human adipose tissue. *British Journal of Nutrition*, *104*(5), 633-636. https://doi.org/doi:10.1017/S0007114510001169

John, G., & Vemula, P. K. (2006). Design and development of soft nanomaterials from biobased amphiphiles. *Soft Matter*, *2*(11), 909-914.

Kafle, A., Akamatsu, M., Bhadani, A., Sakai, K., Kaise, C., Kaneko, T., & Sakai, H. (2020). Phase Behavior of the Bilayers Containing Hydrogenated Soy Lecithin and β - Sitosteryl Sulfate. *Langmuir*, *36*, 6025-6032.

Kalogeras, I. M. (2016). Glass-Transition Phenomena in Polymer Blends; Encyclo- pedia of Polymer Blends. In *Encyclopedia of Polymer Blends: Volume 3: Structure* (Vol. 3). Wiley.

Katileviciute, A., Plakys, G., Budreviciute, A., Onder, K., Damiati, S., & Kodzius, R. (2019). A

Sight to Wheat Bran: High Value-Added Products. *Biomolecules*, *9*(12), 887.

Khaw, K.-T., Friesen, M. D., Riboli, E., Luben, R., & Wareham, N. (20 12). Plasma phospholipid fatty acid concentration and incident coronary heart disease in men and women: the epic-norfolk prospective study. *PLoS Medicine*, *9*(7), e 100 1255.

Kurotani, K., Sato, M., Yasuda, K., Kashima, K., Tanaka, S., Hayashi, T., Shirouchi, B., Akter, S., Kashino, I., Hayabuchi, H., & Mizoue, T. (20 17). Even- and odd-chain saturate fatty acids in serum phospholipids are differentially associated with adipokines. *PLoS One*, *12*(5), e0 178 192.

Leung, A. W. Y., Amador, C., Wang, L. C., Mody, U. V., & Bally, M. B. (2019). What Drives Innovation: The Canadian Touch on Liposomal Therapeutics. *Pharmaceutics*, *11*(3), 124.

Linko, A.-M., & Adlercreutz, H. (2007). Whole-grain rye and wheat alkylresorcinols are incorporated into human erythrocyte membranes | British Journal of Nutrition | Cambridge Core. *British Journal of Nutrition*, *93*(1), 11-13. https://doi.org/doi:10.1079/BJN20041281

Linko, A.-M., Ross, A. B., Kamal-Edin, A., Serena, A., Bjørnbak Kjaer, A. K., Jørgensen, H., Peñalvo, J. L., Aldercreutz, H., Åman, P., & Bach Knudsen, K. E. (2007). Kinetics of the appearance of cereal alkylresorcinols in pig plasma. *British Journal of Nutrition*, *95*(2), 282-287.

Linko-Parvinen, A.-M., Landberg, R., Tikkanen, M. J., Adlercreutz, H., & Peñalvo, J. L. (2007). Alkylresorcinols from Whole-Grain Wheat and Rye Are Transported in Human Plasma Lipoproteins. *The Journal of Nutrition*, *137*(5), 1137-1142. https://doi.org/10.1093/jn/137.5.1137

Liu, J., Hao, Y., Wang, Z., Ni, F., Wang, Y., Gong, L., Sun, B., & Wan, J. (2018). Identification, Quantification, and Anti-inflammatory Activity of 5-n-Alkylresorcinols from 21 Different

Wheat Varieties. *Journal of Agriculture and Food Chemistry*, *66*(35), 9241-9247.

Loh, G., Eberhard, M., Brunner, R. M., Hennig, U., Kuhla, S., Kleessen, B., & Metges, C. C. (2006). Inulin Alters the Intestinal Microbiota and Short-Chain Fatty Acid Concentrations in Growing Pigs Regardless of Their Basal Diet. *Journal of Nutrition*, *136*(5), 1198-1202.

Malekar, S. A., Sarode, A. L., BachII, A. C., & Worthen, D. R. (2015). The Localization of Phenolic Compounds in Liposomal Bilayers and Their Effects on Surface Characteristics and Colloidal Stability. *AAPS PharmSciTech*, *17*(6), 1468-1476.

Marklund, M., McKeown, N. M., Blumberg, J. B., & Chen, C.-Y. O. (2013). Hepatic biotransformation of alkylresorcinols is mediated via cytochrome P450 and β-oxidation: A proof of concept study. *Food Chemistry*, *139*(1-4), 925-930.

Marklund, M., Strömberg, E. A., Lærke, H. N., Knudsen, K. E. B., Kamal-Eldin, A., Hooker, A. C., & Landberg, R. (2014). Simultaneous Pharmacokinetic Modeling of Alkylresorcinols and Their Main Metabolites Indicates Dual Absorption Mechanisms and Enterohepatic Elimination in Humans. *The Journal of Nutrition*, *144*(11), 1674-1680. https://doi.org/10.3945/jn.114.196220

Martini, S. (2013). *Sonocrystallization of Fats* (R. W. Hartel, Ed. 1st ed.). Springer.

McClements, D. J., & Gummus, C. E. (2016). Natural emulsifiers — Biosurfactants, phospholipids, biopolymers, and colloidal particles: Molecular and physicochemical basis of functional performance. *Advances in Colloid and Interface Science*, *234*, 3-26.

Mensink, M. A., Frijlink, H. W., Maarschalk, K. v. d. V., & Hinrichs, W. L. J. (2015). Inulin, a flexible oligosaccharide. II: Review of its pharmaceutical applications. *Carbohydrate Polymers*, *134*, 418-428.

Moran-Valero, M. I., Ruiz-Henestrosa, V. M. P., & Pilosof, A. M. R. (2017). Synergistic

performance of lecithin and glycerol monostearate in oil/water emulsions. *Colloids and Surfaces B: Biointerfaces*, *151*(1), 68-75.

Mozafari, M. R., Khosravi-Darani, K., Borazan, G. G., Cui, J., Pardakhty, A., & Yurdugul, S. (2008). Encapsulation of Food Ingredients Using Nanoliposome Technology. *International Journal of Food Properties*, *11*(4), 833-844.

Mozuraityte, R., Kristinova, V., & Rustad, T. (2016). Oxidation of Food Components. In B. Caballero, P. M. Finglas, & F. Toldra (Eds.), *Encyclopedia of Food and Health* (Vol. 1, pp. 186-190). Elsevier.

Mungure, T., & Birch, E. J. (2014). Analysis of intact triacylglycerols in cold pressed canola, flax and hemp seed oils by HPLC and ESI-MS. *SOP Transactions on Analytical Chemistry*, *1*(1), 48-61.

Onipe, O. O., Jideani, A. I., & Beswa, D. (2015). Composition and functionality of wheat bran and its application in some cereal food products. *International Journal of Food Science and Technology*, *50*(12), 2509-2518.

Ozkan, H., Willcox, G., Graner, A., Salamini, F., & Kilian, B. (2011). Geographic distribution and domestication of wild emmer wheat (*Triticum dicoccoides)*. *Genetic resources and crop evolution*, *58*(1), 11-53.

Paglarini, C. d. S., Silva Vidal, V. A., Ozaki, M. M., Badan Ribeiro, A. P., Bernardinelli, O. D., Ignacio Camara, A. K. F., Herrero, A. M., Ruiz-Capilla, C., Sabadini, E., & Rodrigues Pollonio, M. A. (2021). Inulin gelled emulsion as a fat replacer and fiber carrier in healthier Bologna sausage. *Food Science and Technology International*, *0*(0), 1-12.

Paradiso, V. M., Giarnetti, M., Summo, C., Pasqualone, A., Minervini, F., & Caponio, F. (2015). Production and characterization of emulsion filled gels based on inulin and extra virgin

olive oil. *Food Hydrocolloids*, *45*, 30-40.

Petersen, S., Chaleepa, K., & Ulrich, J. (2013). Importance of emulsions in crystallization — applications for fat crystallization. *Frontiers of Chemical Science and Engineering*, *7*(1), 43-48.

Pichot, R., Watson, R. L., & Norton, I. T. (2013). Phospholipids at the Interface: Current Trends and Challenges. *International Journal of Molecular Sciences*, *14*(6), 11767-11794.

Puckler, M., Siebenhangl-Ehn, S., Apprich, S., Holtinger, S., Haas, C., Schmid, E., & Kneifel, W. (2014). Wheat bran-based biorefinery 1: Composition of wheat bran and strategies of functionalization. *LWT- Food Science and Technology*, *56*(2), 211-221.

Ross, A. B., Chen, Y., Frank, J., Swanson, J. E., Parker, R. S., Kozubek, A., Lundh, T. r., Vessby, B., Åman, P., & Kamal-Eldin, A. (2004). Cereal Alkylresorcinols Elevate γ-Tocopherol Levels in Rats and Inhibit γ-Tocopherol Metabolism In Vitro. *The Journal of Nutrition*, *134*(3), 506-505 510.

Ross, A. B., Kamal-Eldin, A., Lundin, E. A., Zhang, J.-X., Hallmans, G., & Aman, P. (2003). Cereal Alkylresorcinols Are Absorbed by Humans. *The Journal of Nutrition*, *133*(7), 2222-2224. https://doi.org/10.1093/jn/133.7.2222

Ruecroft, G., Hipkiss, D., Ly, T., Maxted, N., & Cains, P. W. (2005). Sonocrystallization: The Use of Ultrasound for Improved Industrial Crystallization. *Organic Process Research & Development*, *9*, 923-932.

Sampietro, D., Catalan, C. A., & Vattuone, M. (2013). Alkylresorcinols: Chemical properties, methods of analysis and potential uses in food, industry and plant protection. In C. L. Céspedes, D. A. Sampietro, D. S. Seigler, & M. Rai (Eds.), *Natural Antioxidants and Biocides from Wild Medicinal Plants* (pp. 148-166). CABI.

Scherer, P. E. (2006). Adipose tissue: from lipid storage compartment to endocrine organ. *Diabetes*, *55*(6), 1537-1545.

Schramm, L. L. (2014). *Emulsions, Foams, Suspensions, and Aerosols: Microscience and Applications* (2 ed.). John Wiley & Sons, Incorporated.

Schulte, H. L., Sousa, J. P. B., Sousa-Moura, D., Grisolia, C. K., & Espindola, L. S. (2021). Degradation evaluation and toxicity profile of bilobol, a promising eco-friendly larvicide. *Chemosphere*, *263*, 128323.

Senrayan, J., & Venkatachalam, S. (2020). Ultrasonic acoustic-cavitation as a novel and emerging efficient technique for oil extraction from kapok seeds. *Innovative Food Science & Emerging Technologies*, *62*, 102347.

Servili, M., Veneziani, G., Taticchi, A., Romaniello, R., Tamborrino, A., & Leone, A. (2019). Low-frequency, high-power ultrasound treatment at different pressures for olive paste: Effects on olive oil yield and quality. *Ultrasonics Sonochemistry*, *59*, 104747.

Shahidi, F., & Zhong, Y. (2010). Lipid oxidation and improving oxidative stability. *Chemical Society Reviews*, *39*(11), 467-479.

Shoaib, M., Shehzad, A., Omar, M., Rakha, A., Raza, H., Sharif, H., Shakeel, A., Ansari, A., & Niazi, S. (2016). Inulin: Properties, health benefits and food applications. *Carbohydrate Polymers*, *147*, 444-454.

Shukla, S., Haldorai, Y., Hwang, S. K., Bajpai, V. K., Huh, Y. S., & Han, Y.-K. (2017). Current Demands for Food-Approved Liposome Nanoparticles in Food and Safety Sector. *Frontiers in Microbiology*, *8*, 2398-2398.

Silva, R., Ferreira, H., Little, C., & Cavaco-Paulo, A. (2010). Effect of ultrasound parameters for unilamellar liposome preparation. *Ultrasonics Sonochemistry*, *17*(3), 628-632.

Stasiuk, M., & Kozubek, A. (2010). Biological activity of phenolic lipids | SpringerLink. *Cellular and Molecular Life Sciences*, *67*(6), 841-860. https://doi.org/10.1007/s00018-009-0193-1

Statistics Canada. (2018). *Canadian international merchandise trade: Annual review, 2017* https://www150.statcan.gc.ca/n1/daily-quotidien/180606/dq180606c-eng.htm

Stevenson, L., Phillips, F., O'Sullivan, K., & Walton, J. (2012). Wheat bran: its composition and benefits to health, a European perspective. *International Journal of Food Sciences and Nutrition*, *63*(8), 1001-1013.

Stoyanova, S., Geuns, J., Hideg, E., & Van Den Ende, W. (2011). The food additives inulin and stevioside counteract oxidative stress. *International Journal of Food Sciences and Nutrition*, *62*(3), 207-214.

Symko, S. (2015). *From a single seed - tracing the Marquis wheat success story in Canada to its roots in the Ukraine*. Agriculture and Agri-Food Canada.

Tadros, T. F. (2016). *Emulsions: Formation, Stability, Industrial Applications*. De Gruyter, Inc.

Teles dos Santos, M., Viana, I. S., Ract, J. N. R., & Le Roux, G. A. C. (2016). Thermal properties of palm stearin, canola oil and fully hydrogenated soybean oil blends: Coupling experiments and modeling. *Journal of Engineering*, *185*(2016), 17-25.

Tian, S., Sun, Y., Chen, Z., & Zhao, R. (2020). Bioavailibility and bioactivity of alkylresorcinols from different cereal products. *Journal of Food Quality*, *2020*, 1-6.

van Hoogevest, P., & Wendel, A. (2014). The use of natural and synthetic phospholipids as pharmaceutical excipients. *European Journal of Lipid Science and Technology*, *116*(9), 1088-1107.

Yokota, D., Moraes, M., & Pinho, S. C. (2012). Characterization of lyophilized liposomes produced with non-purified soy lecithin: a case study of casein hydrolysate

microencapsulation. *Brazilian Journal of Chemical Engineering*, *29*(2).

Zhao, X., Huang, B., El-Aooiti, M., & Rousseau, D. (2018). Demulsification to control solute release from Pickering crystal-stabilized water-in-oil emulsions. *Journal of Colloid and Interface Science*, *509*, 192-201.